

**SEALS/ SECONDARY FLOWS**  
Selected NASA LeRC Results  
with Emphasis on CFD

R.C. Hendricks and B.M. Steinmetz  
NASA Lewis Research Center  
Cleveland, Ohio

and

M.M. Athavale and A.J. Przekwas  
CFD Research Corp.  
Huntsville, Alabama

The overview Panel-1 provides a development history of various phases of our interactive seals/secondary/powerstream flow fields with emphasis on the numerical computations instigated by the experimental testing in the YT-700 engine program. The panel summarizes the solver, model and grid along with the results and impact on the industry. Selected references provide more in-depth resources and the viewgraph numbers relate to the terse textual materials.

When changes are made in an engine, the interactive effects between seals, secondary flows and powerstream flows are often considered minor or neglected. But what really happens when for instance you make a significant change as the CDP seal or perhaps even a minor change in the interstage turbine cavity seal? The results can be very enlightening and range from very positive reductions in SFC to catastrophic failure with losses of aircraft and lives of pilots.

**YT-700 Compressor Discharge Pressure Seal Test**  
(Panel-2 provides an overview of the operating conditions and results)

Consider the case of changing the CDP seal in a YT700 engine (fig. 1) from the forward facing 5-tooth labyrinth (knife) seal (fig. 2) to a dual brush seal of standard Cross construction, i.e., 2.8mil Haynes 25 bristles, 2500/in-circumference, free length of approx. 0.38 inches (fig. 3). In this case the leakage was cut in half, the SCF decreased well over 1%, the pressure ratio across the compressor increased - in short flows throughout the entire engine changed (fig 4). So here is a case where by making a rather benign change in the CDP- seal it changed the secondary flow distribution and the power stream flows. That work initiated investigations into the benefits of interactive seals secondary power stream systems. For relatively minor investments, significant gains can be made.

**UTRC Large Scale Test Rig**  
Panels 3-9 background, numerical methods, code capabilities, problem descriptions, flow

conditions, boundary conditions, a description of test runs

To illustrate some of the steps taken to understand this interaction, consider the UTRC simulation of the SSME HPFTP (fig. 5) with multiple cavities , purge flows, power stream simulation modeled to assess how the flow threads through the system, purge flows, ingestion effects and cooling within the pump. CFD studies with a single cavity were unsuccessful in predicting data. It wasn't until the entire multiple connected cavities and purge flows were coupled and gridded (fig. 6) with the power stream at the inlet of the first stage turbine and exit of the second stage turbine that the proper experimental BC's could be satisfied. Streamlines show how the flow threads through the system (figs. 7, 8(a), 8(b)) The interactive effects of purging, ingestion and the powerstream shown were illustrated by CO<sub>2</sub> injection (fig. 9). Ingesting of the power stream, intentional in this case, became a major result to illustrate why single cavity predictions were unsatisfactory (fig. 10) - the reason is apparent when the ingested powerstream partly exits at the low pressure side of the first stage turbine, and a significant portion flowing through the interstage cavities to exit downstream of the second stage turbine. With this understanding, several other programs involving variations in rim sealing as the UTRC single stage turbine program were investigated. Panel-10 compares mass flow rates for selected runs at four seals and three purge cavities.

### The Allison T-56/501D Turbine

Panels-11-15 give the problem simulation set, the characteristics, flow and boundary conditions, and computational grid.

It was necessary to determine the effectiveness of multiply connected cavities. The T56 501D trubine configuration was gridded (fig. 11) and CFD calculations carried out. The results were both enlightening and in good agreement with design data. However more realistic conjugate heat transfer was added and hot spots to 150F over design data appeared (figs. 12 and 13), with some results on panel-16, giving some warning signals. Doubling seal clearances strongly effected leakage and temperature (figs 14 and 15) with a design/prediction results on panel-17. Further, preliminary inclusion of decoupled strain in a model rotor (fig. 16) signaled potential disc warpage problems both of the disc and rim seal interface (figs. 17 and 18).

### Rim Seal Ingestion - Four Basic Configurations

Panels-18 and 19 give an overview along with parameters and conditions to be compared. The UTRC cavity model (figure 19) illustrates the major parameters along with purge locations. Vector plots and comparisons of computations to data are illustrated for each of the four rim seal configurations (figs. 20-21). Panel-20 provides data/computation comparisons. The interaction with the power stream in terms of purge effectiveness of four different rim seals for planar averaged flows show good agreement with the data. Displacing the rotor 1/2-rim seal thickness caused severe heating in the clearance gap (step up) and along the platform (step down), (fig. 22).

### Unsteady and Rotordynamic Effects

Here are shown the CFD results of Hah. The grid (fig. 23) and Mach number of time average flows (fig. 24) and pressures (fig. 25) for another UTRC seal cavity configuration. While these illustrate the highly interactive behavior of the seals secondary and power stream flows, they are for a single stage turbine.

T-56/501D turbine transients simulated using a simple step jump from high-speed ground idle to takeoff showed little if any ingestion for this turbine and purge flows (figs. 26,27).

Unsteady and unexpected flow fields such as occur in this whirling annular seal. The geometry and typical conditions are given on Panel-21. The computational geometry is shown (fig. 28) and the numerical and experimental results (figs. 29-31). For this seal, the flow rotates nearly 270-degrees from the inlet large clearance zone to the exit small clearance zone. This effect was also noted in early SSME LH<sub>2</sub> seals testing. In these calculations, the low Reynolds number model may be slightly better. In a unique study by Prof. Morrison (Texas A&M Univ.) turbulent stress parameters were measured with a 3-color LDV. Typical results include detailed studies of labyrinth seal cavities with tangential velocities (fig. 32) and turbulence kinetic energies (fig. 33). For rotors whirling twice the rotational speed with zero eccentricity, the pressure field appears periodic with the rotor (fig. 34); at an eccentricity of 0.7 and 2.5 times the rotor speed, the has more of a piston effect (fig. 35).

### **Honeycomb and Brush Seal Simulations**

CFD simulations of honeycomb test results from Texas A&M are summarized in panels-22 and 23. The assumed symmetrical grid is (fig. 36) with velocity vectors (fig. 37), and static pressure variations (fig. 38). The conditions for these figures revealed no unsteadiness, yet the data showed large pressure fluctuations - which by the way are simulated by a simplified model.

CFD simulations of flows in brush seals, panel-24, reveals large variations in surface temperatures when flow rivering occurs due to mis-tufting of the bristles (fig. 39).

### **Vortex control studies**

Lid driven cavity studies, Panels-25and 26, illustrated the generic nature of vortices formed under conditions simulating axial turbine or compressor row. The potential for control of these vortices appears feasible, yet requires addition of clockwise or anti-clockwise vortices (fig. 40).

Inlet distortions degrade performance of the entire turbomachine compressor. Extensive work by Anderson is summarized as Panel-27. Distortions are often resolved by placing a swirl device in the flow, such as a swirl brake in the case of labyrinth seals, or by jets or fin arrangements as shown here(figs. 41 and 42) for the engine inlet duct. These distortions must be known and controlled. Anderson, working with DRA in England, has predicted distortion effects in an S-duct as illustrated (fig. 43). The numerical/experimental comparisons are shown here for M=0.44(fig. 44) and M=0.8 (fig. 45). These dynamic effects are currently under investigation.

### **Time Resolved Flows**

Coupling the codes TURBO and SCISEAL , Panel- 28, with a flow chart, Panel -29, will provide the intreactive time resolved solution of mutiple cavity turbomachine components. The proposed workscope appears as Panel-30. A description of the codes SCISEAL and TURBO are Panels 31-34.

### **AST program overview**

The AST program goals, projects, and proposed funding(fig. 46) have been designed to enhance

our understanding of the time resolved interactive behavior of interactive multiple cavity flows from the shaft to the shroud of a turbomachine. CDP, balance-piston, interstage, rim, face/brush seals, and active tip clearance control are under investigation( fig. 47). For example, the GE program is investigating large low leakage robust sealing; Allison is investigating face sealing of CDP for example; UTRC is looking at the turbine rim seal. Program funding projected to the year 2000 will provide validated tools and data bases for current and future engine programs with the overall goal of reductions in cost and SFC, Panel-35, with enhanced reliable engine life "on the wing."

## FIGURES

Figure 1. CDP seal in a YT700 engine

Figure 2. CDP 5-tooth labyrinth (knife) seal

Figure 3. CDP dual brush seal of standard Cross construction

Figure 4. SCF-Power labyrinth to dual brush comparison

Figure 5. UTRC simulation of the SSME HPFTP

Figure 6. Gridding SSME HPFTP Simulation

Figure 7. Streamfunction - Regions I, II

Figure 8(a). Streamfunction - Regions III,IV

Figure 8(b). Streamfunction - Regions II,IV no scale, for overlay

Figure 9. F1 purge concentrations

Figure 10. F4 powerstream concentrations

Figure 11. T56 501D Four Stage Turbine

Figure 12. T56 501D Four Stage Turbine Streamfunction

Figure 13. T56 501D Four Stage Turbine Temperature

Figure 14. T56 501D Stage 1-2 Disk Cavities streamfunction at two seal clearances.

Figure 15. T56 501D Stage 1-2 Disk Cavities temperature at two seal clearances

Figure 16. Simulated rim seal cavity for thermomechanical behavior

Figure 17. Simulated rim seal cavity thermomechanical behavior- streamfunction

Figure 18. Simulated rim seal cavity for thermomechanical behavior - temperatures

Figure 19. UTRC data- four rim seal configurations

Figure 20. UTRC data- four rim seal configurations - velocity vectors.

Figure 21. UTRC data- four rim seal configurations - numerical/data comparison.

Figure 22. Displace rotor rim-seal temperature effects.

Figure 23. UTRC cavity flow (Hah)- grid

Figure 24. UTRC cavity flow (Hah)- Mach number

Figure 25. UTRC cavity flow (Hah)- pressure

Figure 26. T56-501D 1-2 Disc Cavity grid

Figure 27. T56-501D 1-2 Disc Cavity -step jump - thermal effects

Figure 28. Whirling annular seal geometry and transformation

Figure 29. Whirling annular seal normalized axial velocity contours- numerical

Figure 30. Whirling annular seal normalized axial velocity contours - experimental

Figure 31. Whirling rotor normalized pressure distribution- two turbulence models and data

Figure 32. Whirling annular seal tangential velocities for a labyrinth seal.(after Morrison)

Figure 33. Whirling annular seal kinetic energies for a labyrinth seal. (After Morrison)

Figure 34. Time dependent perturbations, 0-eccentricity, whirl =  $2 \times$  rotor speed

Figure 35. Time dependent solutions, 0.7 eccentricity, whirl = 2.5 rotor speed

Figure 36. Flow domain for honeycomb grid.

Figure 37. Velocity vectors in honeycomb configuration

Figure 38. Static pressure within the honeycomb configuration

Figure 39. Brush seal simulations

Figure 40. Lid driven cavity vortex injection studies

Figure 41. Inlet duct and fin arrangements (Anderson)

Figure 42. Inlet duct and fin geometries (Anderson)

Figure 43. Inlet S-duct grid (Anderson)

Figure 44. Inlet distortion predictions, DRA data  $M=0.44$  (Anderson)

Figure 45. Inlet distortion predictions, DRA data  $M= 0.8$  (Anderson)

Figure 46. AST Goals

Figure 47. Seals Locations and project description

## PANELS

Panel-1 Overview of programs, models, grids, solvers, results, impact, reference, figures

Panel-2 YT-700 Engine test overview

Panel-3 Disc cavity flow simulation, background

Panel-4 Numerical methodology for SCISEAL

Panel-5 Capabilities of SCISEAL

Panel-6 Description of problem UTRC large scale rig

Panel-7 Flow conditions for test

Panel-8 Boundary conditions on simulation

Panel-9 Test run parameters

Panel-10 Seal mass flow rates numerical/ experimental simulation of SSME - HPFTP

Panel-11 T56/501D Four stage turbine simulation

Panel-12 T56/501D Characteristics and parameters

Panel-13 Flow and boundary conditions for simulation

- Panel-14 Modeling parameters**
- Panel-15 Grid and boundary conditions**
- Panel-16 Comparison of numerical and design data for T56-501D four stage turbine**
- Panel-17 Comparison of numerical and design data for clearance of 0.012-inch and 0.024-inch.**
- Panel-18 Rim seal ingestion study overview**
- Panel-19 Purge and rotor parameters and boundary conditions**
- Panel-20 Comparison of numerical/experimental data for four rim seal configurations**
- Panel-21 Whirling annular seal conditions**
- Panel-22 CFD Simulation of honeycomb tester ( insufficient storage, and time )**
- Panel-23 CFD results and summary of honeycomb simulation**
- Panel-24 SCISEAL brush seal clearance characterization**
- Panel-25 SCISEAL simulation of lid driven cavity simulation blade-shroud effects**
- Panel-26 Co- and counter- rotation vortices placed near suction and pressure sides**
- Panel-27 Inlet distortion overview (Anderson)**
- Panel-28 Features of SCISEAL and TURBO codes**
- Panel-29 Proposed flow chart for parallel execution of codes SCISEAL and TURBO**
- Panel-30 Proposed scope of work for combining SCISEAL and TURBO**
- Panel-31 SCISEAL and TURBO features**
- Panel-32 TURBO applications (Janis)**
- Panel-33 TURBO release specifications (Janis)**
- Panel-34 TURBO future releases (Janis)**
- Panel-35 Potential SFC gains seals/secondary flow program**

Topic	Solver	Flow Resolution	Model Dimension	Grid	Results	Impact	Selected References	Viewgraph Number
1. T-700 Engine Test	1%	Full Scale Ground idle to Full power 765F ; 530 fps	Full Scale	CDP Labyrinth Seal Replaced by Dual Brush Seal	SCF decrease >1% Pressure ratio increased Changed flow throughout engine	Initiated investigations of interactive seal/secondary/powerstream multicavity flows	94-GT-266	1 Geometry 2 Labyrinth 3 Dual Brush 4 SCF vs HP
2. SSME HPFTP Simulation UTRC Large Scale Test Rig SCISEAL	0.5%	Axisym N.S . + Scalar transport	Axisym	20k cell/ 52 block Body fit coord.	Simulate powerstream multiple cavities/seals flows, purge flows and fluid ingestion - code validation results	Interactive seals/power/ secondary flows are required to validate code/experimental results	95-GT-325	1 Geometry 2/3 Streamlines Stage 1 & 2 4/5 CO2 purge F1 & F4
3. T56-501D Engine 4-stage turbine	Planar Design Data/ SCISEAL	Average N. S. Conjugate heat trans.	Axisym	91 k cell/140 block Body fit coord.	All multiple connected cavities pairs stage 1-2,2-3 3-4 required for integrated seals/secondary/power flow - conjugate heat trans. Rim seal leakage and gas temperature > design data M>1 interface showed no flow shock field Thermomechanical distortions of interface are significant Clearance change 0.012" to 0.024" initiates powerstream ingestion -cavity with large temperature increases	4-stage gas turbine validation of SCISEAL code Local hot regions defined Rim seal leakage and gas temperature > design data M>1 interface showed no flow shock field Thermomechanical distortions of interface are significant Clearance change 0.012" to 0.024" initiates powerstream ingestion -cavity with large temperature increases	96-GT-067 AIAA95 2620	1 Geometry 2 Streamlines 3 Temperature 4 M > 1 5 Thermal distortion 6 0.012/0.024 Streamlines Temperature
4. Rim Seal Cavity	SCISEAL	Planar average	Axisym	90x130	Rim seal temperature depends on gap recirculation zone cavity geometry/powerstream purge flow strength Small changes in rotor radius, as eccentric rotor effects significant temp changes 4 UTRC rim seal/cavity numerical/experimental parameters,good agreement	Demonstrates effectiveness of platform cooling Rotor eccentricity causes large changes in rim seal temperature and recirculation zone SCISEAL code validation , rim seals	ISROMAC-4 Vol A p 122 1992 AIAA94 2803	1 Geometry 2 Streamlines 3 Rotor radius changes 4 4 UTRC rim seals
5. Tip Seal Chunill Hah	UNS3D Time Resolve	3-D NS			Time dependent wakes due to blade passing engenders large pressure velocity fluctuations	Need to compute Time resolved flow fields		1 Geometry 2 Streamlines 3 Velocity 4 Pressure
6. T56-501D Operation Envelope	SCISEAL	Planar Average	Axisym NS	90k 34 blocks	No powerstream ingestion for changes from fast ground idle to takeoff power	Necessary to compute component flows over operations envelope	AIAA96 3305	1 Geometry 2 Takeoff
7. Seal Dynamics	SCISEAL	periodic	3-D NS BFC	12k cells	Whirling annular seal flowfield rotates 270-degrees from inlet to exit Good agreement with experimental data Pressure/forces distribution sub/super/synchronous interactive rotor/flow field	Seal dynamics strongly effect system flow and rotordynamics	ISROMAC 6 1996	1 Geometry 2 velocity contour 3 pressure contour 4 Sub/super rim seals 5 Synchronous
8. Honeycomb Seal	SCISEAL	periodic	3-D NS	90k 6 cells each 14x14x45	Pressure drop not predicted Experimental unsteady flow not predicted	Cell structure complex requires more cells in axial direction Large computer time	TAM-Workshop 96	1 Geometry 2 velocity 3 pressure
9. Lid Driven Cavity	SCISEAL	Planar average periodic	3-D No Coriolis No body force	12 k cells	Leading edge/ tip vortex root vortex fills up to 1/3 of the powerstream passage Counter vortex insertion alters this effect	Vortex insertion can control vortices and instabilities	AIAA93-0390	1 Geometry 2 Vortex 3 Insertion vortex

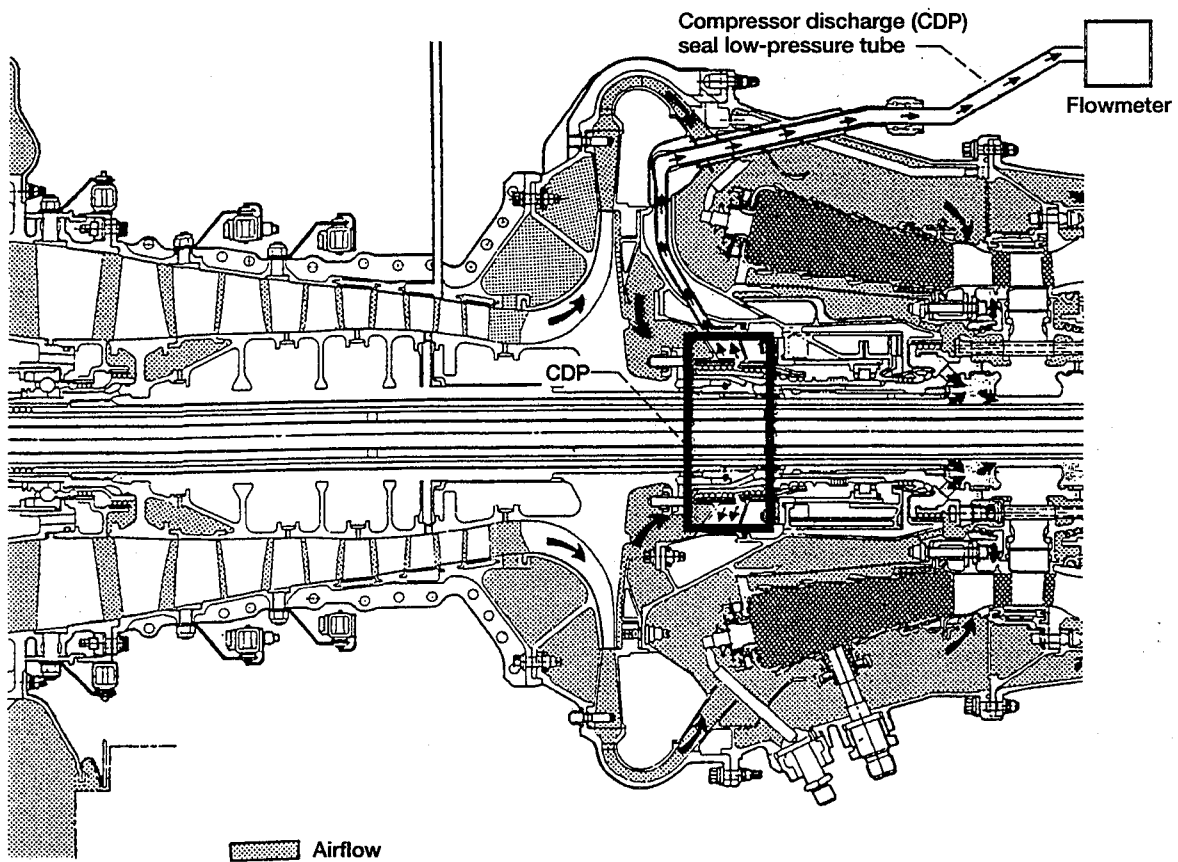
10.	Inlet Distortion	RNS3D Bernie Anderson	3D Euler + Boundary	49x49x107	Good agreement with DRA experimental inlet Vortex vanes provide to 80% distortion reduction	Inlet flow distortions change flow field & BC's & can not be ignored Vortex control appliances effective in controlling distortion	AIAA96 3279	1 Geometry 2 Vanes 3 Distortion 4 Controlled flows
11	Powerstream Seal Secondary TURBO Coupling	SCISEAL	3D NS P-based 3D NS rho-based	Time resolved Time resolved	Code coupling in progress to provide time resolved multi-stage turbomachine component computation - hub to rim.		1 Work scope 2 Codes TURBO/SCISEAL 3 Coupling 4 Video	
12.	AST Advance Subsonic Transport	1. Goals and Budget 2. Programs and Engine Locations 3. Performance Benefits						

### Panel-1 Overview of programs, models, grids, solvers, results, impact, reference, figures

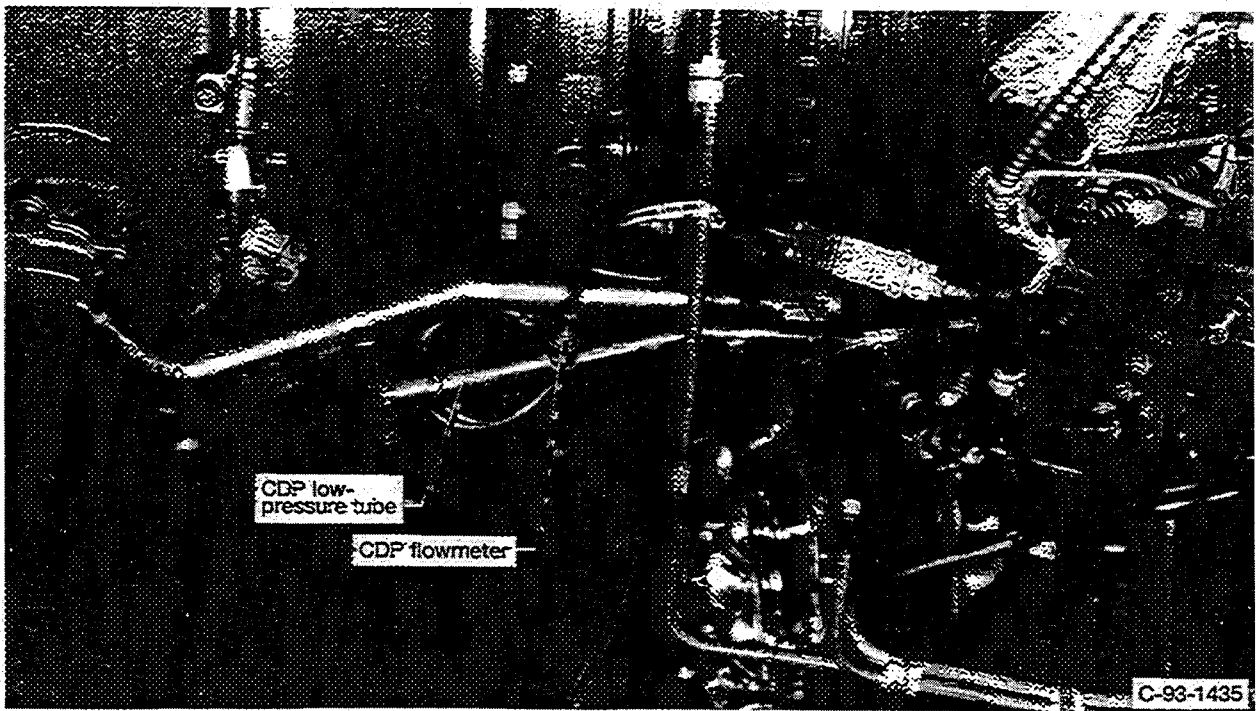


## YT-700 Compressor Discharge Pressure Seal Test

- Direct comparison between BOM CDP labyrinth seal and dual brush CDP seal
- Compressor:
  - ◊ Rotor speed to 43000 rpm
  - ◊ Surface speed to 530 fps (160 m/s)
  - ◊ Pressure drop to 145 psia (1 MPa)
  - ◊ Temperature to 765C (680K)
- Dual brush: Haynes-25/CrC standard Cross Mfg.
- Wear: < 1 mil (.025 mm) 46 hr. operation
- Leakage: Labyrinth = 2.5 X dual brush
- SCF > 1% decrease
- Increased engine pressure ratio
- Distributed flow throughout the entire engine
- Modifications of secondary flow path changes engine
  - ◊ Powerstream
  - ◊ Cooling and tribology stream
  - ◊ Engine dynamics



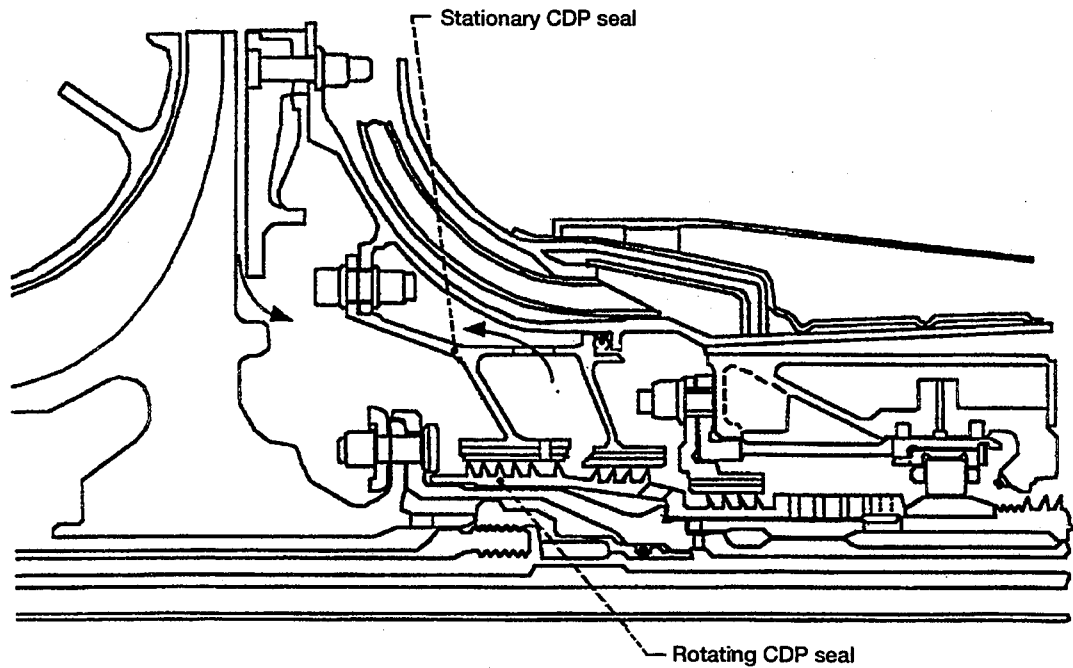
(a) Airflow schematic.



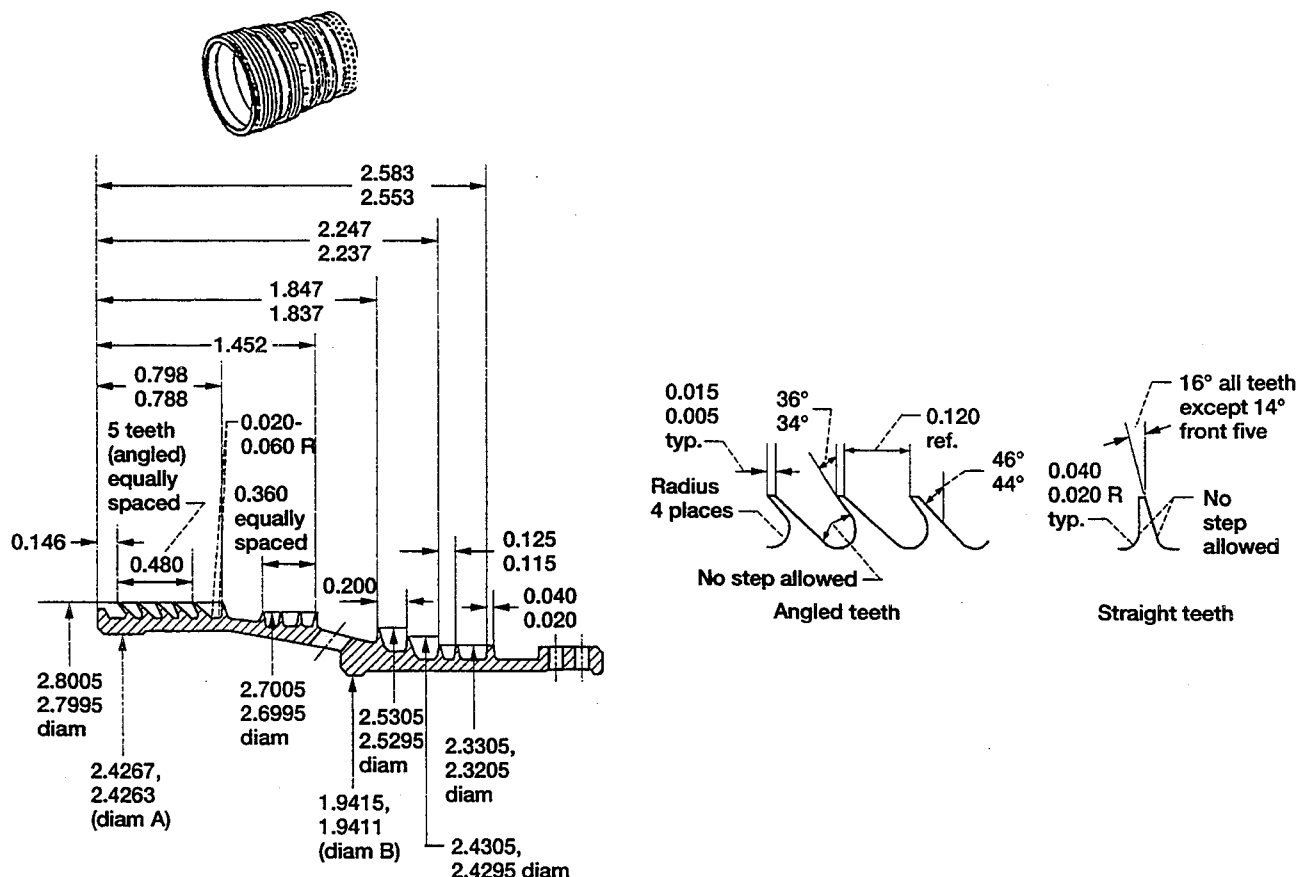
(b) Location of CDP flowmeter.

Figure 1.—Schematic of engine airflow and location of flowmeter.

Figure 1. CDP seal in a YT700 engine



(a) Labyrinth seal package and airflow.



(b) Schematic of labyrinth compressor discharge seal. (Seal teeth and axis established by diameters A and B to be concentric within 0.003 full indicator reading. No steps allowed on tooth face or at fillet radius. All dimensions are in inches.)

Figure 2.—Labyrinth compressor discharge seal system.

Figure 2. CDP 5-tooth labyrinth (knife) seal

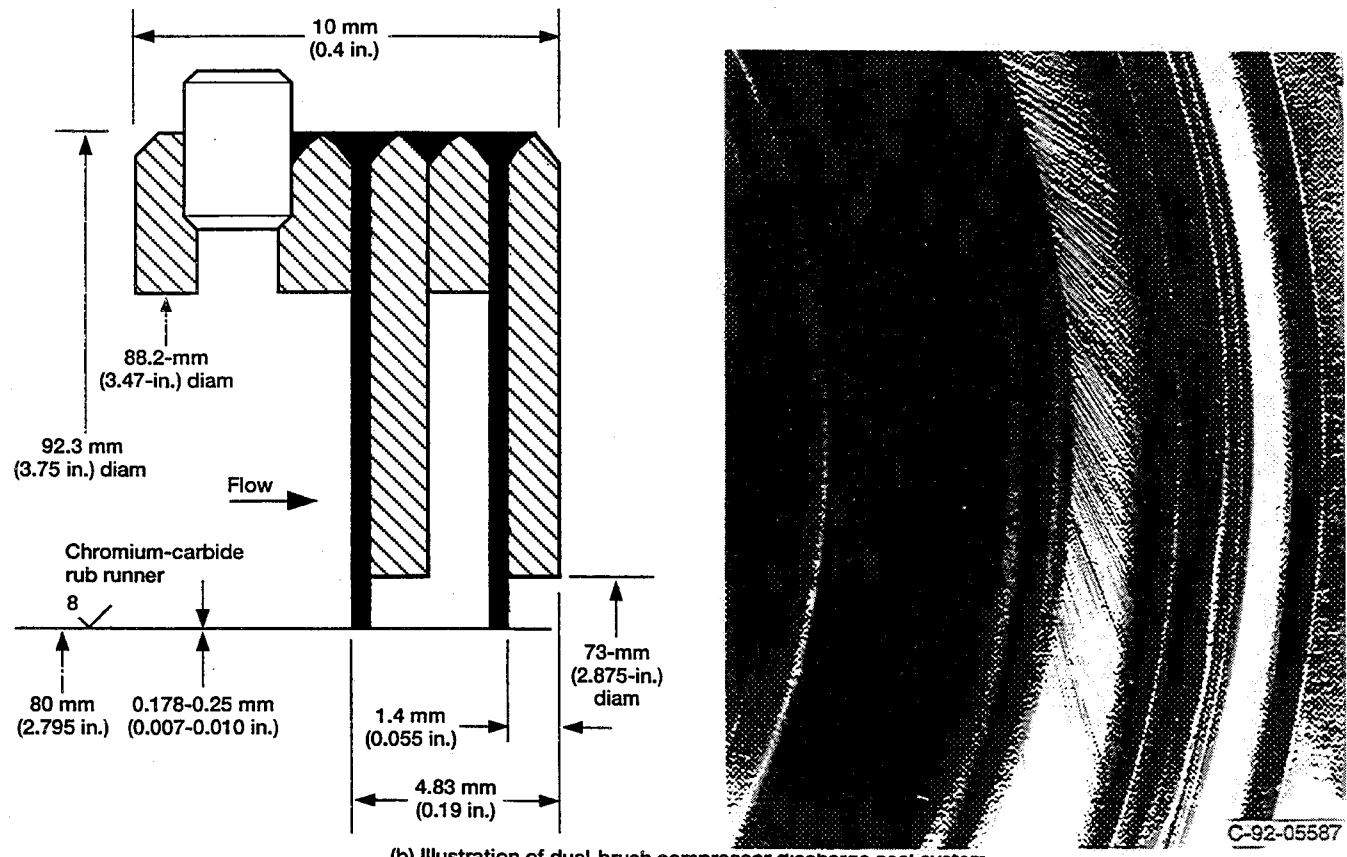
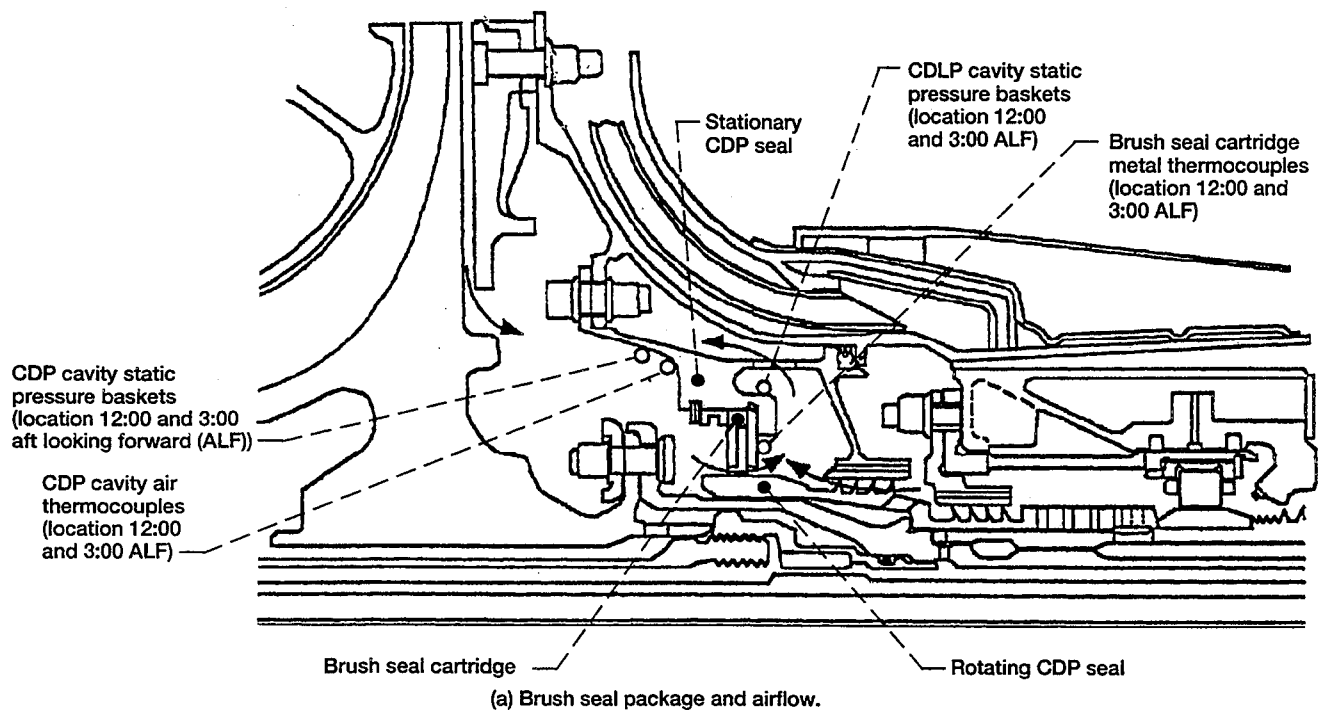


Figure 4.—Dual-brush compressor discharge seal system and schematic of airflow.

Figure 3. CDP dual brush seal of standard Cross construction

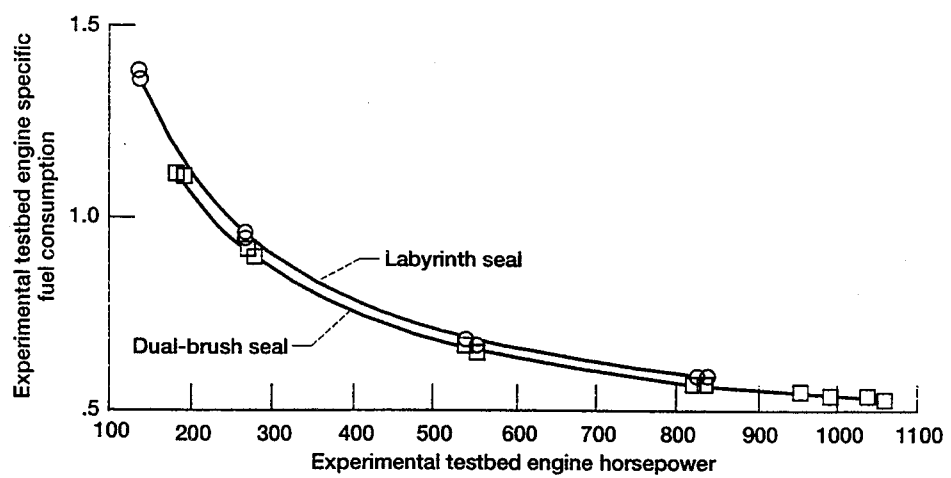


Figure 16.—Experimental testbed engine specific fuel consumption as a function of horsepower.

Figure 4. SCF-Power labyrinth to dual brush comparison

## DISC-CAVITY-MAIN-PATH FLOW SIMULATIONS



- Single Cavity & Rim Seal (1992)
  - different flow and geometric conditions
- Disc Pumping Test, 1994 (Graber et. al., 1987)
  - Cold flow simulations with tracer gas, cooling effectiveness studies, validation
- Large Scale Rig Simulations 1994, (Daniels and Johnson, 1993)
  - Multiply connected, multicavity & main path
  - Cold flow with tracer gaser, simulations compared with experiments
- Allison T-56 Turbine Disc Cavities 1994 → 1996 (with J. Forry & J. Munson)
  - Stage 1-2 cavity simulations with labyrinth seal clearance variations (1994)
  - Conjugate heat-transfer for cavity pairs (1995)
  - Conjugate flow & heat transfer for entire turbine drum (1996)

## **NUMERICAL METHODOLOGY**

---



- Computations Presented here Performed using  
**SCISeAL**
  - 3D CFD Code Developed for Fluid Flow and Forces in Turbomachinery Seals; Under a NASA LeRC Contract No. NAS3-25644
- SCISeAL Code Description
  - Finite-Volume Pressure-Based Algorithm
  - Implicit Multi-Domain Flow Treatment
  - Incompressible and Compressible Flow Treatment
  - Collocated Variable Storage with Strong Conservation Approach for Convective Fluxes

## CODE CAPABILITIES (continued)

**CFDRc**

- SCISEAL Capabilities
  - High Order Spatial (up to 3rd) and Temporal (2nd Order Crank-Nicholson) Differencing schemes
  - A Comprehensive Set of Boundary Condition Types
  - Seal Rotordynamic Coefficient Calculation Methods
  - Variety of Turbulence Models (Standard and Low-Re K- $\epsilon$ , multiple scale K- $\epsilon$ , 2-layer), Surface Roughness Treatment
  - Transport Equations for Passive Scalars e.g. Mixture Fractions (M-F) of Gas Mixtures, of Vital Importance to Present Study

## PROBLEM DESCRIPTION



- 2 Rotor, 4 Cavity Configuration in the UTRC Large Scale Rig by Daniels and Johnson
- Simulates the Turbine Section of the SSME HPFTP
- 4 Rim Seals with Associated Main-Path Flows
- Purge Flows at 3 Locations
- Different Concentrations of Tracer Gas ( $\text{CO}_2$ ) Injected in Different Flow Streams and Measured at Several Locations
- Flow Rates in Main Path and Flow Paths Measured and Varied for Parametrics
- Shanks of the Blades also Simulated by Openings in the Rotors with Curved Passages Under the Blade Platforms.

Panel-6 Description of problem UTRC large scale rig

## FLOW CONDITIONS

**CFDRIC**

- Flow Conditions
  - 2D Axisymmetric Flow of Compressible Gas at Near Room Temperature
  - Convective Terms Discretized Using Central Differencing with 20% Damping
  - Standard k- $\varepsilon$  Equation of Turbulence with Wall Functions
  - A Total of Seven Gas Compositions used for Main and Purge Flows. M-F of Each Composition Solved for using a Scalar Transport Equation

Panel-7 Flow conditions for test

## BOUNDARY CONDITIONS

**GDI<sup>RC</sup>**

- Specified Mass Fluxes at the Inlets of Main Path Flows, Specified Pressures at Main Path Exits
  - M-F of 100% of One of F4 through F7 at Different Inlets; e.g. at Mainpath 1, F4=100%, F1, F2, F3, F5, F6, F7=0
- Specified Mass Fluxes at Purge Flow Inlets, M-F of 100% of one of F1, F2, or F3
- Rotating Walls on all Rotor Surfaces, Stationary Walls on Other Surfaces
- All Walls Assumed Adiabatic, Sufficient for Small T Variation in this Study
- In an Actual Turbine, T Variations are High, and Wall Conditions Unknown
  - Conjugate Heat Transfer Necessary which Treats Flows and Solids Together in Energy Equation

## DESCRIPTION OF TEST RUNS

**CFDR**

- Simulations Carried Out at Three Different Conditions
  - Variations in  $Re_\theta$  as well as Purge Flow Rates

Test No.	rpm	Pressure psia	Reynolds Number	Forward Cavity purge F1= $\phi_{12}$	Center Cavity purge F2= $\phi_{13}$	Aft Cavity purge F3= $\phi_{14}$
102	1004	60.55	1.64E6	.027	.012	.012
202	1502	57.24	2.19E6	.017	.008	.013
205	1504	57.79	2.24E6	.030	.015	.014

Powerstream flow concentrations      Herein      UTRC      Seal No.  
Nomenclature

First stage blade	leading edge	$F4 = \phi_{01}$	1
	trailing edge	$F5 = \phi_{03}$	2
Second stage blade	leading edge	$F6 = \phi_{05}$	3
	trailing edge	$F7 = \phi_{07}$	4

# LARGE-SCALE MODEL RIG

CDRC

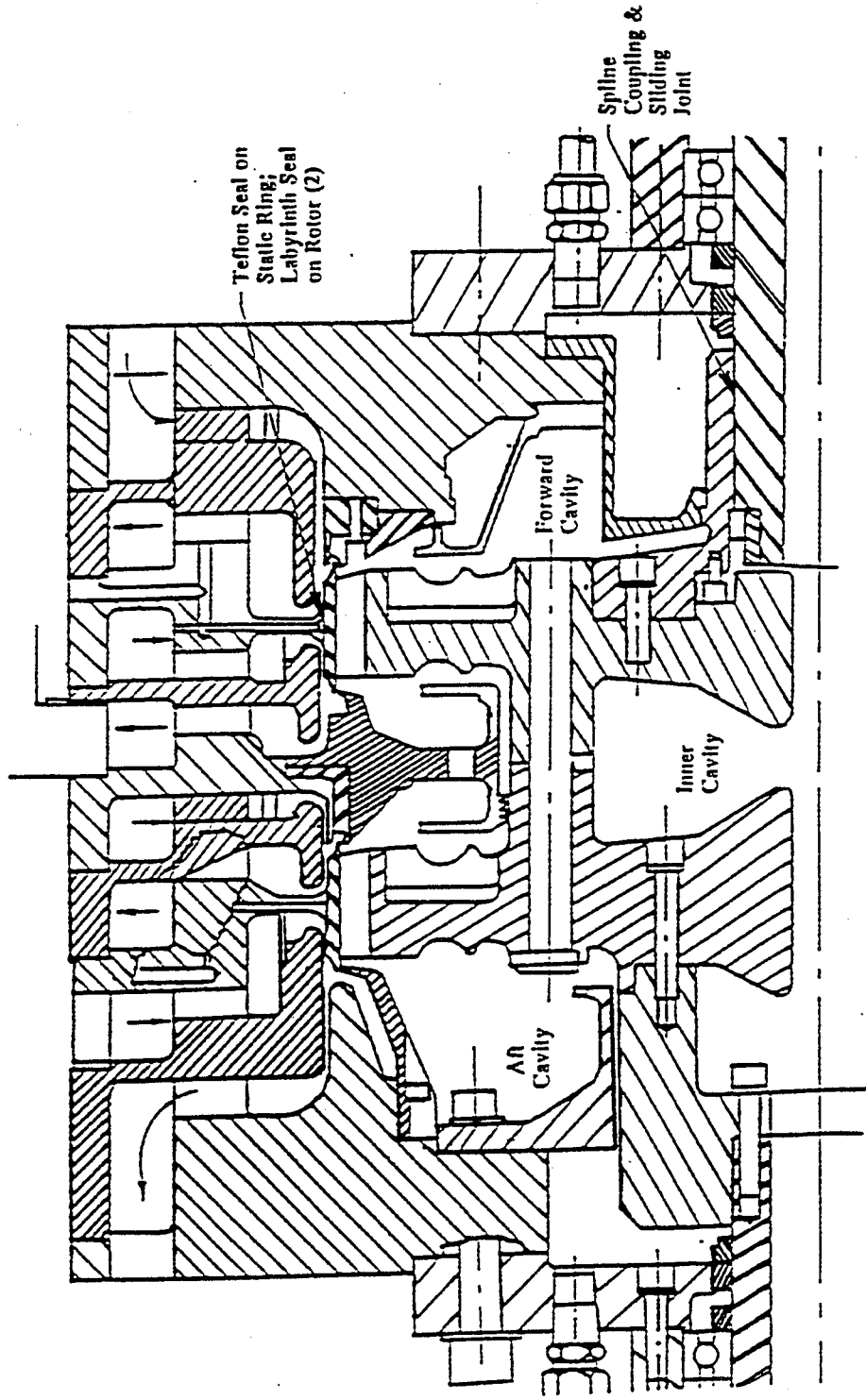
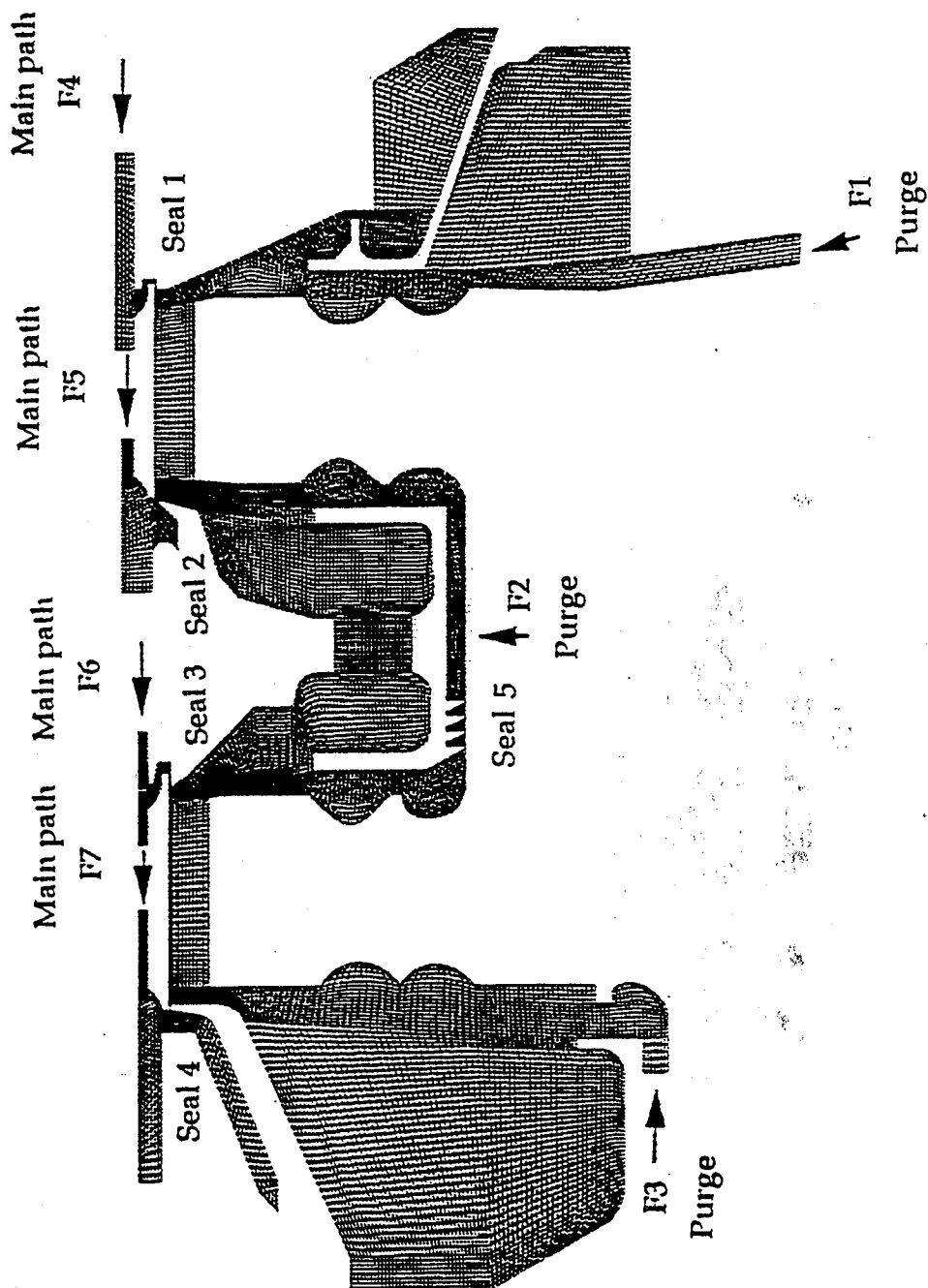


Figure 5. UTRC simulation of the SSME HPFTP

# FLOW DOMAIN

CFDR<sup>C</sup>



# Streamfunction Plot

## Regions I, II and Blade Shanks, Run No. 202

CFDRC

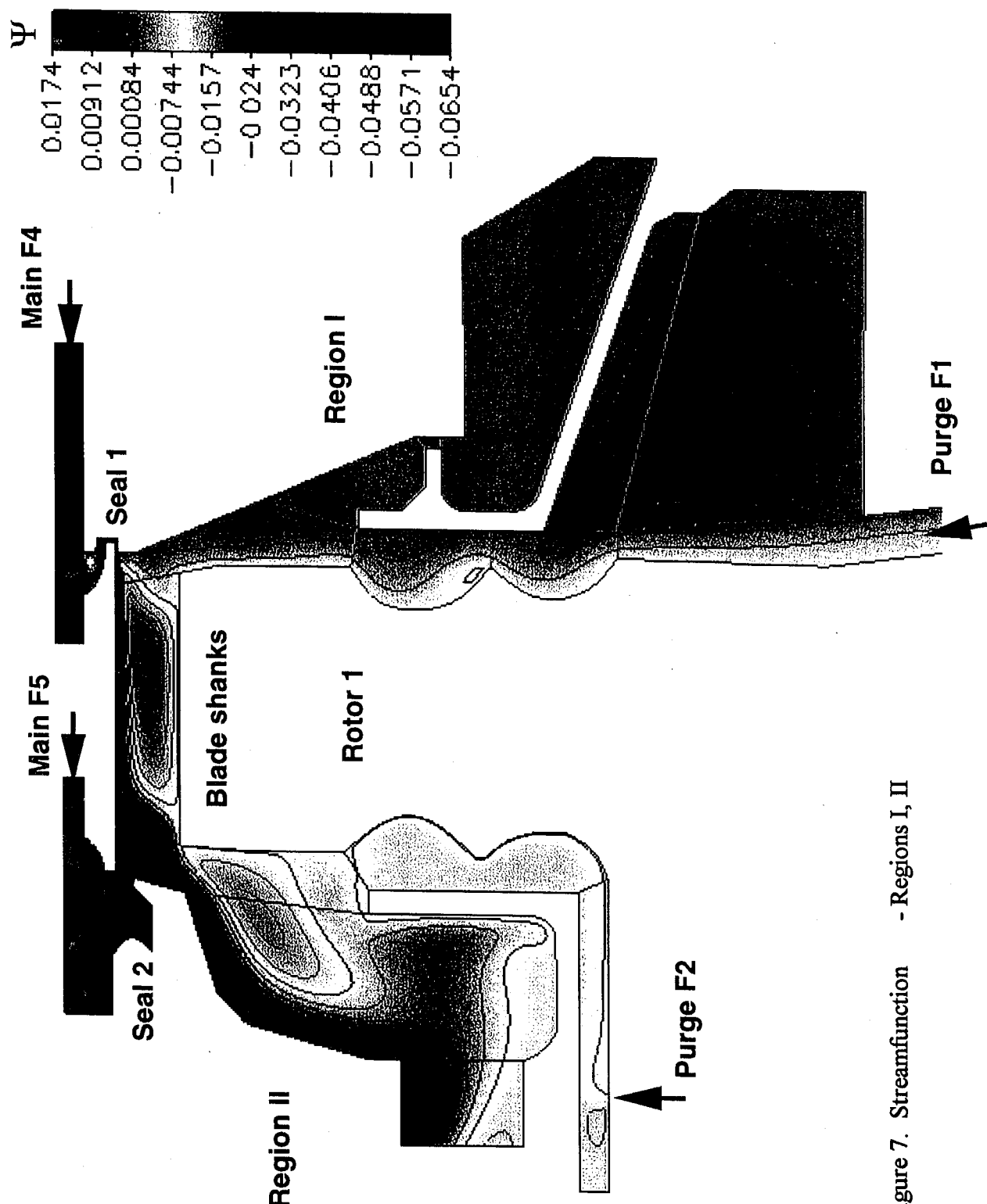


Figure 7. Streamfunction - Regions I, II

# Streamfunction Plot

CFDRC

Regions III, IV and Blade Shanks, Run No. 202

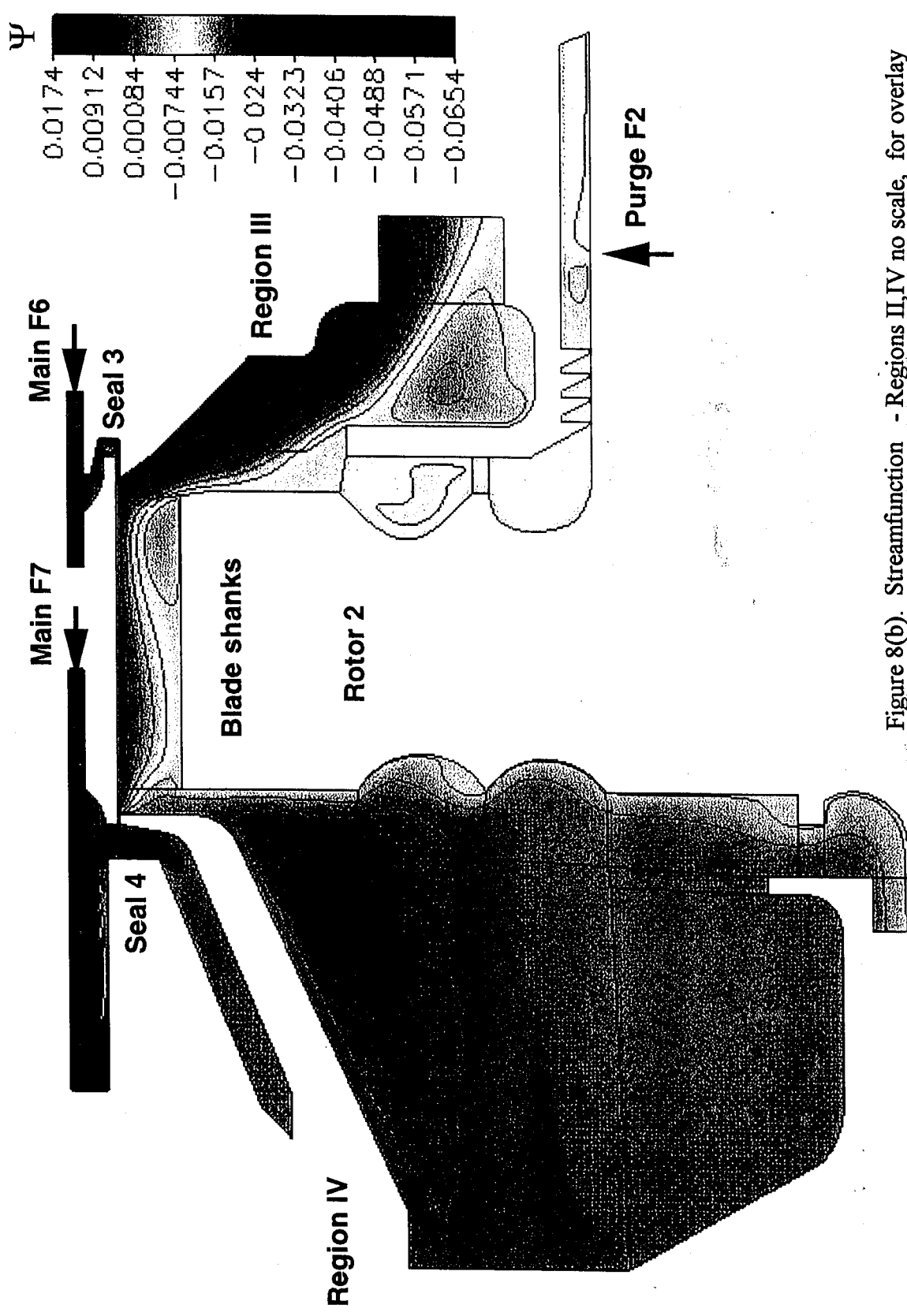


Figure 8(b). Streamfunction - Regions II,IV no scale, for overlay

# Mixture Fraction (Concentrations)

## Computed Values of F1 Concentrations, Run No. 202

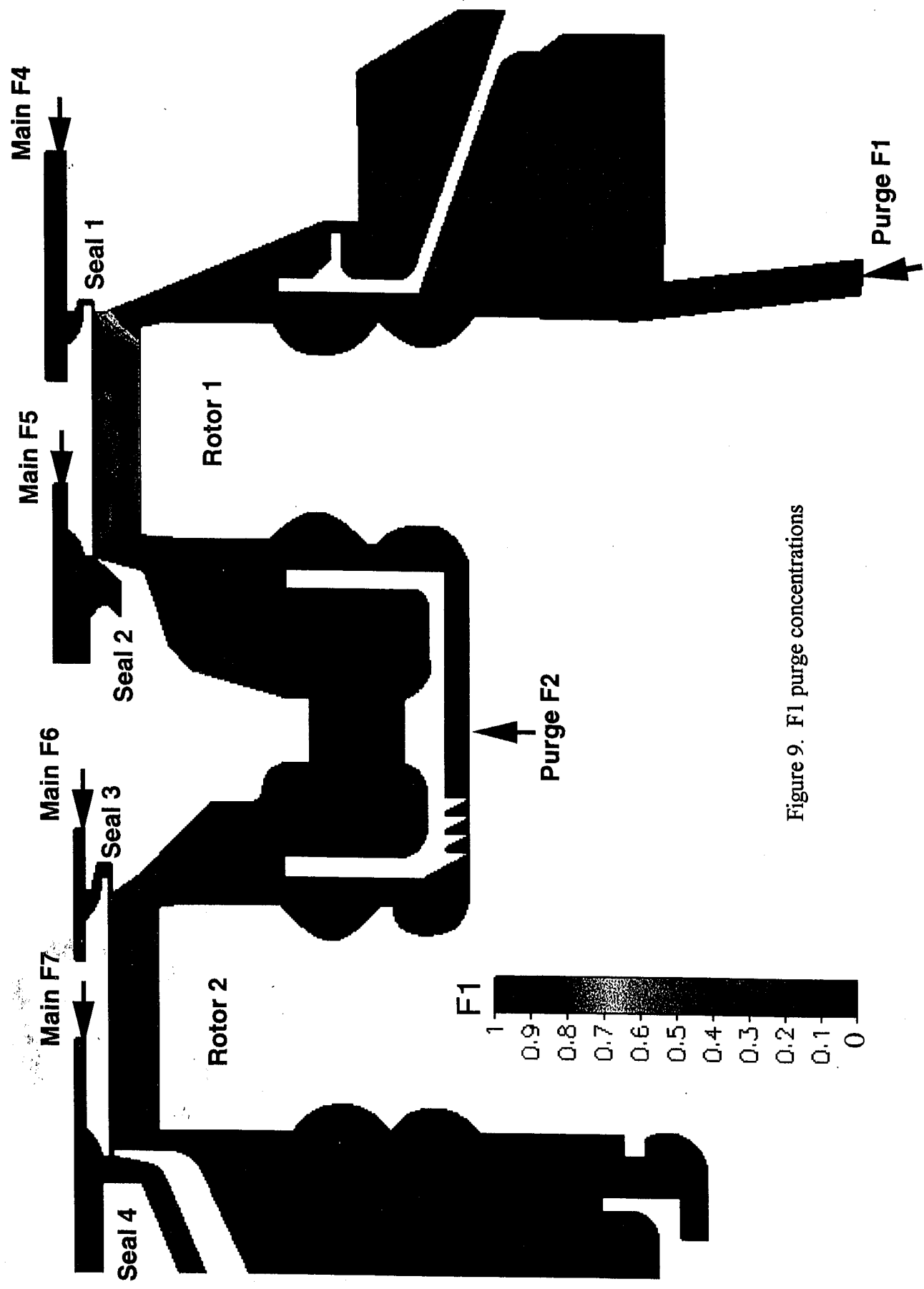


Figure 9. F1 purge concentrations

# Mixture Fraction (Concentrations)

# CFDRC

Computed Values of F4 Concentrations, Run No. 202

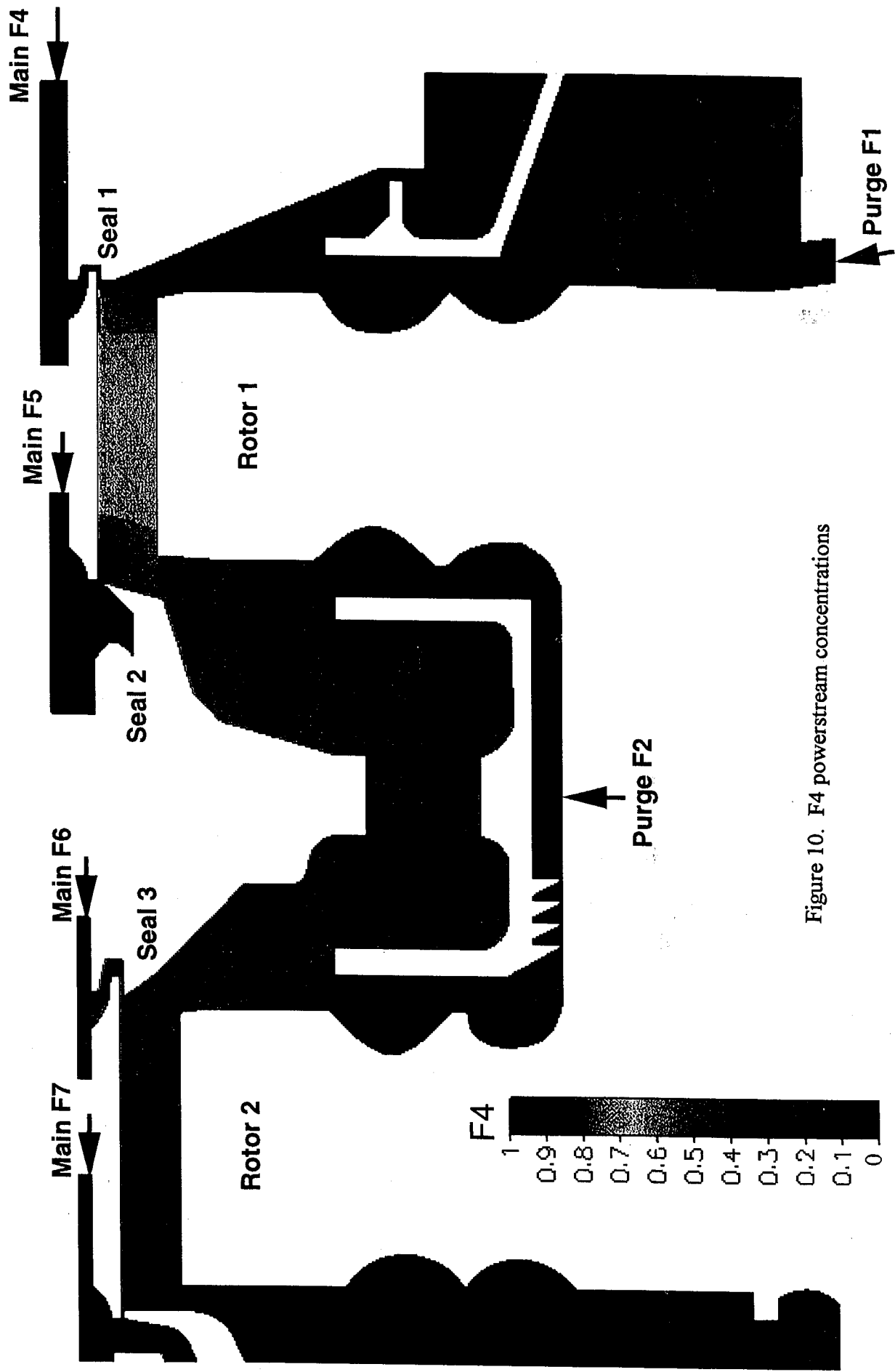
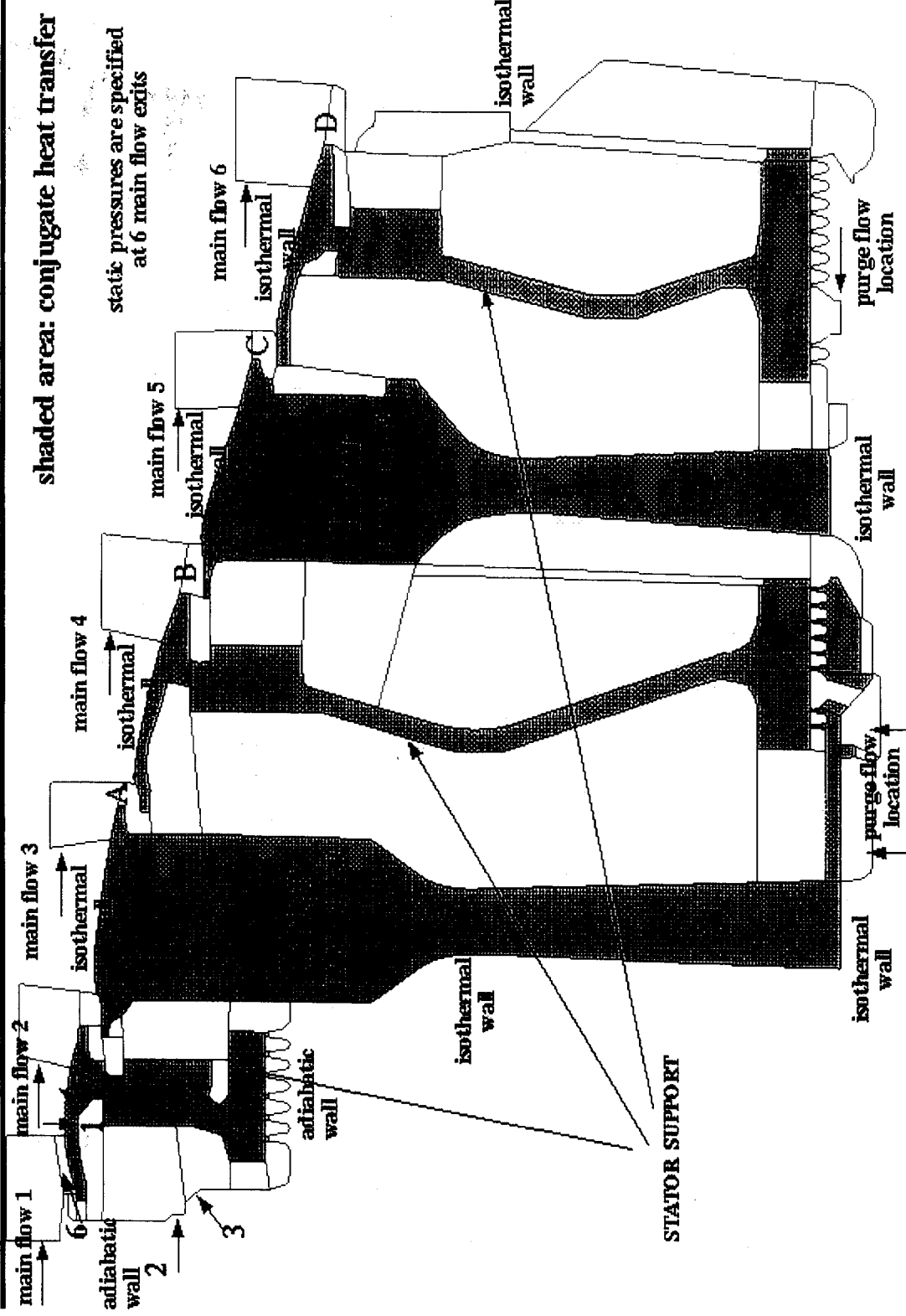


Figure 10. F4 powerstream concentrations

# Allison T56 Engine Turbine Cavities

CFDRC



# SEAL MASS FLOW RATES



- Rim Seal Ingestion Flow Rates is an Important Parameter**
- Computed and Experimental Values Given Below**

(Mass Flow rates in lbs/s)

Run No.	Rim Seal Flows				Specified Purge Flows				
	Seal 1	Seal 2	Seal 3	Seal 4	Forward Cavity	Center Cavity	Aft Cavity	Net, in $\dot{m}$	Net, out $\dot{m}$
<b>102</b>									
numerical	-0.150	-0.072	0.233	0.260	0.1425	0.0637	0.064	0.4923	0.4923
experimental	-0.126	-0.094	0.265	0.208	0.143	0.062	0.066	0.491	0.473
(exp-num)/exp	.19	-.23	.12	-.25	0	-.03	.03	.003	-.04
<b>202</b>									
numerical (18K grid)	-0.236	-0.139	0.286	0.353	0.1168	0.0552	0.0904	0.6374	0.639
numerical (30K grid)	-0.237	-0.126	0.283	0.33	0.1168	0.0552	0.0904	0.6374	0.639
experimental	-0.224	-0.154	0.257	0.271	0.115	0.057	0.087	0.637	0.528
(exp-num)/exp	.05	-.10	-.11	-.30	-.02	.03	.04	0	-.21
<b>205</b>									
numerical	-0.223	-0.1025	0.357	0.381	0.208	0.103	0.0985	0.7351	0.738
experimental	-0.186	-0.113	0.302	0.302	0.208	0.105	0.095	0.707	0.604
(exp-num)/exp	.20	.09	.18	.26	0	.01	.04	.04	.22

$$\text{Net } \dot{m}_{in} = |\text{seal 1}| + |\text{seal 2}| + |\text{all purge flows}|$$

$$\text{Net } \dot{m}_{out} = |\text{seal 3}| + |\text{seal 4}|$$

$$\Delta \dot{m} = (\dot{m}_{in} - \dot{m}_{out})$$

$\Delta \dot{m} > 0$  implies net mass accumulation in apparatus

$$\Delta \dot{m}$$

Run No.	102	202	205
experimental	+ 0.018	+ 0.109	+ 0.103
numerical	- 0.005	- 0.0006	- 0.0029

## ALLISON T-56 TURBINE CAVITIES



- **Several Sets of Simulations**
  - Stage 1-2 cavities with labyrinth seal clearance changes
  - Stage 2-3 and 3-4 cavities with conjugate heat transfer
  - Complete turbine drum with conjugate heat transfer

Panel-11 T56/501D Four stage turbine simulation

- The T56/501D Engine of Allison Engine Company, Rolls Royce Aerospace Group
- Characteristics of the T56/501D Engine
  - \* Pressure Ratio = 14.1
  - \* Mass Flow Rate = 15.7 kg/s
  - \* Engine Speed = 14239 rpm
  - \* Max. Turbine Inlet Temperature = 1364K
- Simulated the Turbine Section of the T56/501D
- Three Interstage Pairs of Disc Cavities and the Interstage Labyrinth Seals with Associated Main-Path Flows
- Purge Flows at 3 Locations for Stage 1-2, Two Purge Flow Locations for Stage 2-3, and One Purge Flow for Stage 3-4
- Conjugate Heat Transfer Predictions of All Stages

## FLOW AND BOUNDARY CONDITIONS

—CFDRc

- Computational Grids
  - A 34-Domain, 8800 cells Grid for Stage 1-2 with 0.012 in. Labyrinth Clearance
  - A 34-Domain, 9500 cells Grid for Stage 1-2 with 0.024 in. Labyrinth Clearance
- Boundary Conditions
  - Main Flow Paths: Specify Inlet gas velocity and temperatures, Constant Static Pressure at the Exits
  - Purge Flows Conditions (Mass, P, and T) are specified at the Appropriate Locations in All Cavities

Panel-13 Flow and boundary conditions for simulation

## FLOW AND BOUNDARY CONDITIONS

**CFDR<sup>C</sup>**

- 2-D, Axisymmetric Flow Model
- Compressible Flow
- Air is the Working Fluid with Sutherland's Viscosity Law to Account for Variations in the Viscosity due to Temperature
- Central-Differencing with 10 % Damping (upwinding) for the Convective Fluxes in the Momentum Eqn.
- Standard K- $\epsilon$  Turbulence Model with Wall Functions

Panel-14 Modeling parameters

- Computational Grid

- a 140 domain, 91000 cells grid

- Boundary Conditions

- main flow paths: specify inlet gas velocity and temperatures, constant static pressure at the exits
- purge flows conditions (mass, P and T) are specified at the appropriate locations in all cavities
- conjugate heat transfer predictions of stages 1-2, 2-3, and 3-4; do not require BC at the fluid-solid interfaces
- outer walls of stage 1-2 assumed to be adiabatic; all other walls are assumed to be adiabatic

# COMPARISON OF ANALYSIS AND DESIGN DATA

## Stage 1-2 Cavities

Path No.	Design		Prediction (include conjugate heat transfer for solid parts)		Prediction (Without Conjugate Heat Transfer for Stage 1-2 and Rotors)	
	Massflow (kg/s)	Temperature (K)	Massflow (kg/s)	Temperature (K)	Massflow W (kg/s)	Temperature (K)
4	0.1129	843	0.1284	870	0.1397	829
5	0.0186	843	0.0249	984	0.0136	827
6	0.0449	843	0.0481	893	0.0431	866

## Stage 2-3 and 3-4

Panel-16 Comparison of numerical and design data for T56-501D four stage turbine

Locations (Center of Leakage Path)	Prediction for Stage 2-3 and 3-4 (Include Conjugate Heat Transfer for All Solid Parts)				Prediction for Stage 2-3 and 3-4 (Without Conjugate Heat Transfer for Stage 1-2 and Rotors)				
	Mass (kg/s)	Pressure (Pa)*x10 <sup>5</sup>	Temperature (K)	Mass (kg/s)	Pressure (Pa)*x10 <sup>5</sup>	Temperature (K)	Mass (kg/s)	Pressure (Pa)*x10 <sup>5</sup>	Temperature (K)
A	0.0567	3.309	741	0.0390	3.282	790	0.0376	3.275	786
B	0.0376	2.137	698	0.0522	2.089	794	0.0540	2.068	716
C	0.0340	1.724	705	0.0249	1.682	769	0.0240	1.689	700
D	0.0209	1.103	703	0.0263	1.082	732	0.0272	1.069	666

# CEDRC

## Stream Function

### Stage 1-2 Disk Cavities

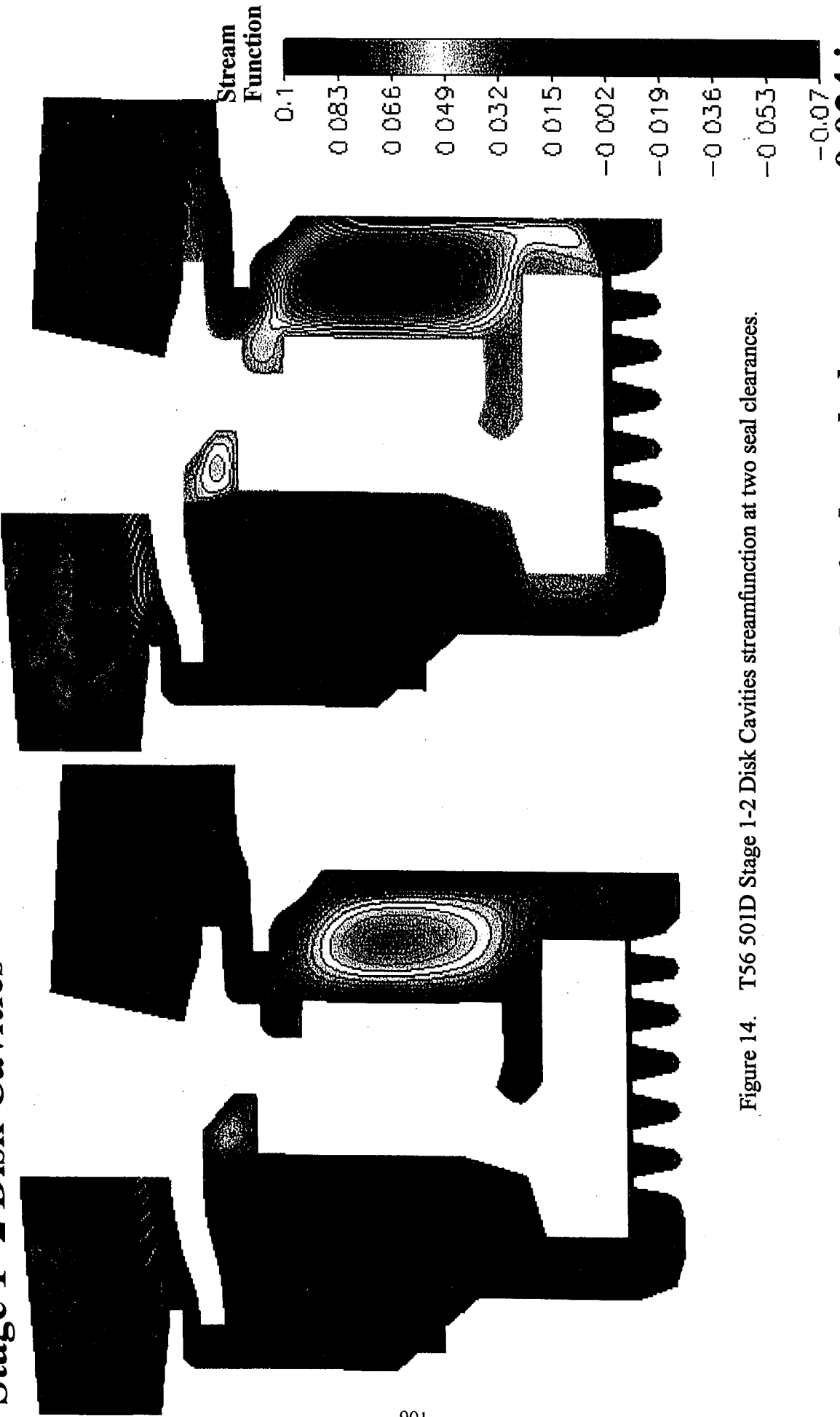


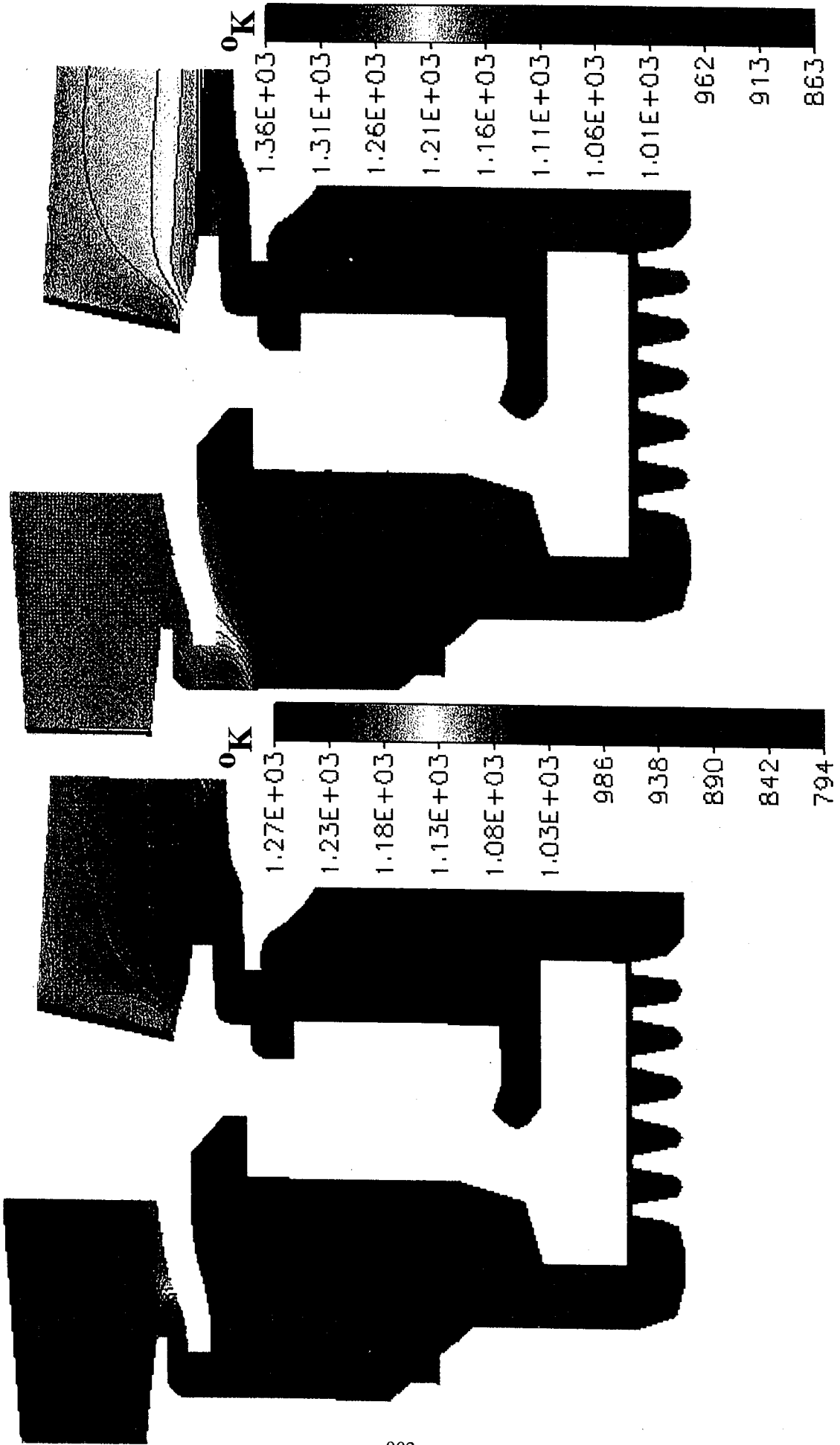
Figure 14. T56 501D Stage 1-2 Disk Cavities streamfunction at two seal clearances.

**Labyrinth seal clearance = 0.012 in**    **Labyrinth seal clearance = 0.024 in**

**Note:** The magnitude is greater than 0.1 in the free stream region (red color with no contours)

# Temperature

## Stage 1-2 Disk Cavities



Labyrinth seal clearance = 0.012 in      Labyrinth seal clearance = 0.024 in

Figure 15. T56 501D Stage 1-2 Disk Cavities temperature at two seal clearances

# Comparison of Analysis and Design Data

CFDRC

## Stage 1-2 Disc Cavities

(a) Labyrinth Seal Clearance=0.012 in.

Path No.	Design		Prediction	
	Massflow (lb/s)	Temp (°F)	Massflow (lb/s)	Temp (°F)
4	0.249	1058	0.308	1032
5	0.041	1058	0.030	1029
6	0.099	1058	0.095	1100

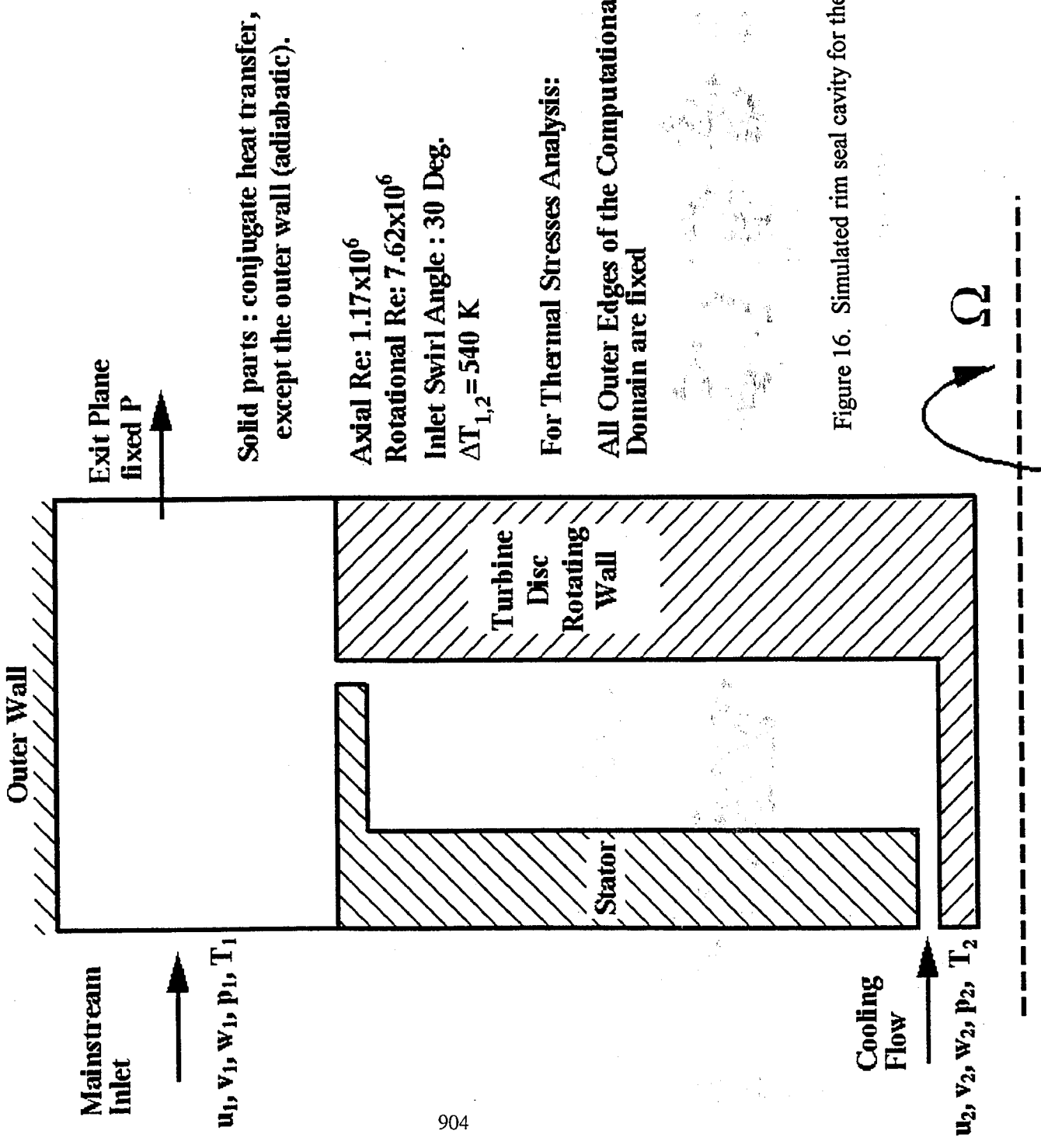
(b) Labyrinth Seal Clearance=0.024 in.

Path No.	Design		Prediction	
	Massflow (lb/s)	Temp (°F)	Massflow (lb/s)	Temp (°F)
4	0.510	1223	0.610	1315
5	0.038	1223	0.041	1148
6	-0.153	1691	-0.220	1830

Panel-17 Comparison of numerical and design data for clearance of 0.012-inch and 0.024-inch.

# Flow and Thermal Stresses Interaction CFDRC

## Problem Description



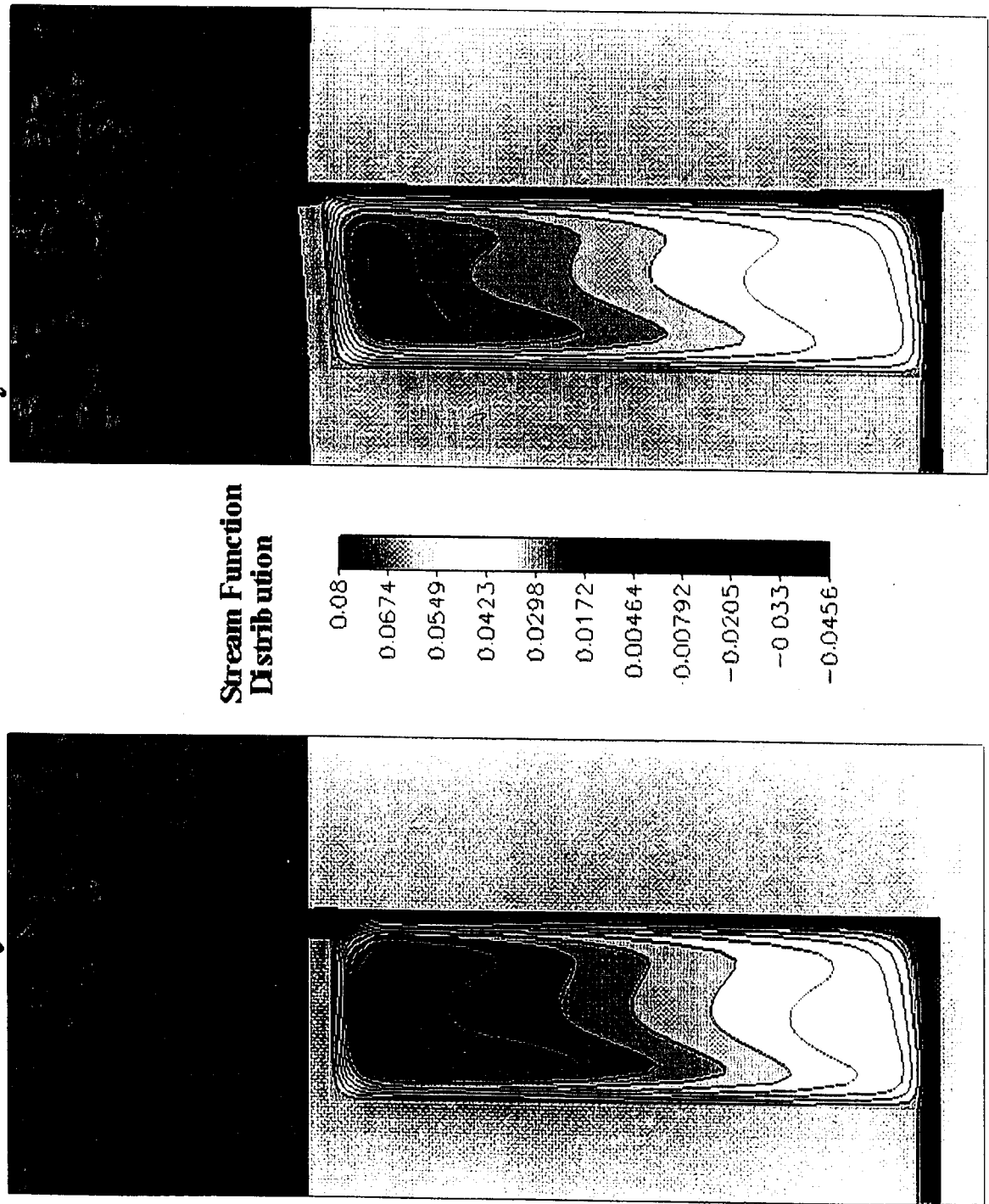
# Streamfunction

# CFDRC

Figure 17. Simulated rim seal cavity thermomechanical behavior- streamfunction

Flow Simulation  
with Deformation  
by Thermal Stresses

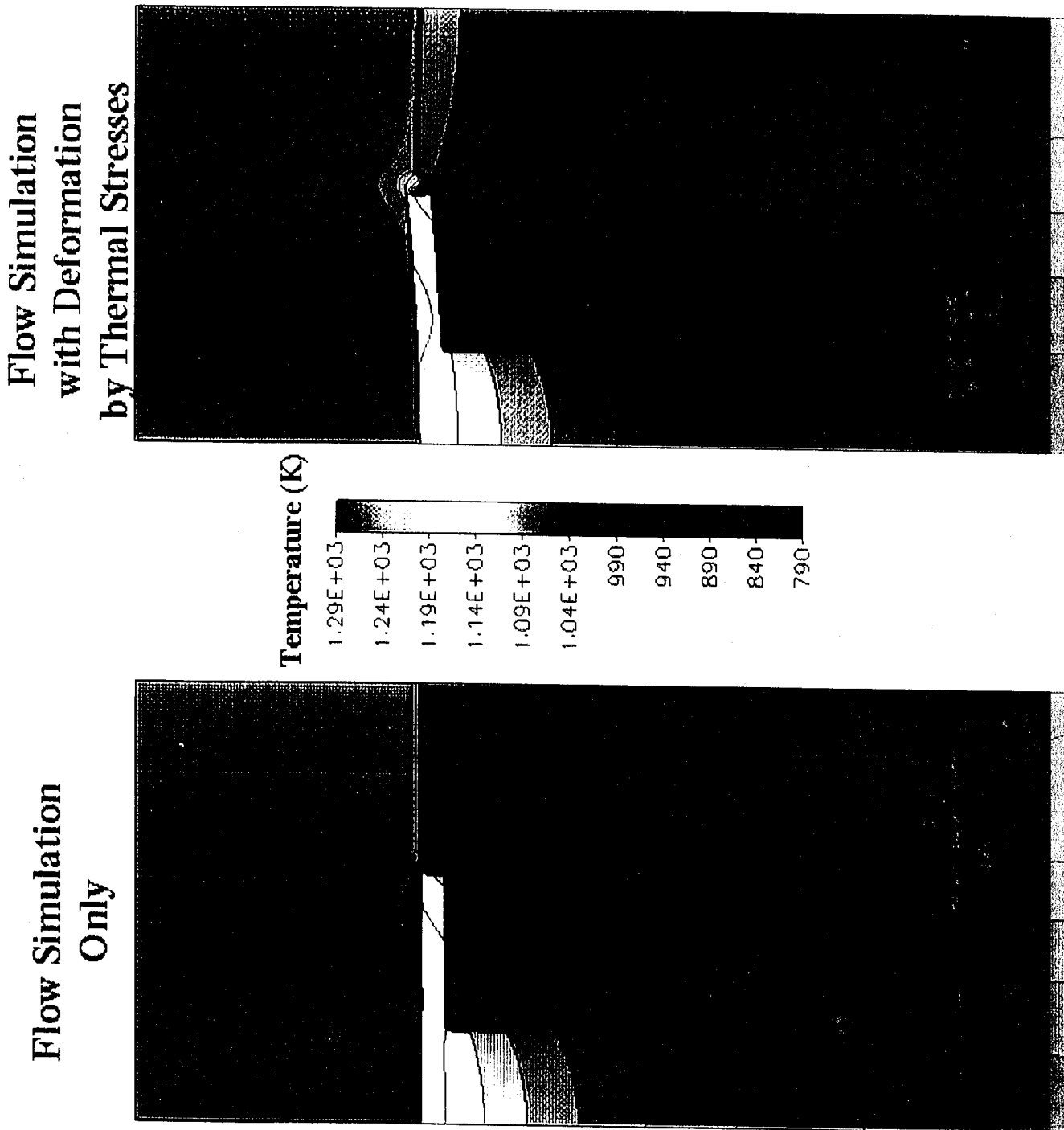
Flow Simulation  
Only



# Temperatures

# CFDRC

Figure 18. Simulated rim seal cavity for thermomechanical behavior - temperatures



## RIM SEAL INGESTION COMPUTATIONS

---



- Variation of Cooling Effectiveness due to Purge Mass Flow
- Fixed Inlet Swirl Reynolds Number
- Four Configurations Tested (reported by UTRC in AFWAL-TR-87-2050, Sept. 1987)
- Each Configuration Tested at Two Purge Flow Rates
- Ingestion Experiments Simulated Using Passive Scalar Transport of Inert Species

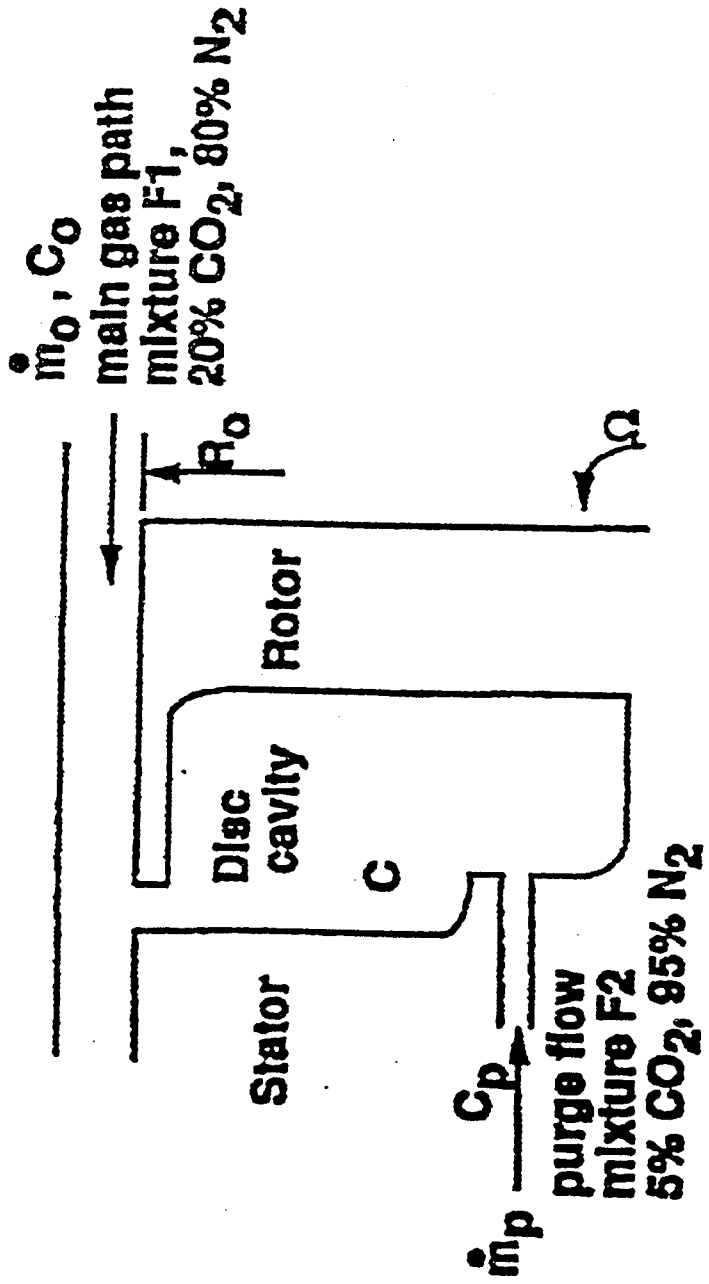
## COMPUTATIONAL CONDITION

CFDRC

- Two Purge Flow Rates  $\eta_t = 1 \times 10^{-3}, 8 \times 10^{-3}$
- Rotor Speed - 2450 rpm,  $Re_t = 5.0 \times 10^5$
- Inlet Swirl = Rotor Tangential Velocity
- Axial Velocity Range 120-150 m/s for the Four Configurations
- Computational Grids:
  - 50-60 cells in axial direction
  - 60-70 cells in radial direction

# Disc Cavity and Rim Seal Apparatus and Notation

Figure 19. UTRC data- four rim seal configurations



$$\eta_t = \text{nondimensional purge mass flow} = \left( \frac{\dot{m}_p}{4\pi\mu R_o} \right) (Re_t)^{-0.8}$$

$$\phi = \text{cooling effectiveness} = \frac{C_p - C_o}{C_p - C_o}$$

$$Re_t = \text{tangential Reynolds number} = \frac{\Omega R_o^2}{V}$$

# Calculated Velocity Vectors: All Configuration

$$\eta = 10^{-3} \text{ and } \eta = 8 \times 10^{-3}$$

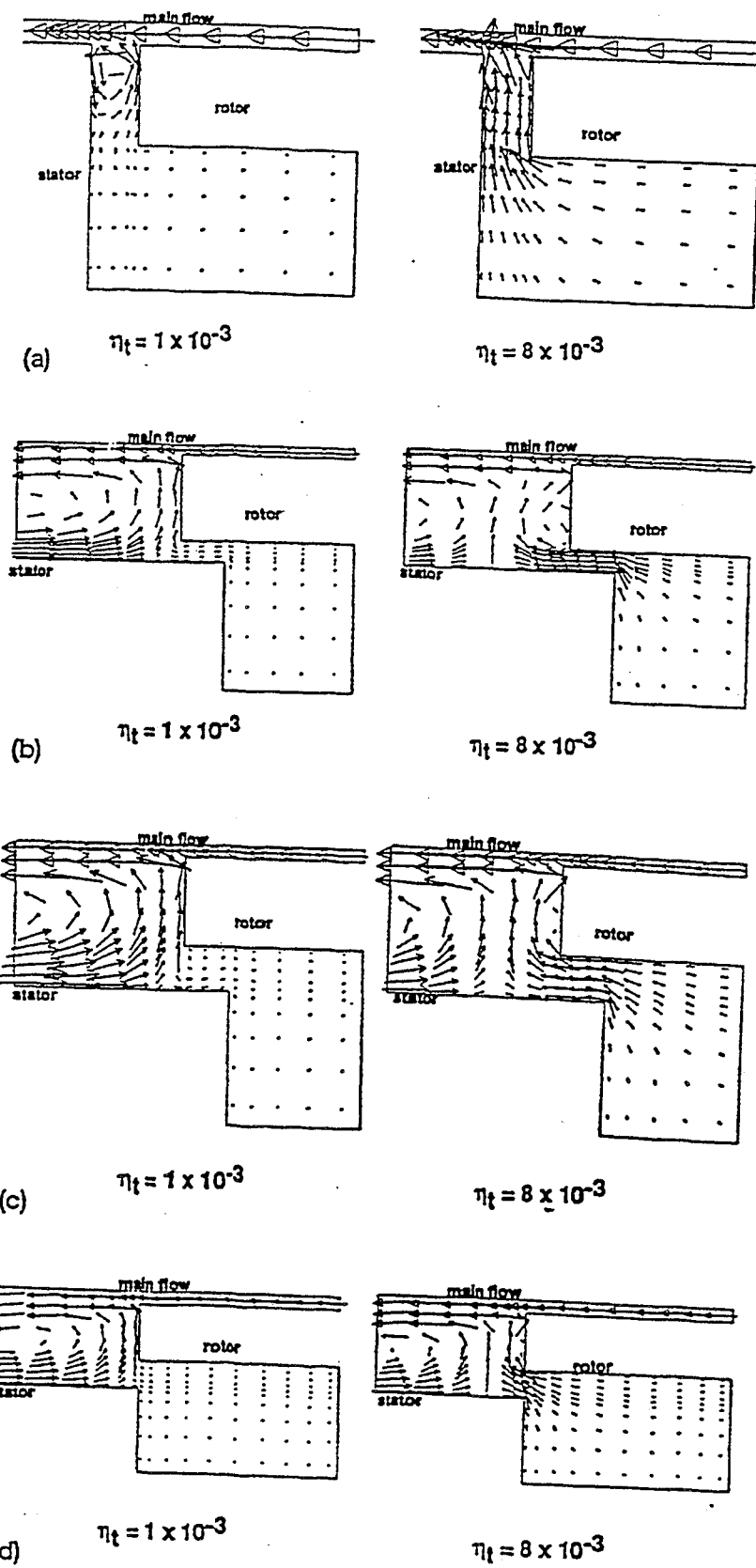


Figure 20. UTRC data- four rim seal configurations - velocity vectors.

# Comparison of Calculated and Experimental Data All Configurations

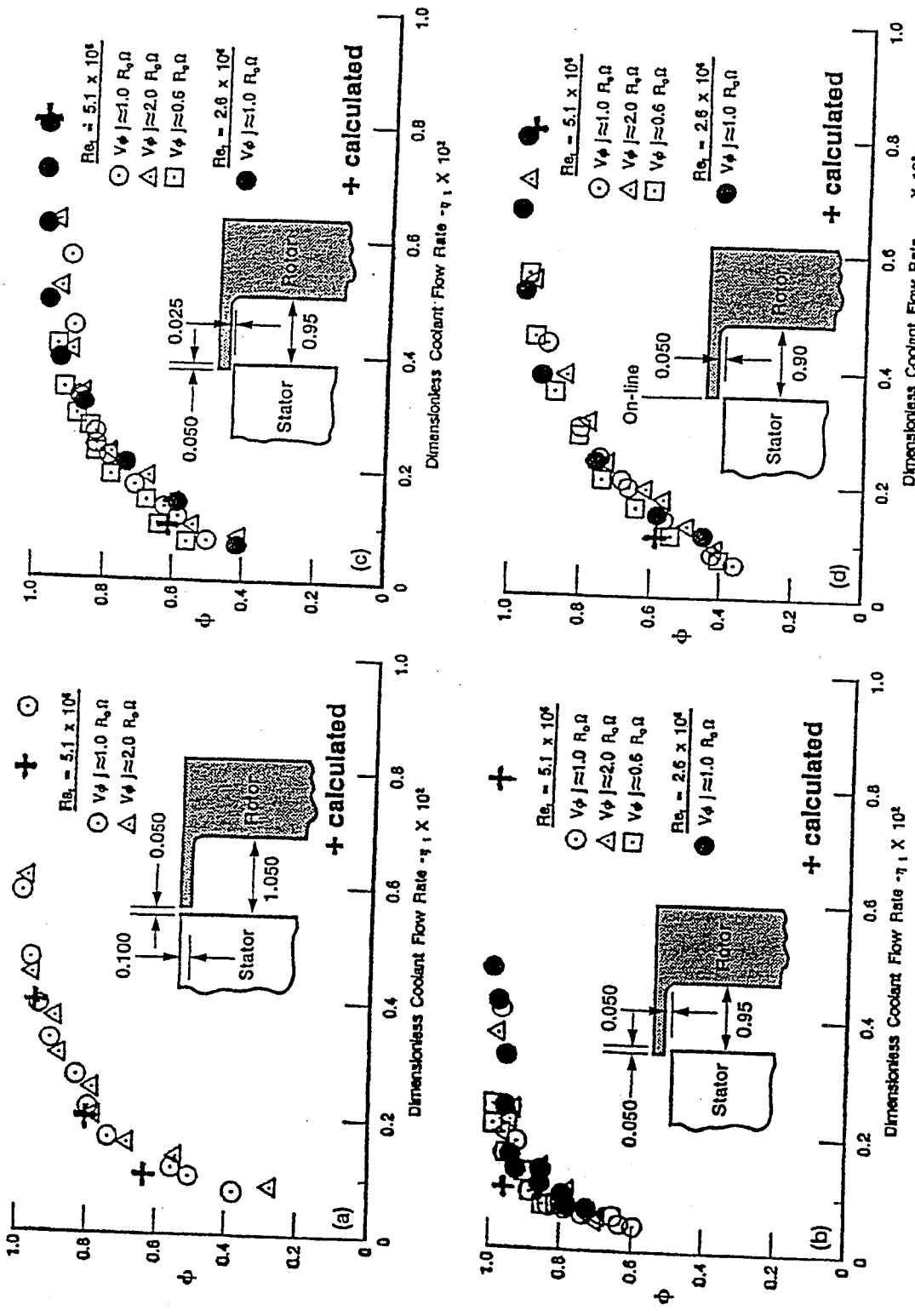


Figure 21. UTRC data- four rim seal configurations - numerical/data comparison.

# Comparison of Calculated and Experimental Data All Configurations

Deviation in Percent

[Cooling effectiveness parameter,  $\phi^a$ ;  $Re_f = 5.0 \times 10^6$ ,  $V_{\phi f} \approx R\Omega$ .]

Configuration	Dimensionless coolant flow parameter, $\eta_c$	$\phi$ experimental <sup>b</sup>	$\phi$ calculated	Deviation, percent
1	0.001	0.53	0.63	19
	.002	.77	.802	4
	.004	.94	.972	3
	.008	1	.997	-0.3
2	0.001	0.89	0.95	7
	.008		.99	---
3	0.001	0.57	0.611	7
	.008	.98	.99	1
4	0.001	0.5	0.589	18
	.008	.98	.965	-2

<sup>a</sup>Numerical results computed using assumed main-flow conditions with axial velocity ranging from 120 to 150 m/s.  
<sup>b</sup>Experimental data from Gruber et al. [1987].

STRM CONTOURS  
 FMIN -1.172E-02  
 FMAX 1.466E+00  
 CONTOUR LEVELS

1	-1.170E-02
2	7.111E-04
3	1.312E-02
4	2.553E-02
5	3.794E-02
6	5.035E-02
7	6.277E-02
8	7.518E-02
9	8.759E-02
10	1.000E-01
11	1.000E+00
12	2.000E+00

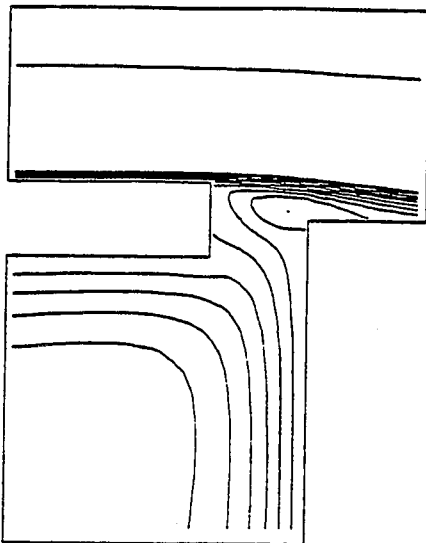


Figure Enlarged View of Streamlines Near the Disk Tip

STRM CONTOURS  
 FMIN -3.177E-02  
 FMAX 1.344E+00  
 CONTOUR LEVELS

1	-3.170E-02
2	-2.477E-02
3	-1.784E-02
4	-1.091E-02
5	-3.974E-03
6	2.555E-03
7	9.889E-03
8	1.682E-02
9	2.375E-02
10	3.068E-02
11	3.752E-02
12	4.435E-02
13	5.118E-02
14	5.841E-02
15	6.534E-02
22	2.000E+00

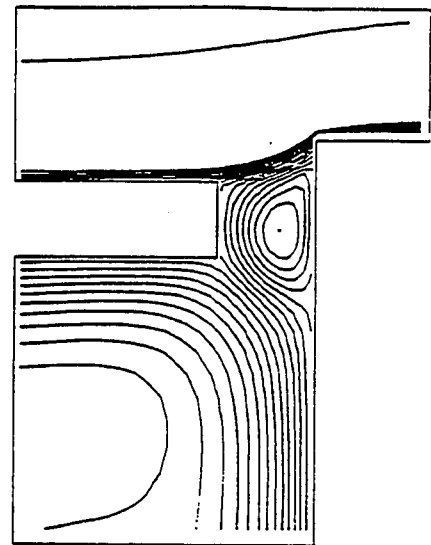


Figure Enlarged View of Streamlines Near the Disk Tip

TEMP CONTOURS  
 FMIN 9.872E+02  
 FMAX 1.235E+03  
 CONTOUR LEVELS

1	9.000E+02
2	9.367E+02
3	9.733E+02
4	1.010E+03
5	1.047E+03
6	1.083E+03
7	1.120E+03
8	1.157E+03
9	1.193E+03
10	1.230E+03

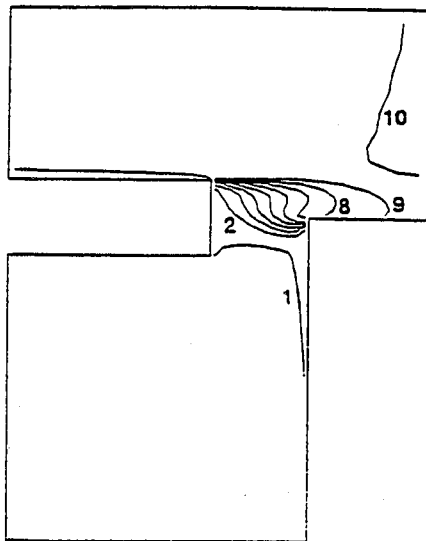


Figure Enlarged View of the Isotherms Near the Disk Tip

TEMP CONTOURS  
 FMIN 9.189E+02  
 FMAX 1.256E+03  
 CONTOUR LEVELS

1	9.367E+02
2	9.733E+02
3	1.010E+03
4	1.047E+03
5	1.083E+03
6	1.120E+03
7	1.157E+03
8	1.193E+03
9	1.230E+03

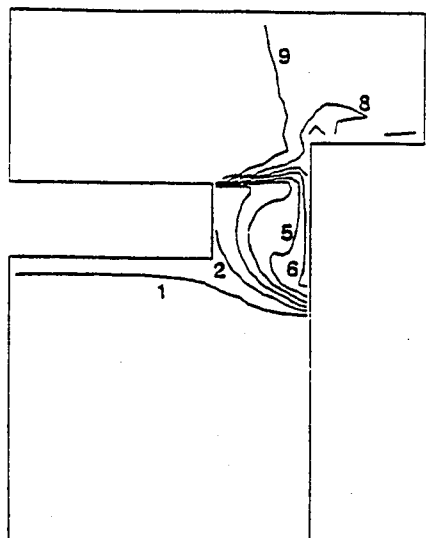


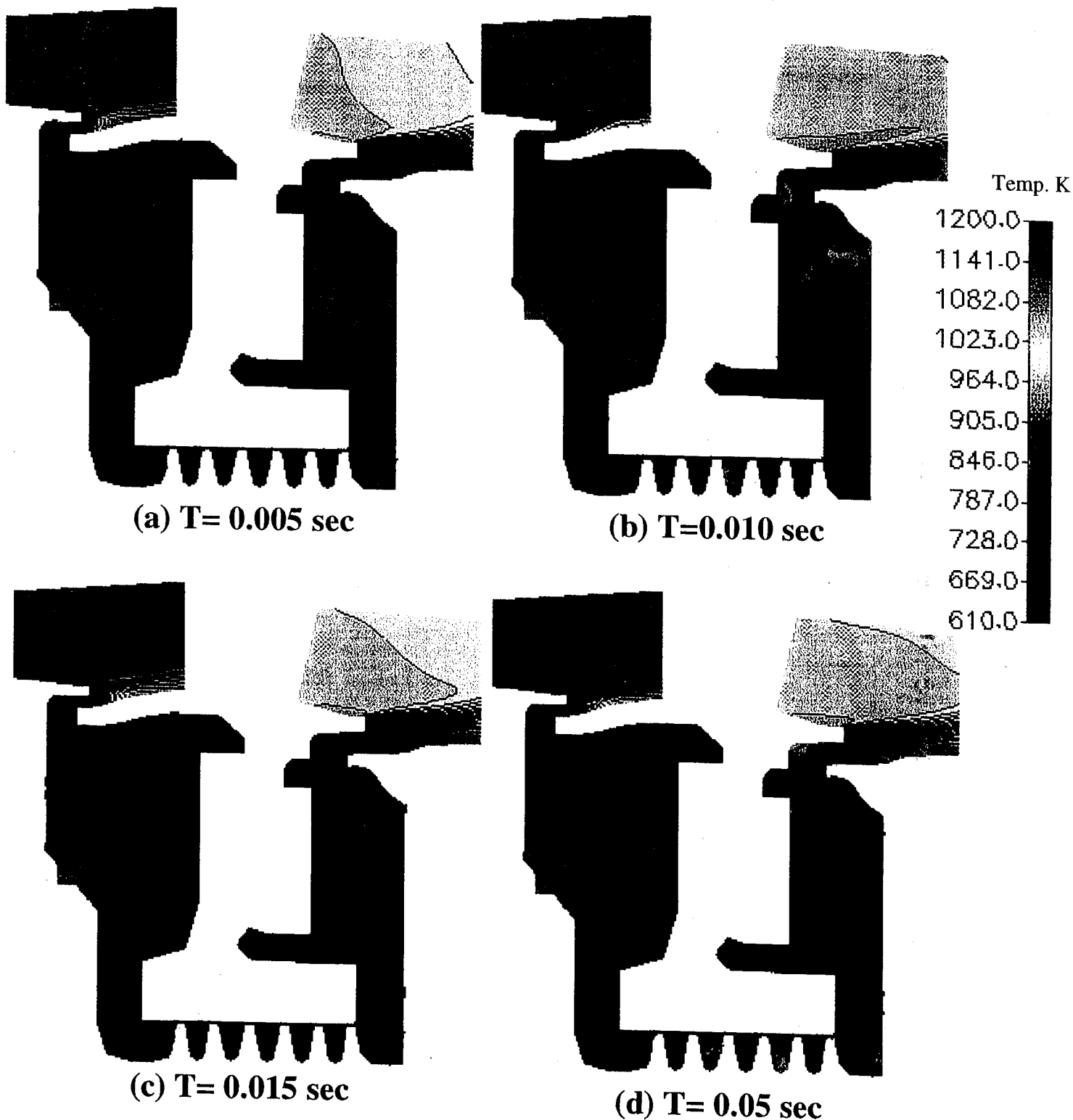
Figure Enlarged View of the Isotherms near the Disk Tip

Figure 22. Displace rotor rim-seal temperature effects.

# Temperature Distribution

CFDRC

High-Speed Ground Idle to Takeoff Conditions with  
Simple Step Jump Approach



## Combined Turbine Stage and Rim Seal Grids

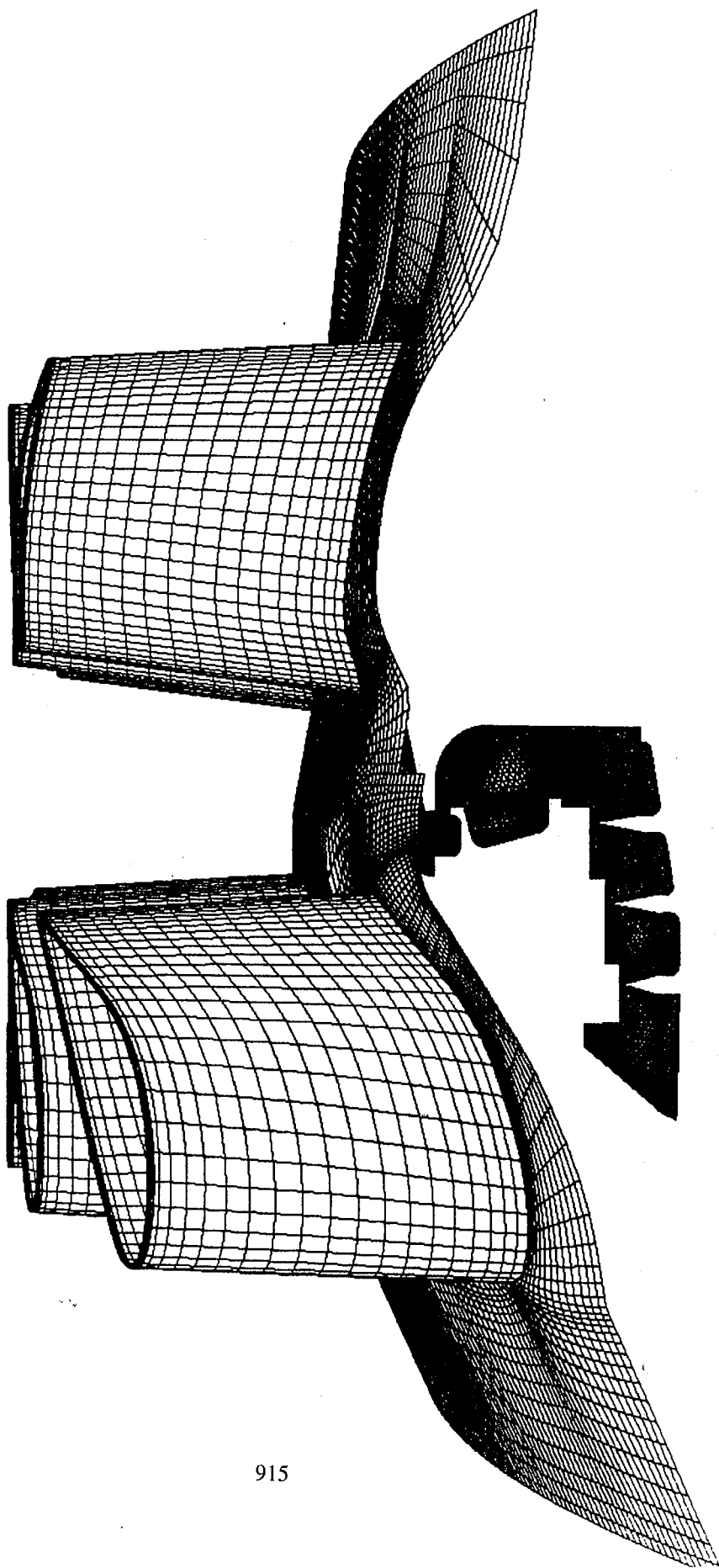
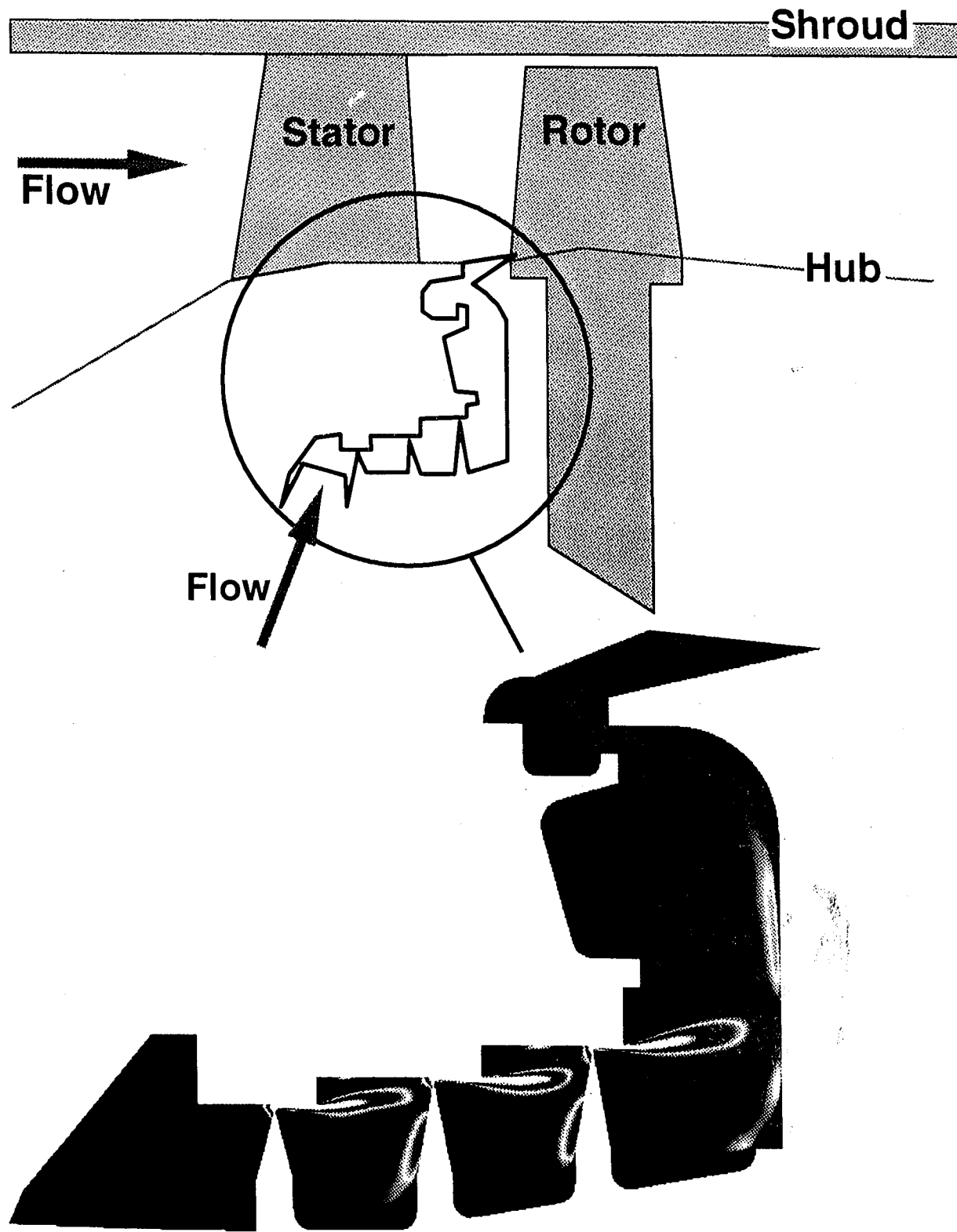


Figure 23. UTRC cavity flow (Hah)- grid



## Mach-Number Contours inside Rim-Seal Geometry

Figure 24. UTRC cavity flow (Hah)- Mach number

Instantaneous Pressure Distribution

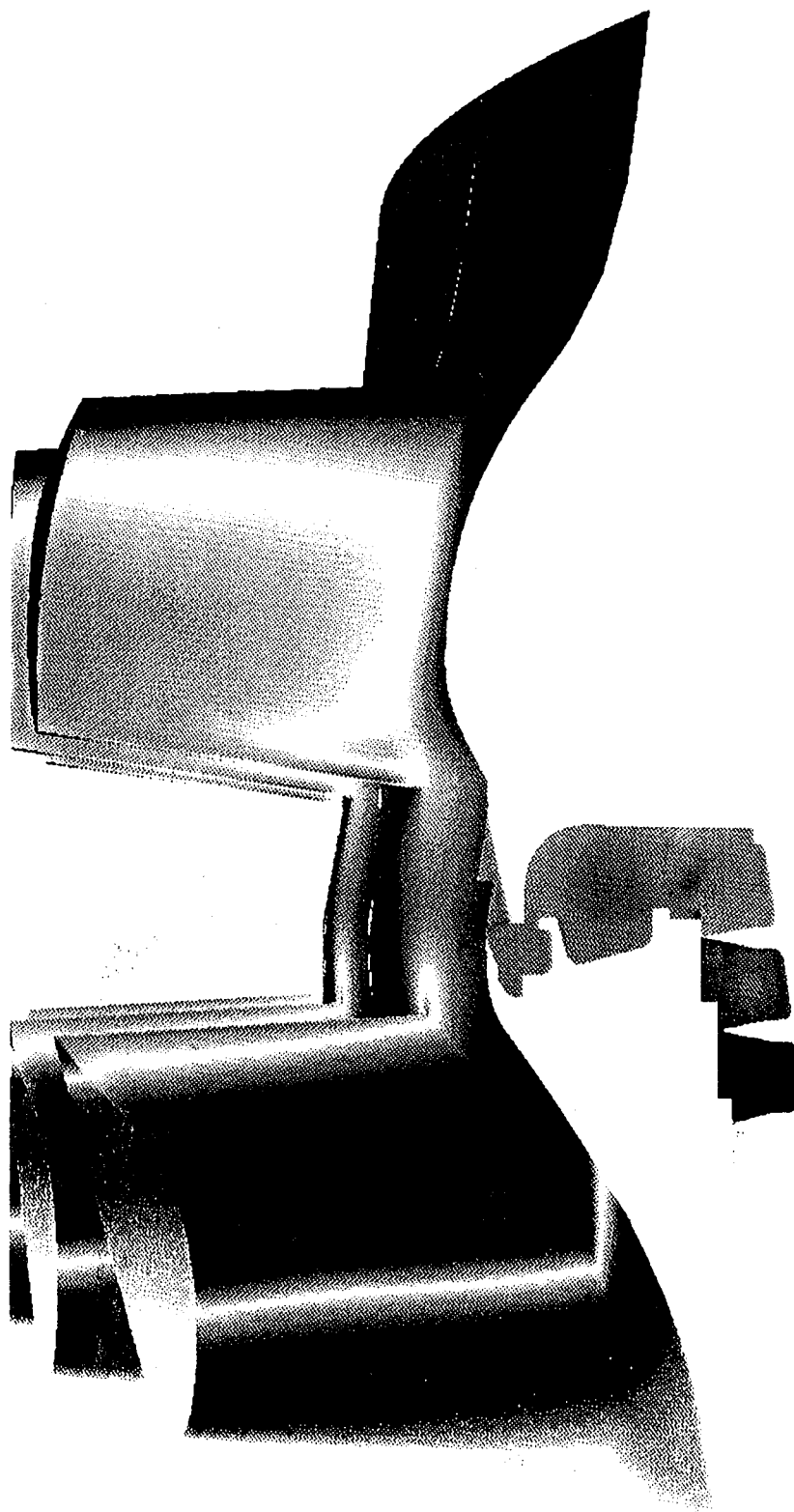
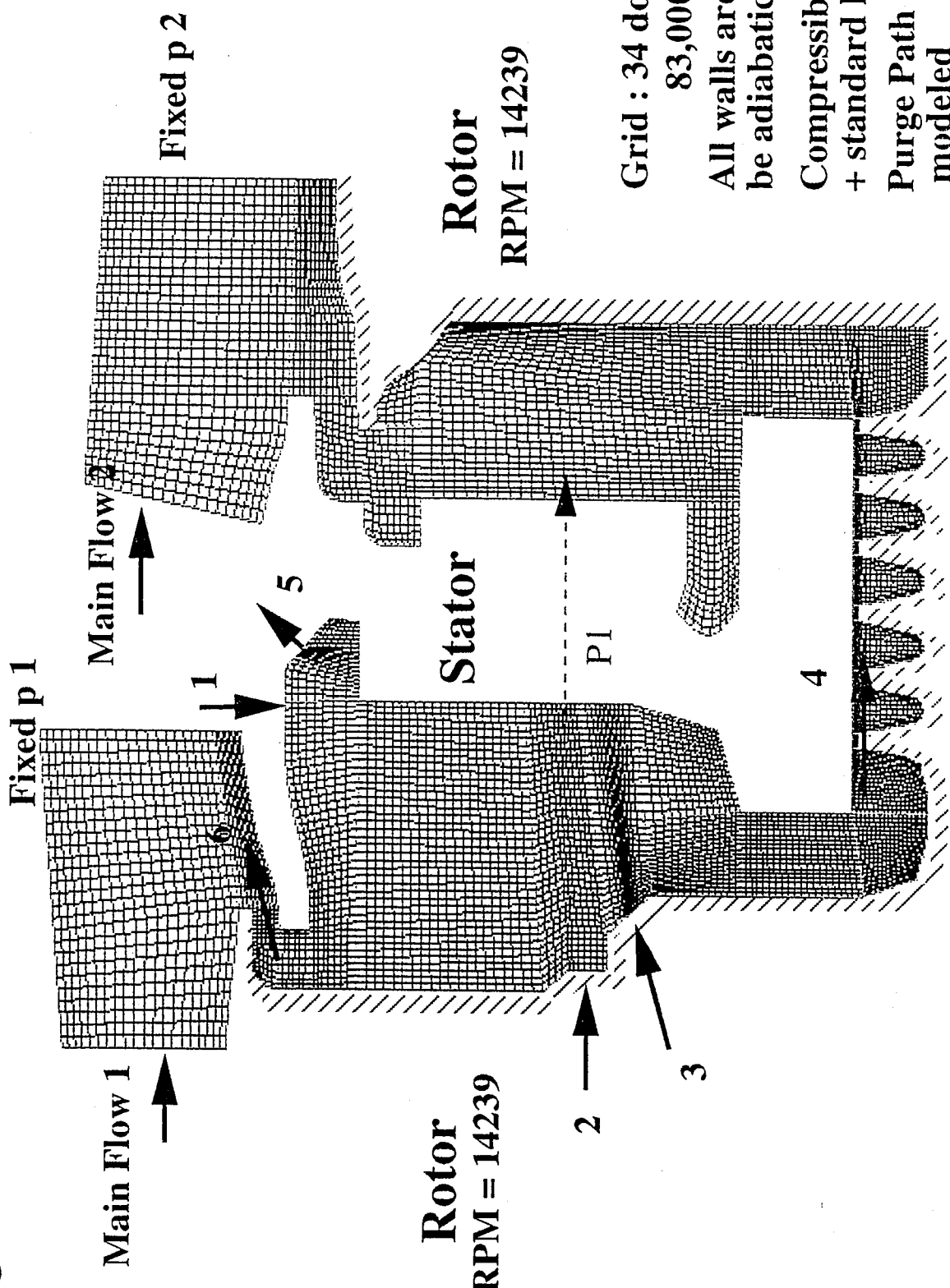


Figure 25. UTRC cavity flow (Hah)- pressure

# CEDRC

## Allison T56 Engine Turbine Cavity

### Stage 1-2 Disk Cavities



Labyrinth seal clearance is 0.012 in

Figure 26. T56-501D 1-2 Disc Cavity grid

# Temperature Distribution

CFDRC

High-Speed Ground Idle to Takeoff Conditions with  
Simple Step Jump Approach

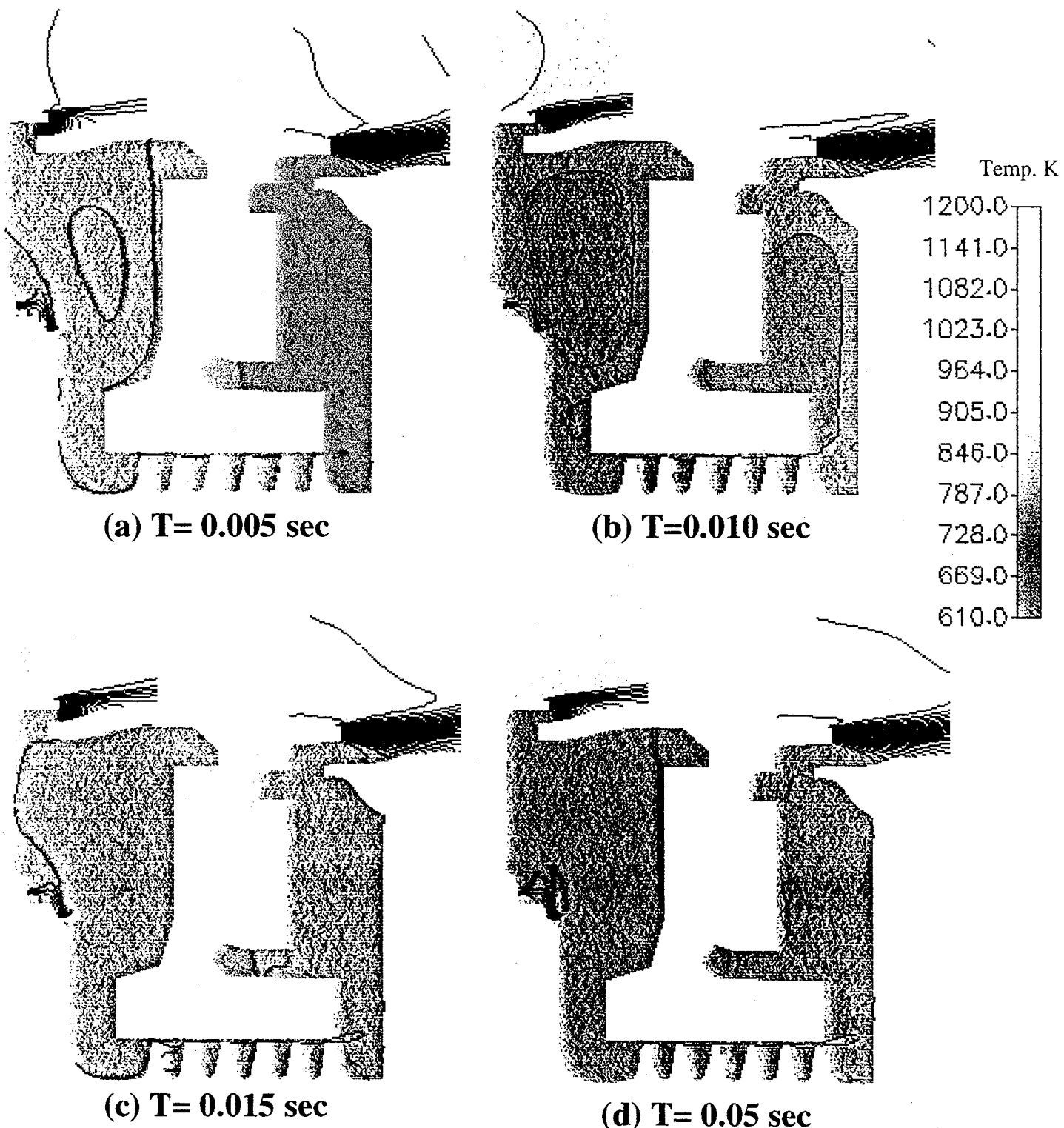


Figure 27. T56-501D 1-2 Disc Cavity -step jump - thermal effects

## Whirling Annular Seal

### Geometry

- $L = 37.3 \text{ mm}$
- $R = 82.05 \text{ mm}$
- $C = 1.27 \text{ mm}$

### Typical Test Condition

- $\text{rpm} = 3600$
- $\text{Reynolds No} = 24\ 000 \ (\text{Uav} = 7 \text{ m/s})$
- $\text{Taylor No} = 6600$
- Test fluid: water

### Grid

- 40 and 20 axial
- 16 and 30 radial
- 20 circumferential

### Data

- 3-D color laser
- Pressure
- Reynolds stress
- Turbulence KE

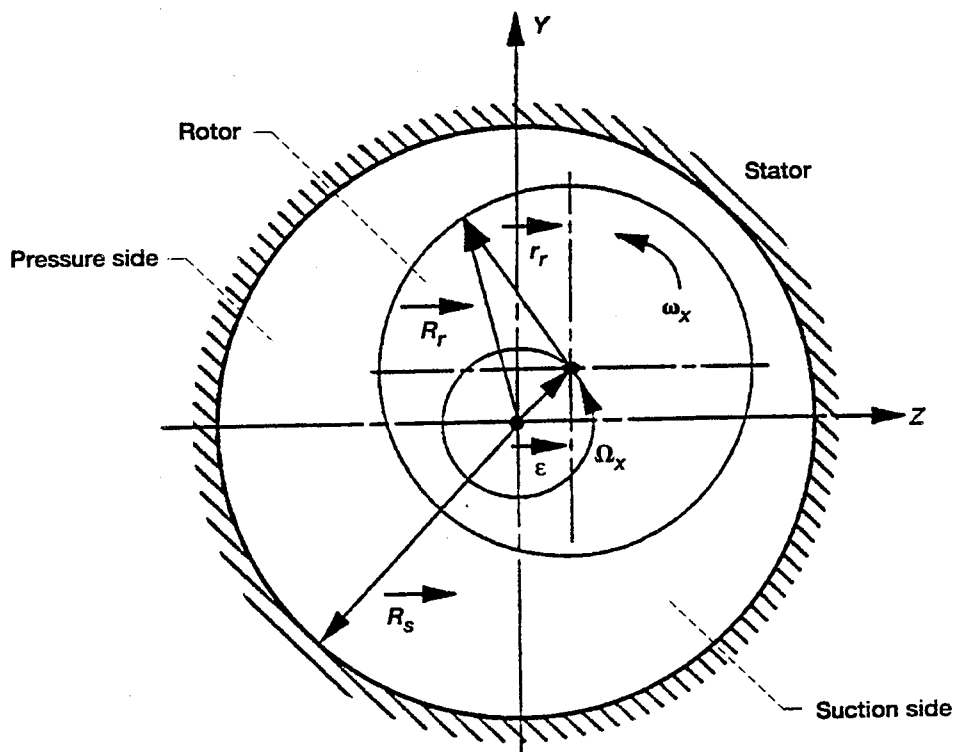


Figure —Details of annular seal with whirling rotor. Axial flow and x axis point into plane of paper.

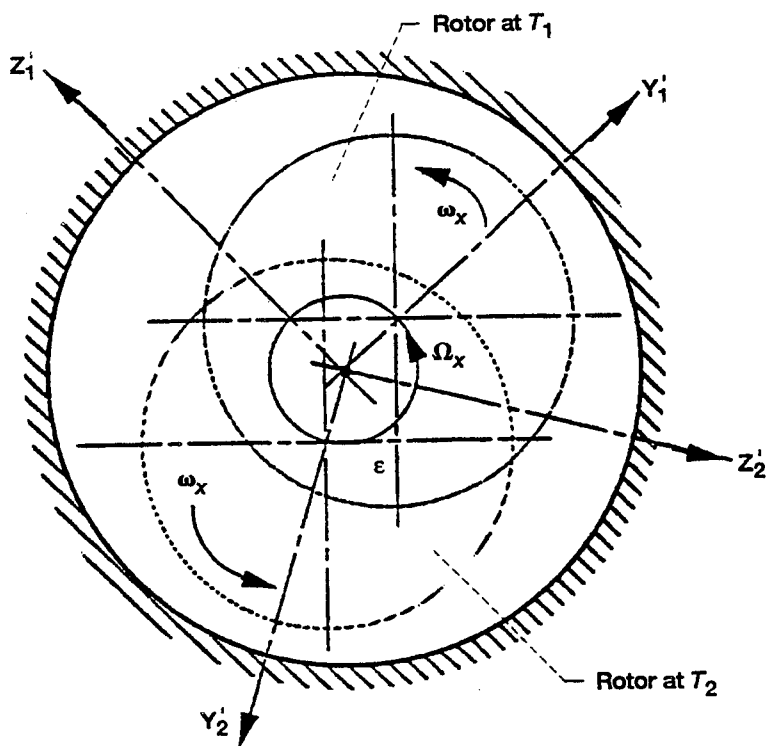


Figure —Rotor positions and associated coordinate frames at two different times,  $T_1, T_2$ .

Figure 28. Whirling annular seal geometry and transformation

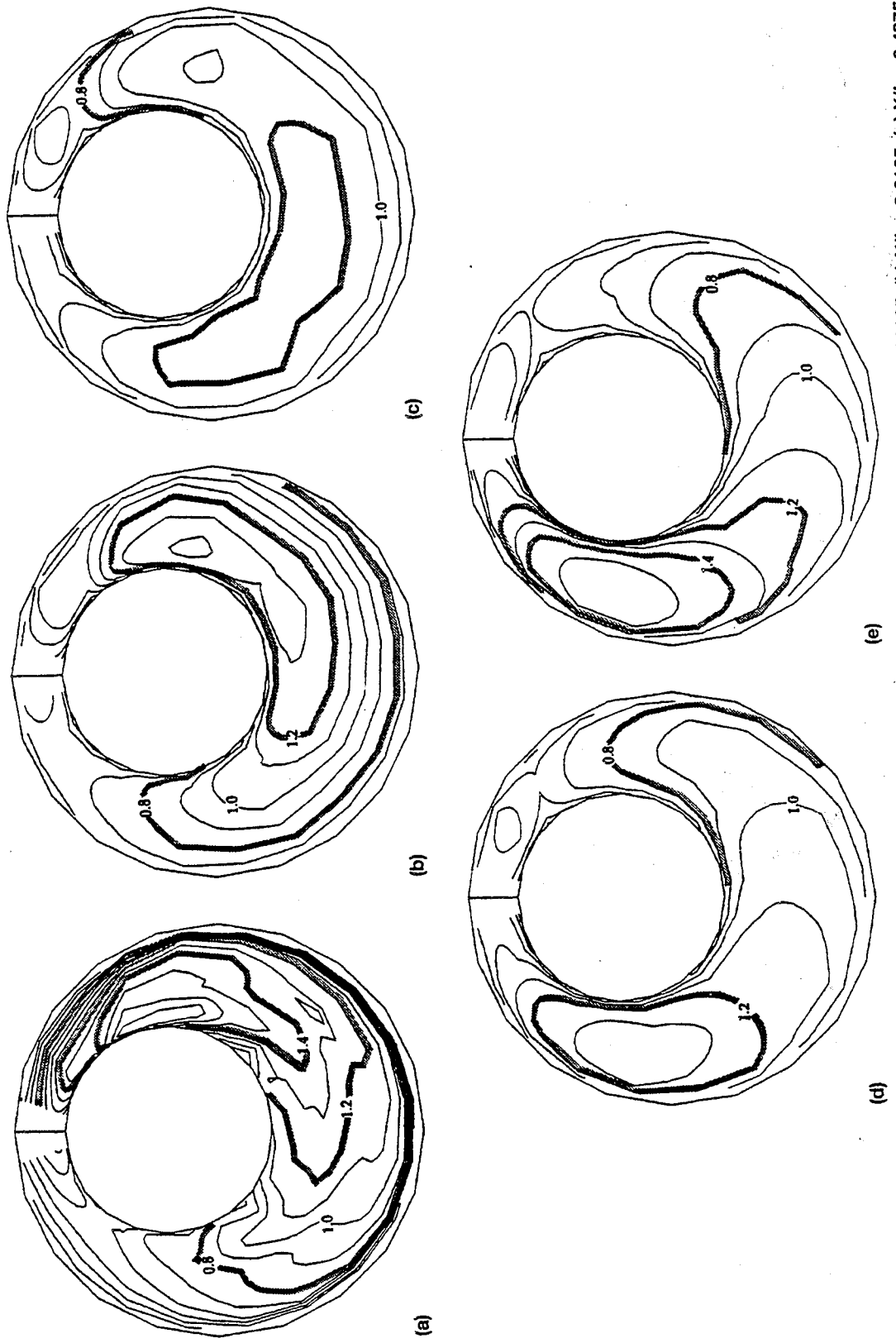


Figure 29. Whirling annular seal normalized axial velocity contours- numerical  
 (a)  $X/L = 0.00125$ . (b)  $X/L = 0.2125$ . (c)  $X/L = 0.4875$ .  
 (d)  $X/L = 0.7625$ . (e)  $X/L = 0.9825$ .

Figure 29. Whirling annular seal normalized axial velocity contours- numerical

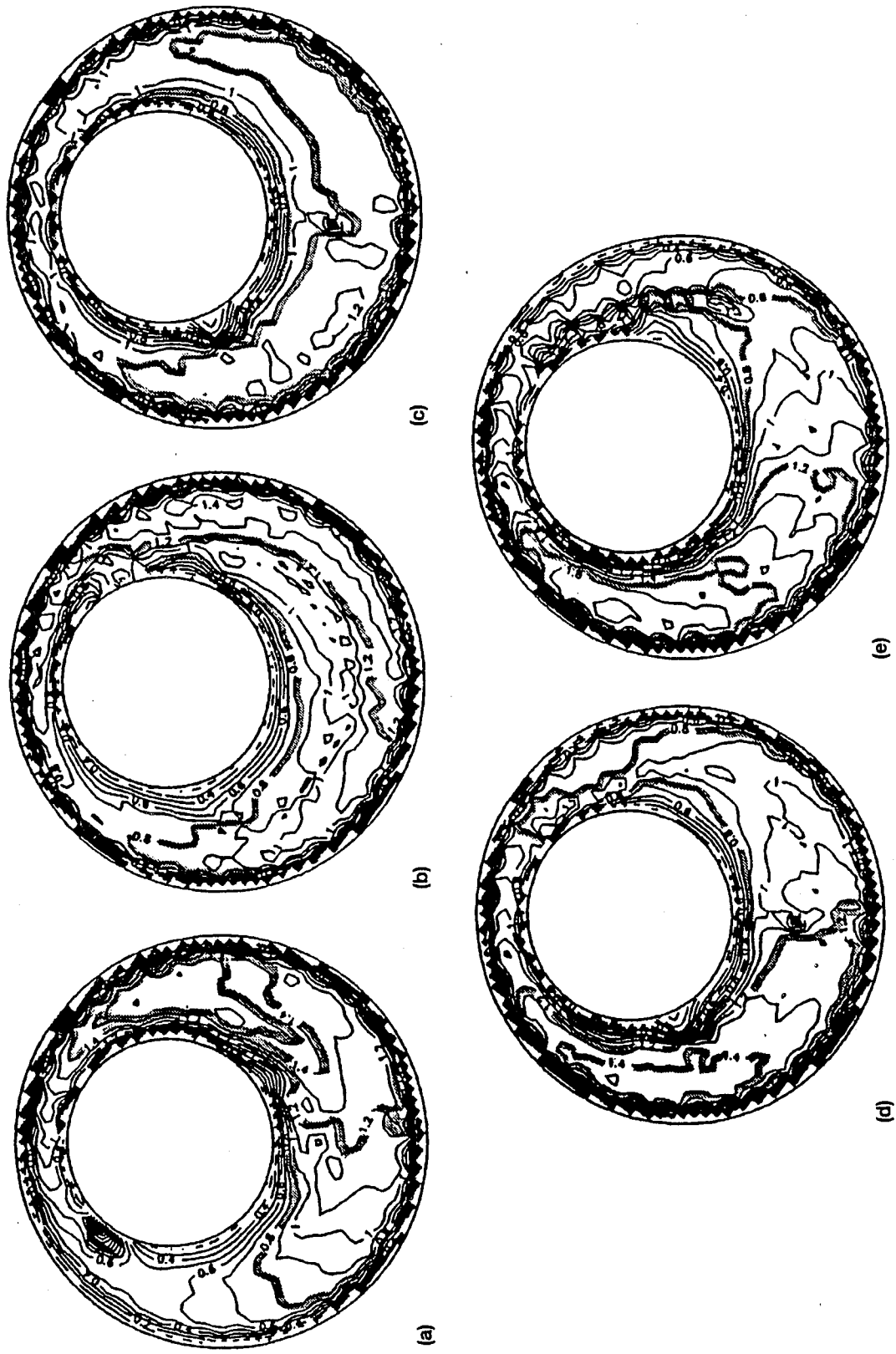
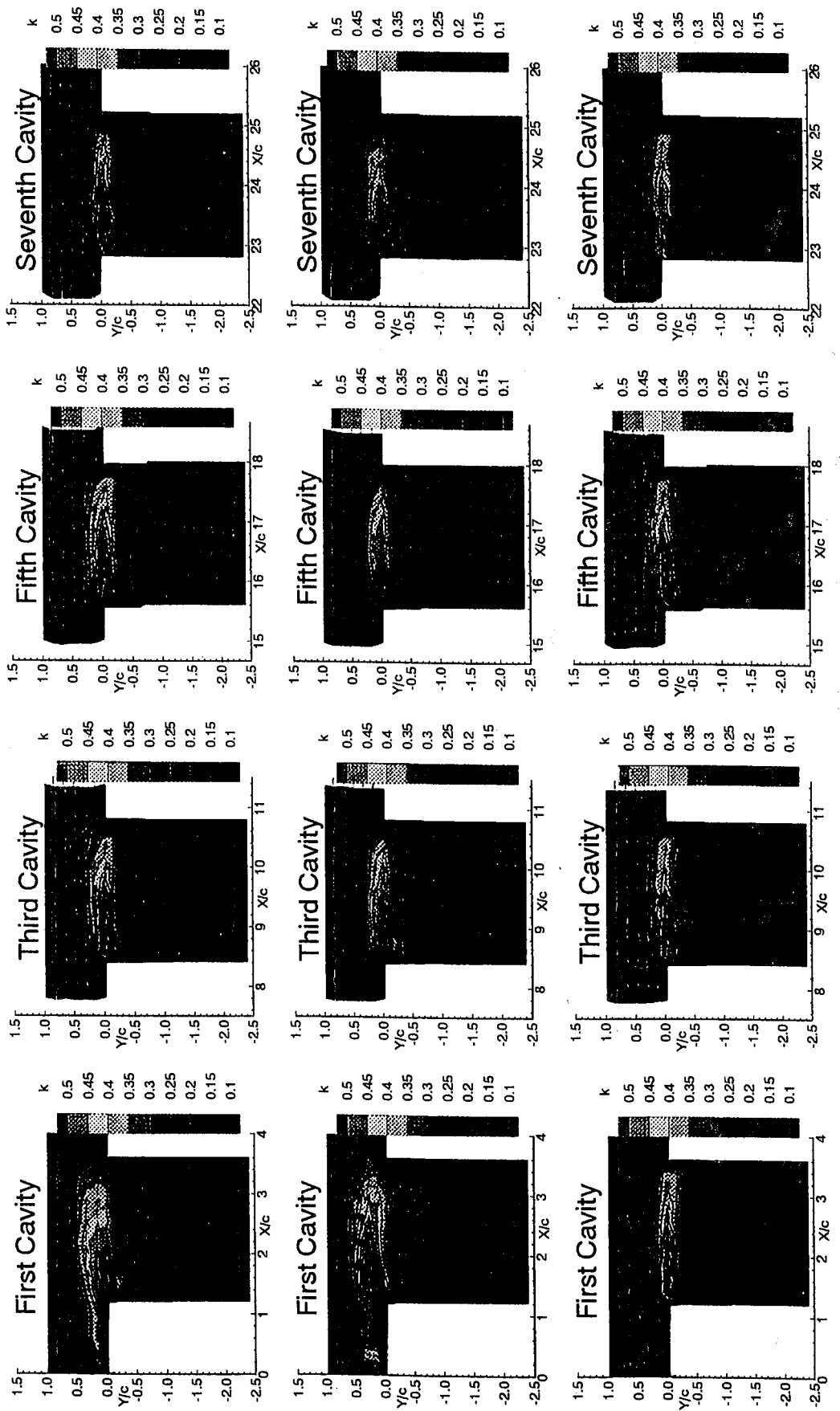


Figure 30.—Experimental data for normalized axial velocity [15, 16]. (a)  $X/L = 0$ . (b)  $X/L = 0.22$ . (c)  $X/L = 0.49$ . (d)  $X/L = 0.77$ . (e)  $X/L = 0.99$ .

Figure 30. Whirling annular seal normalized axial velocity contours - experimental



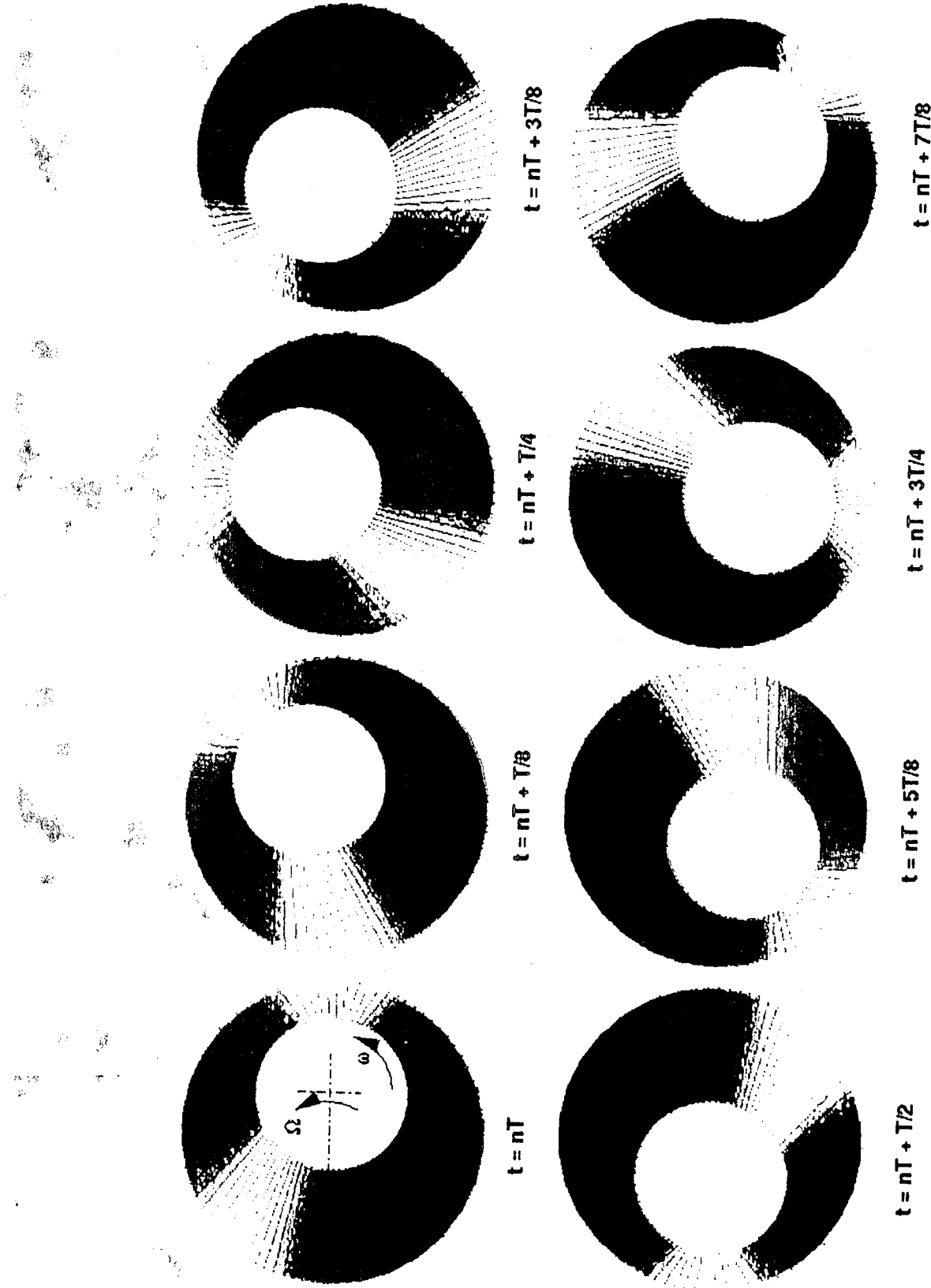
Turbulence kinetic energy contours, first row - negative preswirl, second row - no preswirl, third row - positive preswirl.

Figure 33. Whirling annular seal kinetic energies for a labyrinth seal. (After Morrison)

# Dynamic Analyses

## Time-Dependent Solutions of Perturbation Pressure No Eccentricity; Whirl Speed = 2 x Rotor Speed

Figure 34. Time dependent perturbations, 0-eccentricity, whirl =  $2 \times$  rotor speed

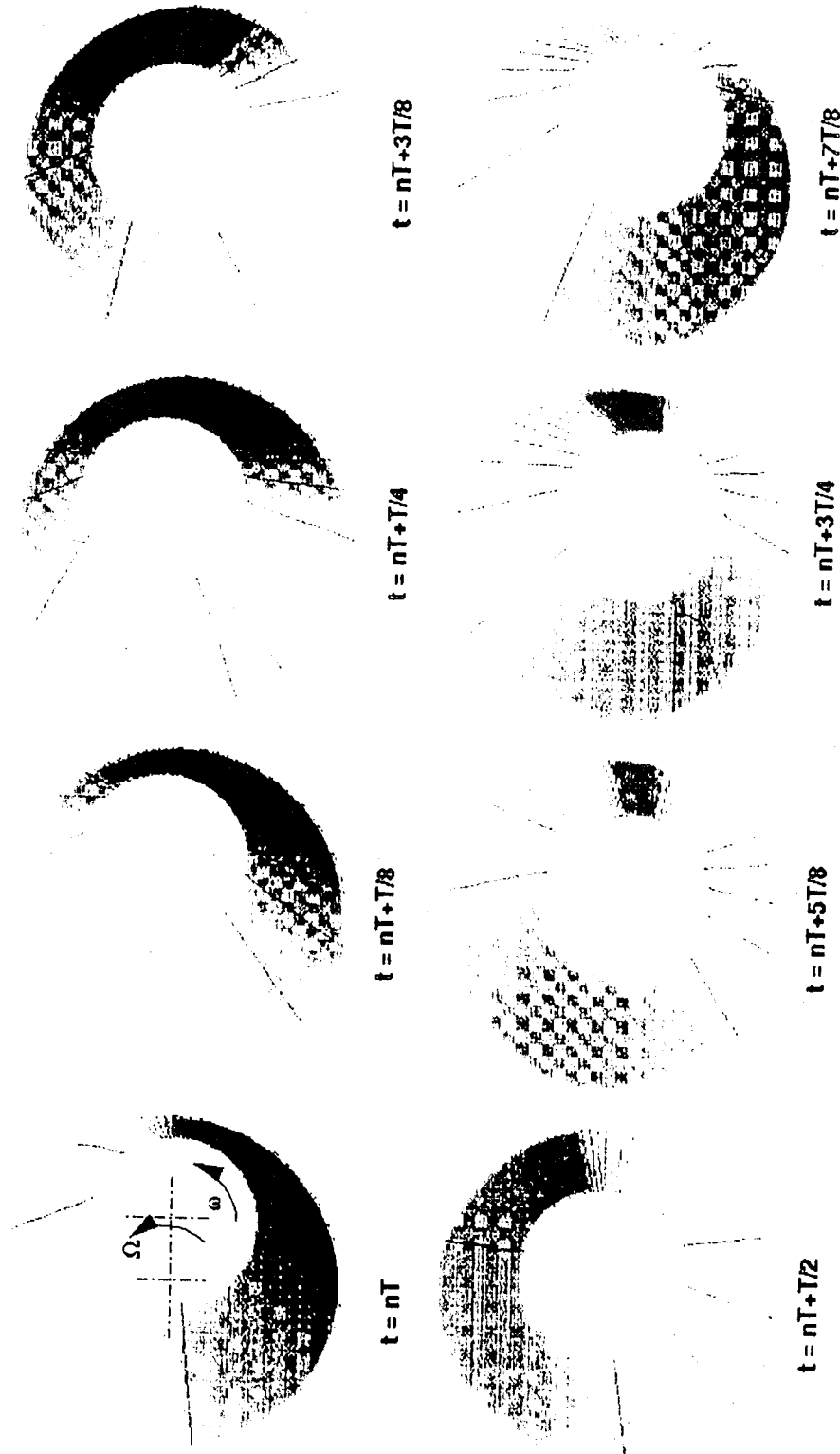


# Dynamic Analyses

## Time-Dependent Solutions of Perturbation Pressure

Eccentricity = 0.7 x Clearance; Whirl Speed = 2.5 x Rotor Speed

Figure 35. Time dependent solutions, 0.7 eccentricity, whirl = 2.5 rotor speed



## CFD Simulations of Honeycomb Tester

- Compressible flow simulations of the flat plate tester
  - ◊ Code used: SCISEAL
  - ◊ Compressible turbulent flow
- Geometries considered
  - ◊ Honeycomb width = 0.79 mm, clearance = 0.38 mm
  - ◊ Depth = 3.05 mm for friction factor jump, 3.8 mm for normal
- Flow model
  - ◊ Steady-state flow, central differencing
  - ◊ 2-Layer k- $\varepsilon$  turbulence model
  - ◊ Standard k- $\varepsilon$  not valid, cavity flow too slow

## CFD Results Summary

- Steady state simulations performed at 2 cell depths clearance  
= .38 mm
- Calculated friction factors:
  - ◊ 0.043 for 3.8 mm depth, experimental range 0.027 - 0.037
  - ◊ for 3.05 nm depth, experimental range 0.06 - 0.149
- Friction factors at higher pressure drops in progress
- Issues involved in CFD modeling:
  - ◊ Compressible flow precluded periodicity conditions, need to model several cells
    - ◊ Grid sizes prohibitively large for good resolution in cavities
    - ◊ Stead-state results will not predict friction factor jump phenomenon
    - ◊ Time-accurate results needed for jump predictions, but obviously will be computationally expensive - need to consider entire plate, 6 cells in axial are not enough

# FLOW DOMAIN AND BOUNDARY CONDITIONS

Grid size: approx. 90000 cells, Flow symmetry allows treatment of half tester.  
6 honeycomb cells used with approx.  $14 \times 14 \times 45$  grid in each cell

Pressure drop across the tester scaled to reflect 6 cells

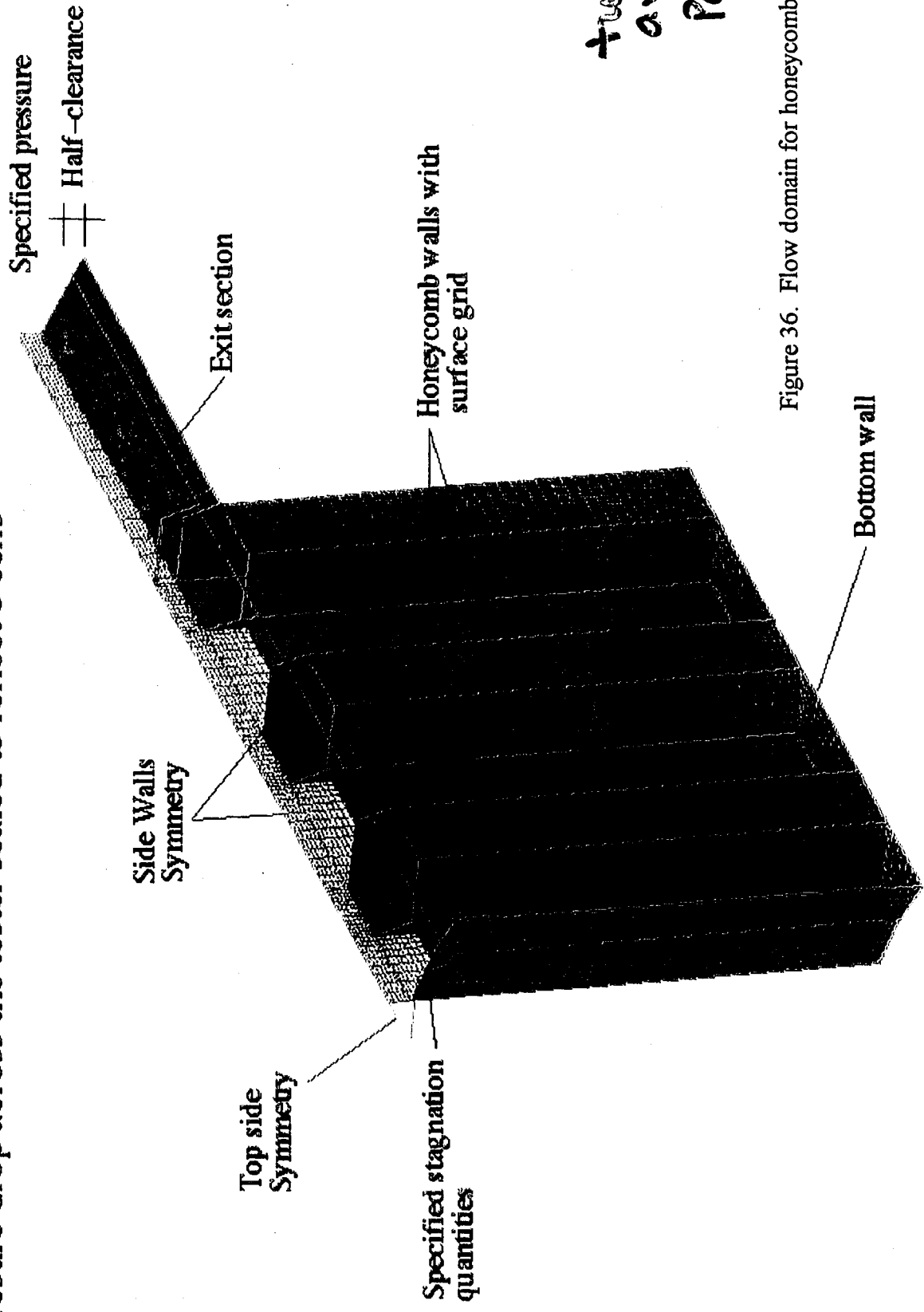


Figure 36. Flow domain for honeycomb grid.

# VELOCITY VECTORS

Upstream pressure = 6.9 Bar, Cell depth=3.8 mm.  
Vectors normalized to unit length

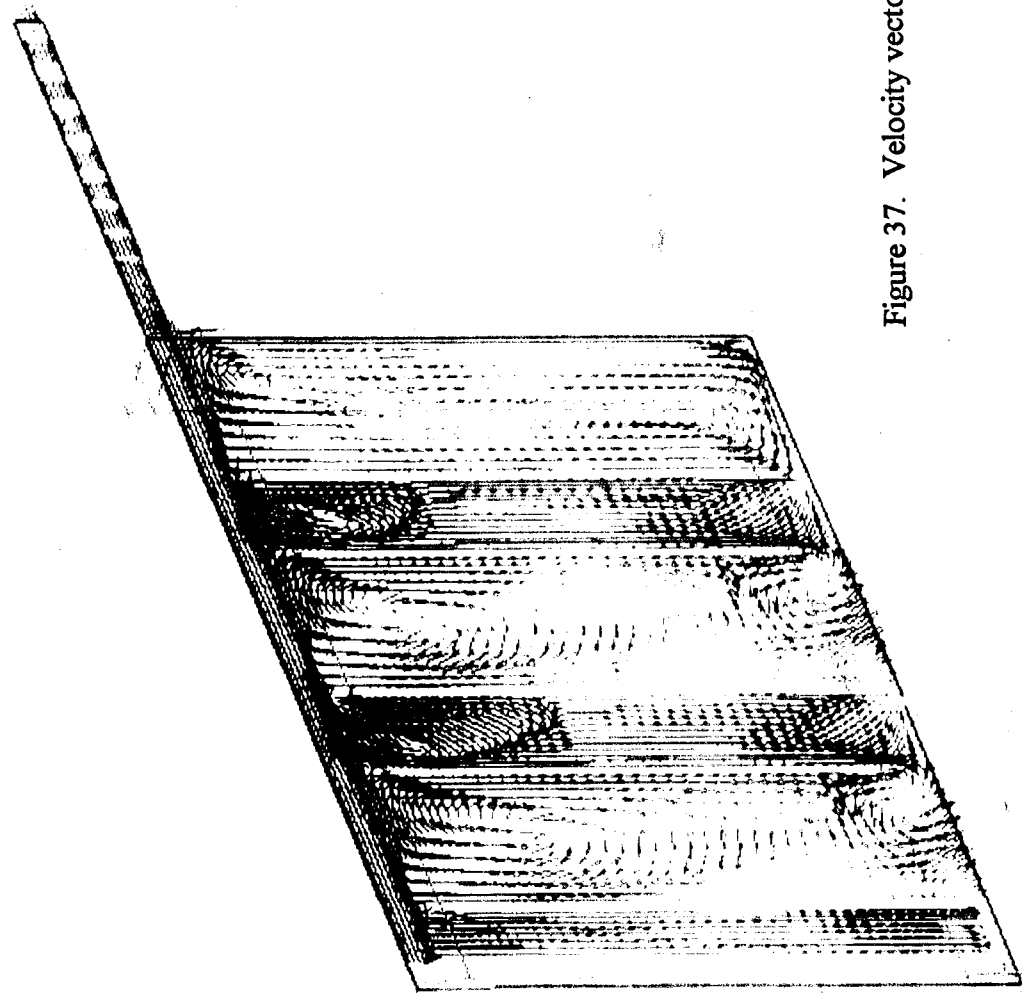


Figure 37. Velocity vectors in honeycomb configuration

Velocity vectors in the center plane

# STATIC PRESSURE

Static pressure along the center plane

Upstream pressure = 6.9 Bar, cell depth = 3.8 mm

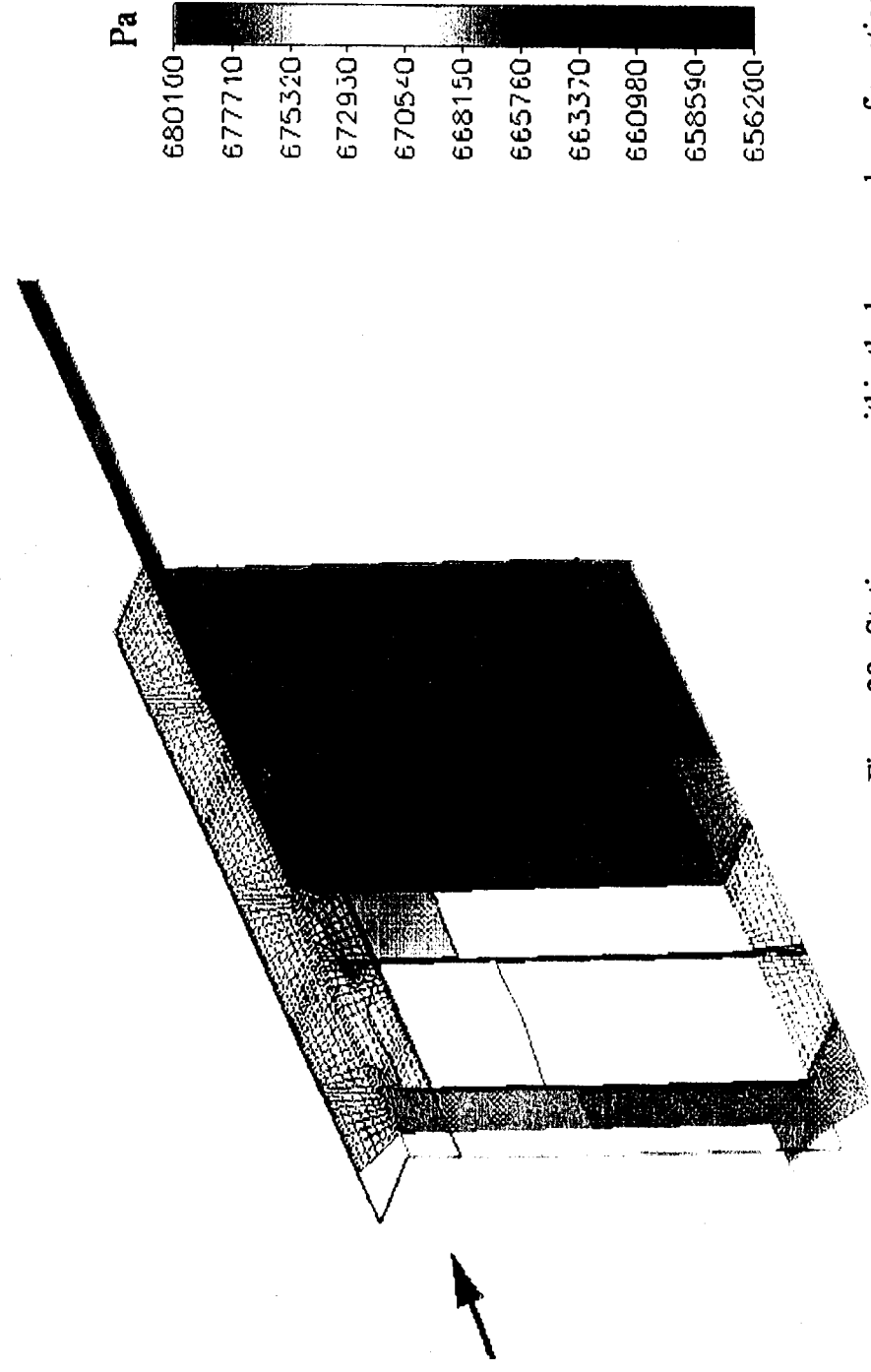


Figure 38. Static pressure within the honeycomb configuration

## SCISEAL - Brush Seal Characterization

### Grid

- Triangular unstructured grid
- Extruded to give prismatic 3-layer grid
- 15 K cells

### Boundary Conditions

- Slug flow inlet
- Pressure boundary outlet
- Adiabatic side and top walls
- Bristle tip heat generation at interface wall
- Flow conditions

### Flow Restraints

- Laminar
- Incompressible

### Results

- Flow factors show:
  - ◊ Rivering
  - ◊ Jetting
  - ◊ Starvation
- High velocity rivering and jetting regions are cool
- Flow starvation regions are hot

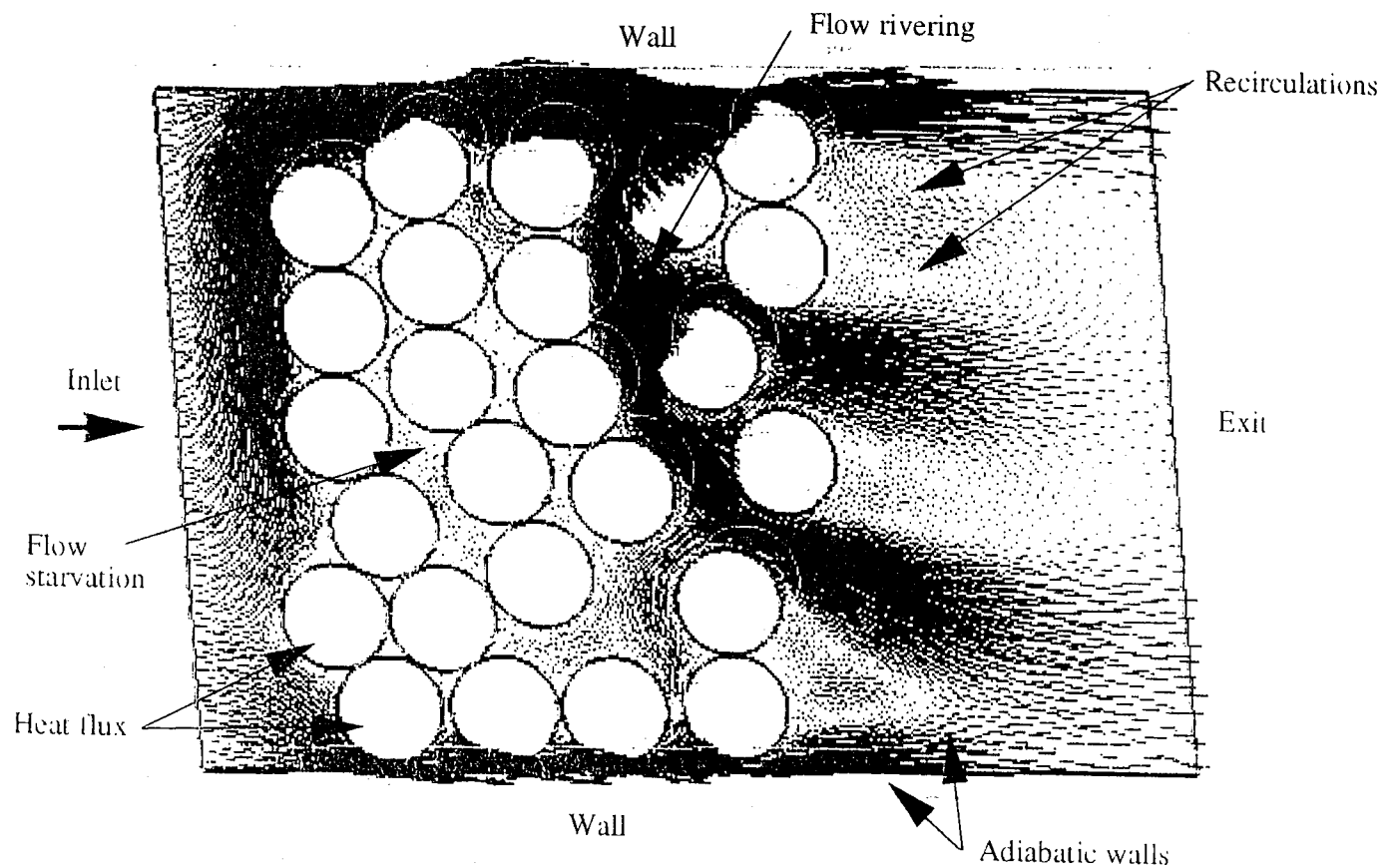


Figure Boundary conditions and velocity vectors in the mid-plane for the linear brush.

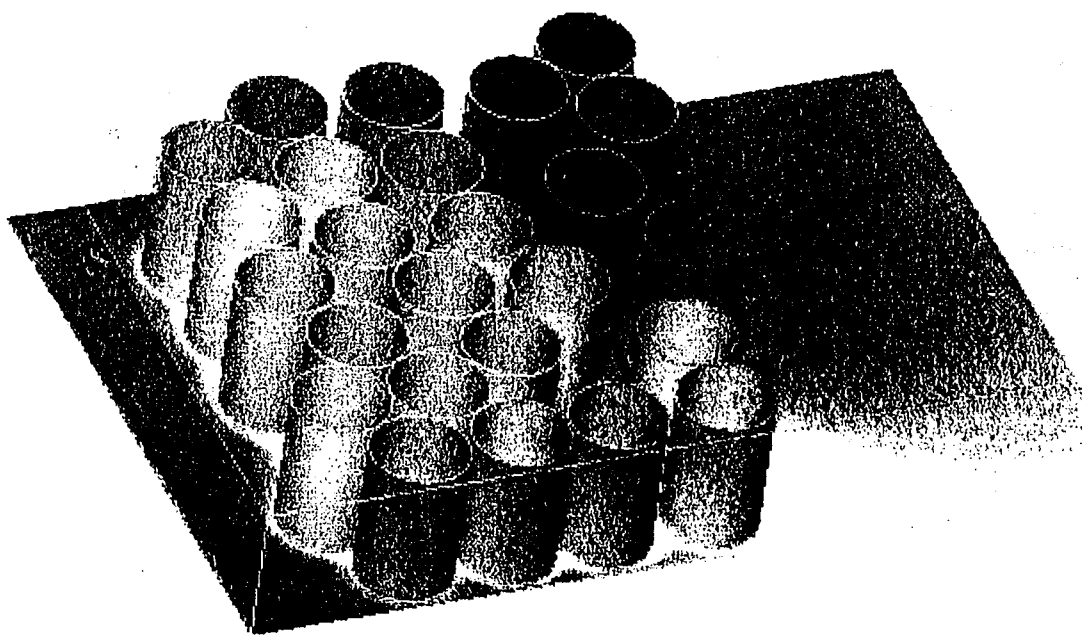


Figure Surface temperature plot for the linear brush with tip heat transfer. Note the high temperatures corresponding to the flow starvation zone.

**Figure 39. Brush seal simulations**

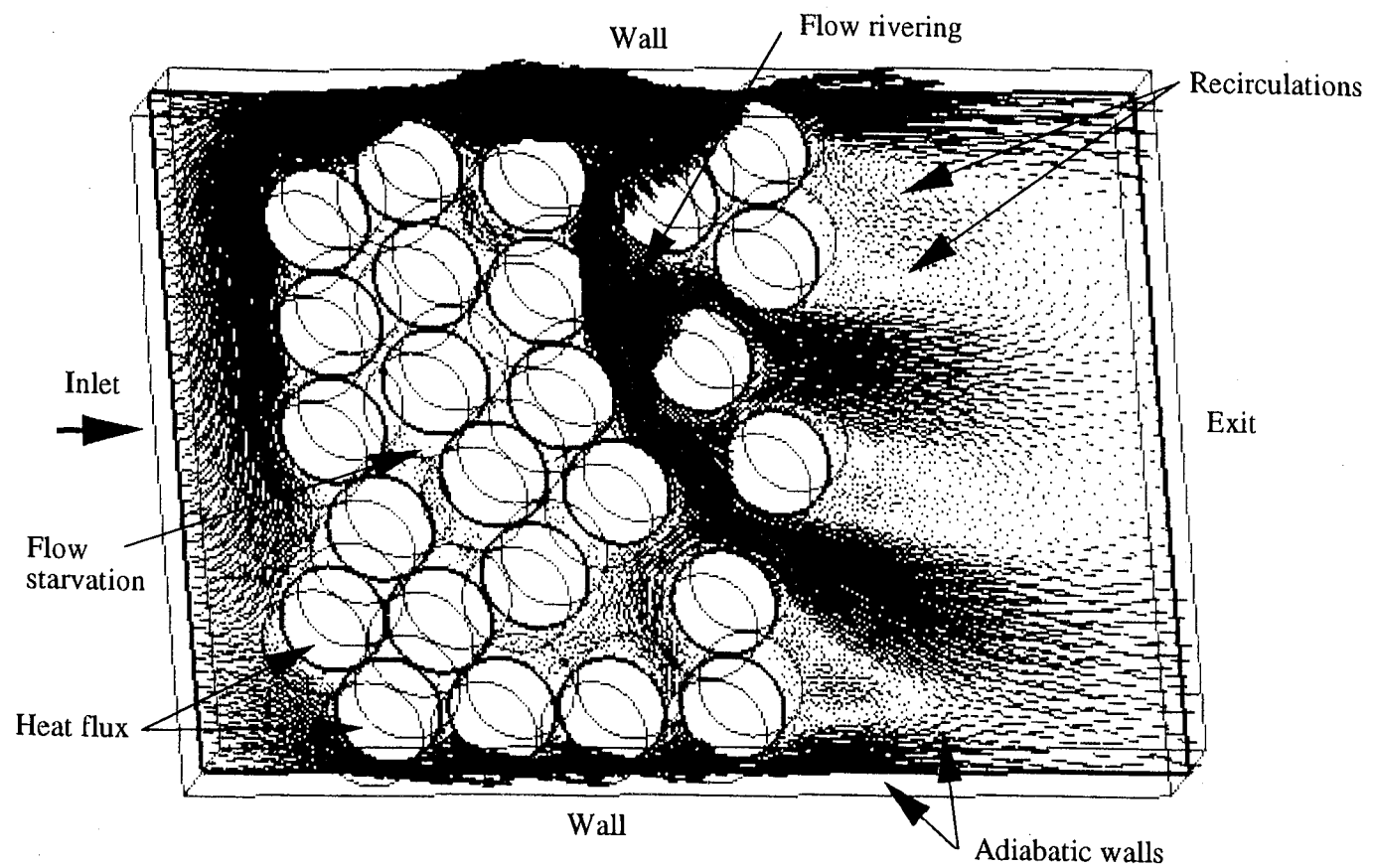


Figure Boundary conditions and velocity vectors in the mid-plane for the linear brush.

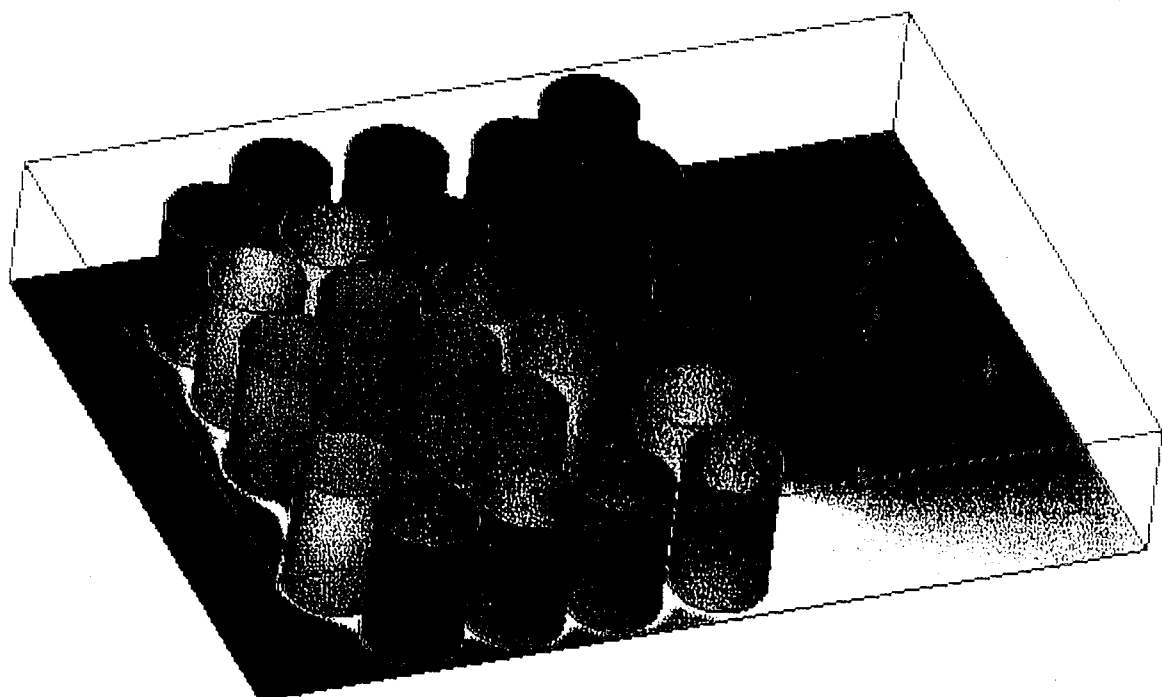


Figure Surface temperature plot for the linear brush with tip heat transfer. Note the high temperatures corresponding to the flow starvation zone.

## SCISEAL - Lid Driven Cavity

### Geometry

- $L = 1$ ,  $D = 0.5$ ,  $c = 0.025$ ,  $T = 0.2$  (permits upstream and downstream flow field)

### Grid

- $NX \times NY \times NZ = 25 \times 18 \times 25$  (Includes upstream and downstream flow field)
- $nx \times ny \times nz = 19 \times 15 \times 19$  (Gridding within the cavity)

### Boundary Conditions

- $U_{lid} = 150$  m/s
- $P_{max} = 10$  atm
- $P_{min} = 8$  atm
- Periodic in the gap

### Flow

- $Re = 42,000$
- Turbulent  $k-\epsilon$

### Vortex Control

- Co-vortex Counter-vortex
- 10% of lid driven vortex strength
- $1/r$  decay
- Placement at  $XY = 4$ 
  1. Near pressure side
  2. Near suction side

## SCISEAL - Lid Driven Cavity (Continued)

### Results

- Lid initiates a small vortex initiated near inlet plane and close to pressure side
  - ◊ Grows as it moves downstream
  - ◊ Moves downward and toward center of cavity
- At bottom of cavity about 1/3 is undisturbed, thereafter
  - ◊ Strong draft induced near pressure side by migrating vortex

### Co-Vortex

- Placed near inlet near pressure side
  - ◊ Two revolving vortices develop  $XY = 13$  and merge near the exit  $XY = 22$
  - ◊ Strong flow from pressure to suction side develops near bottom
  - ◊ Inducing flow reversals
- Placed near inlet suction side
  - ◊ No flow reversal is observed
  - ◊ Single layer vortex maintained

### Counter-Vortex

- Placed near inlet pressure side
  - ◊ Flow of main lid generated vortex is reduced
  - ◊ Influence of imposed vortex to  $XZ = 15$
  - ◊ Generally axial flow at bottom
- Placed near inlet suction side
  - ◊ Mean flow near bottom has diagonal direction
  - ◊ Strong secondary vortex formed midplane  $XZ = 8$
  - ◊ Inlet vortex flow  $XY = 13$  and 22 merge with main vortex
  - ◊ Resultant vortex shifted left of center

Panel-26 Co- and counter- rotation vortices placed near suction and pressure sides

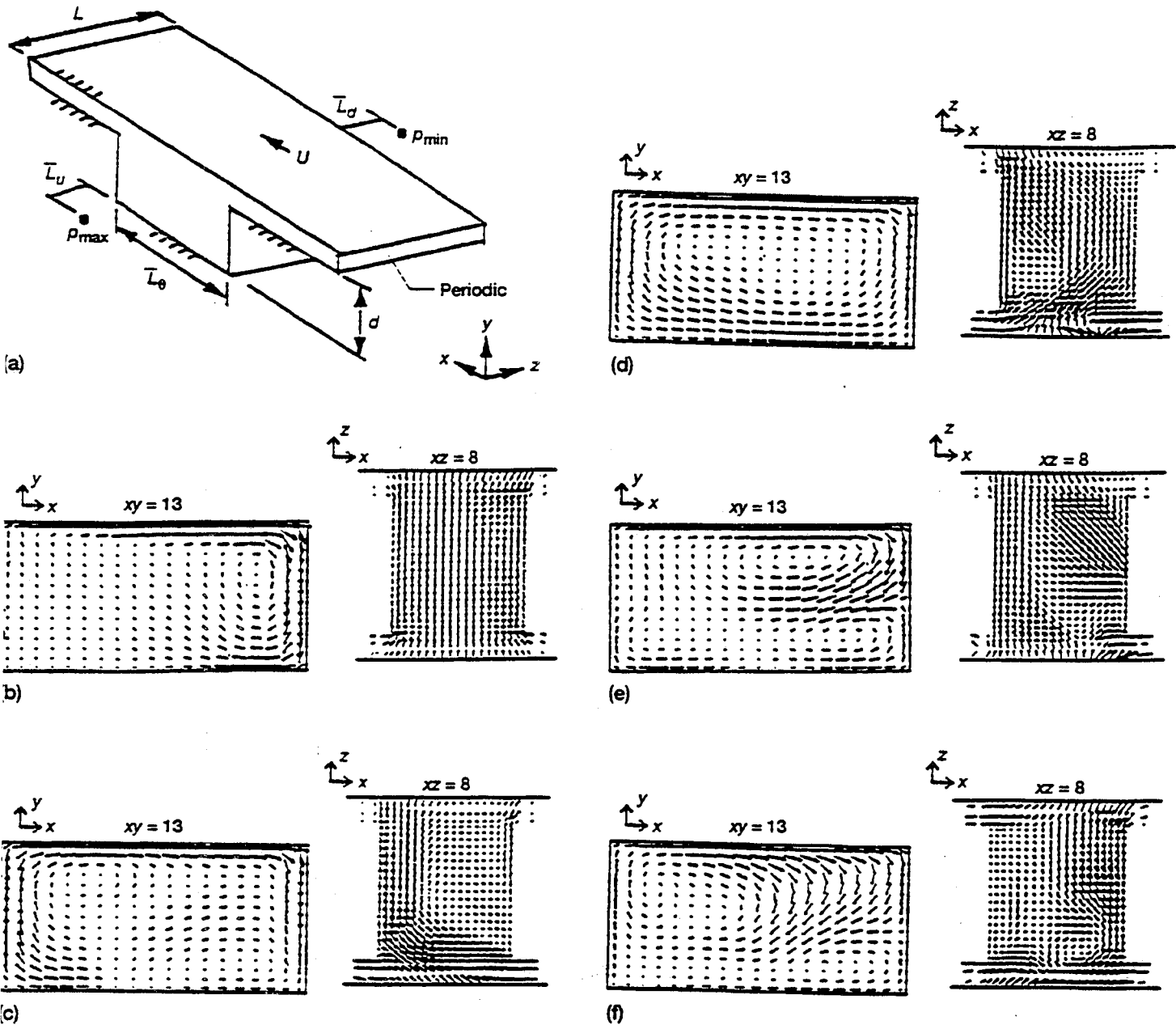


figure —Velocity vector plots for a lid-driven cavity simulating a turbine blade passage at axial plane  $xy = 13$  (near midplane) and radial plane  $xz = 8$  (near midplane). (a) Flow geometry. (b) Base test case velocity vector plots at three selected axial planes:  $xy = 4$  (near inlet),  $xy = 22$  (near exit and radial planes),  $xz = 1$  (near cavity bottom),  $xy = 15$  (near cavity top). (c) Inlet corotating vortex injection near pressure side of simulated blade. (d) Inlet corotating vortex injection near suction side of simulated blade. (e) Inlet counterrotating vortex injection near pressure side of simulated blade. (f) Inlet counterrotating vortex injection near suction side of simulated blade.

Figure 40. Lid driven cavity vortex injection studies

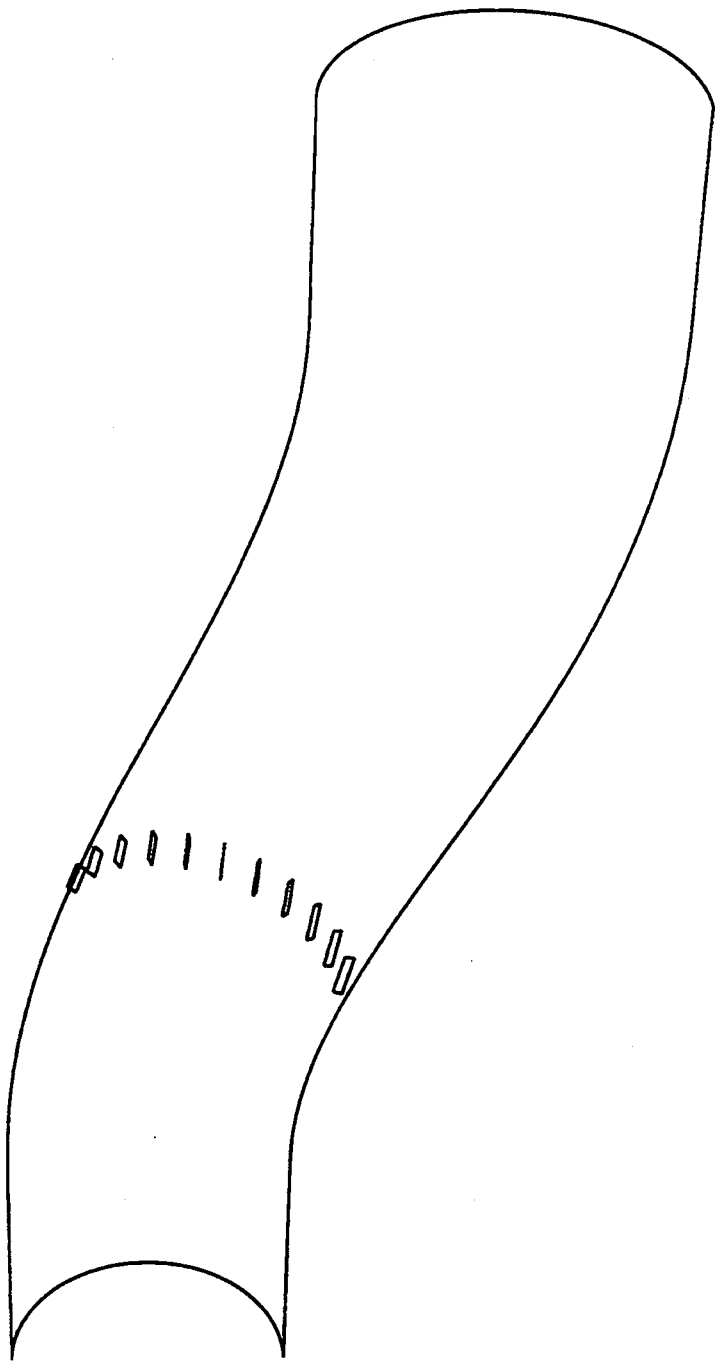
## Inlet Distortion Bernie Anderson

- Inlet distortions little understood
- Local vortex generation controls separation one flow condition
  - ◊ Adaption of external aerodynamics
  - ◊ Mixes low and high momentum streams
  - ◊ Spreads out low momentum region
  - ◊ Prevents separation
- Limitations
  - ◊ Not effective in S-ducts
  - ◊ Separation controlled at one flow (cruise)
- Global vortex control generators
  - ◊ Restructure of secondary flow
  - ◊ Increase total pressure recovery
  - ◊ Optimize
    - ⇒ Inlet total pressure recovery
    - ⇒ Face distortion level
- Reductions
  - ◊ Engine face distortion to 80%
  - ◊ Unsteadiness to 80%

## Vortex Generator Configuration VG170

$n_{vg} = 11, h/R_i = 0.070, c/R_i = 0.280, d/R_i = 0.227$

$\alpha_{vg} = 15.0^\circ, \beta_{vg} = 16.0^\circ, \theta_s = 157.5^\circ$   
 $X_{vg}/R_i = 2.0$



vg170.eps

Figure 41. Inlet duct and fin arrangements (Anderson)

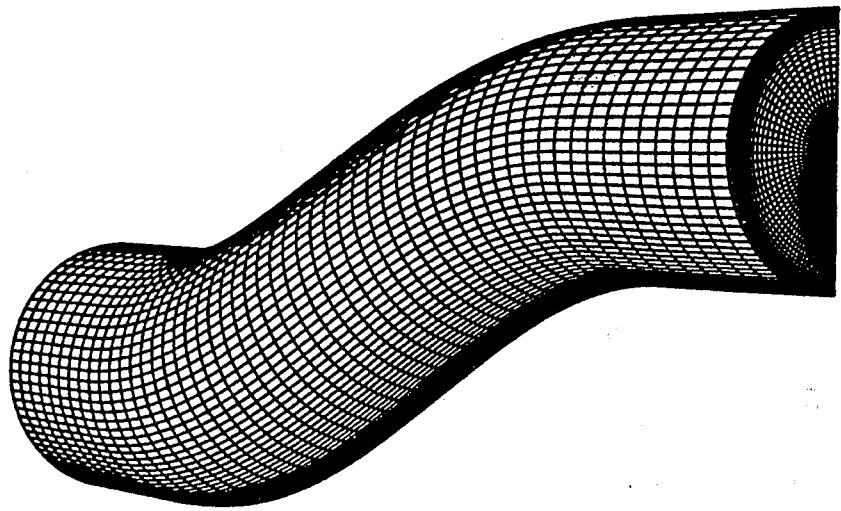


**Fig. Geometry and grid definition for the M2129 inlet S-duct,  $L/R_i=7.10$ ,  $A_{ef}/A_i=1.40$ ,  $\Delta Z/R_i=2.13$ .**

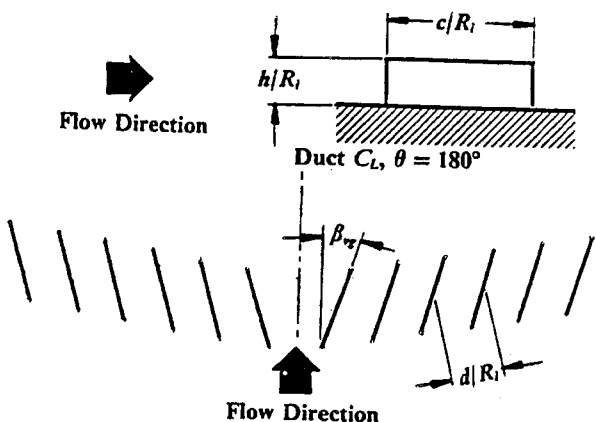


**Fig. Geometry definition for co-rotating vortex Generators**

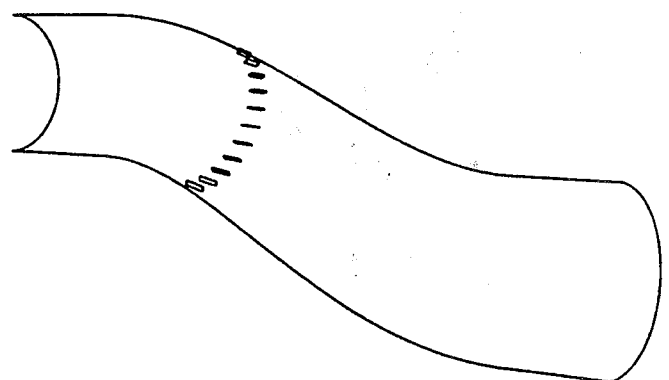


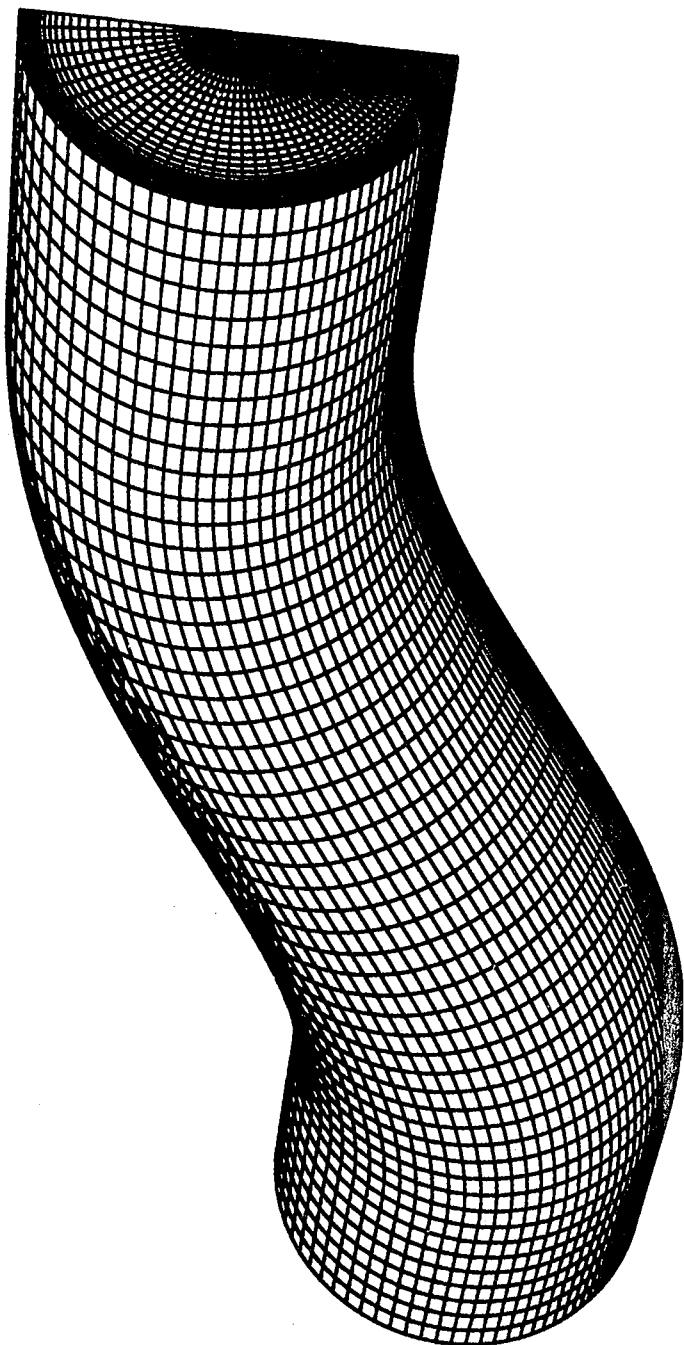
**Fig. Vortex generator configuration VG170 installed in the DRA M2129 inlet S-duct.**

**Figure 42. Inlet duct and fin geometries (Anderson)**

Vortex Generator Configuration VGI/0  
Engine Face Total Pressure Recovery Contours  
Throat Mach Number,  $M_i = 0.80$



DRA/M2129 Intake S-Duct Configuration  
 $L/D_i = 3.550$ ,  $A_{ef}/A_i = 1.400$ ,  $\Delta Z/D_i = -1.650$   
Geometry and Grid Definition

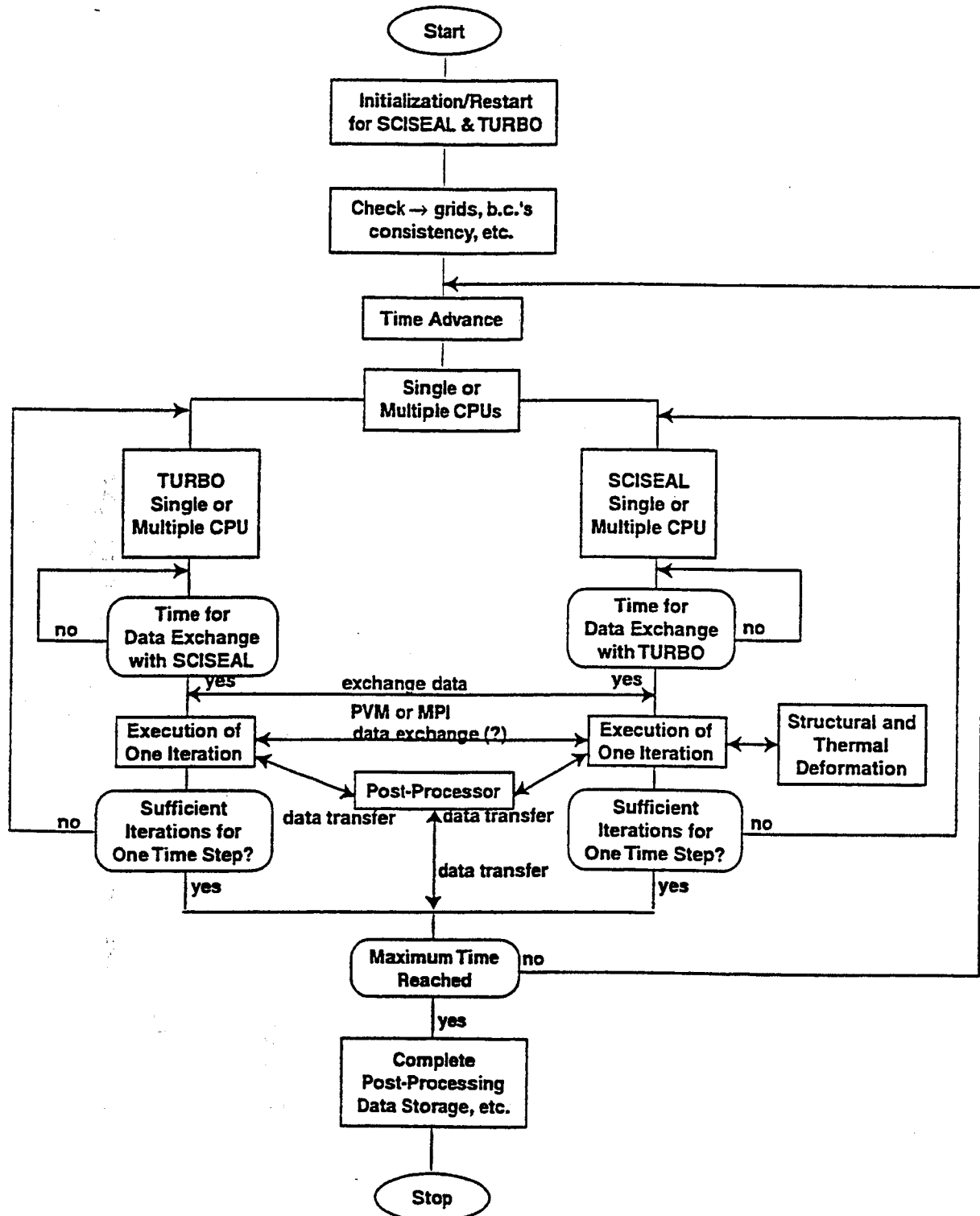


- SCISEAL
  - transfer of unstructured, adaptive Cartesian grid methodology
  - pressure-based, include conjugate heat transfer
- TURBO Code
  - addition of the boundary condition for coupling
  - data transfer procedure addition
- Coupling Interface for SCISEAL-TURBO
  - coupling strategy
  - data transfer procedures

# CODE COUPLING STRATEGY

**CFDRC**

## Proposed Flow Chart for Parallel Execution



Panel-29 Proposed flow chart for parallel execution of codes SCISEAL and TURBO

## PROPOSED WORK SCOPE



- Incorporate Unstructured, Hybrid, Adaptive Cartesian Grid Solution Methodology to SCISEAL
- Develop and Verify a Coupling Procedure for Parallel, Coupled Execution of SCISEAL and TURBO Codes
- Validate the Package Against Relevant Experimental Data
- Apply the Coupled Codes to Relevant OEM/USAF/NAVY Problems (may have overlap with above task)
- Delivery of the Codes to NASA,  $\beta$ -Test Sites for Review, Generation of Manuals and Reports

- SCISEAL
  - transfer of unstructured, adaptive Cartesian grid methodology
  - pressure-based, include conjugate heat transfer
- TURBO Code
  - addition of the boundary condition for coupling
  - data transfer procedure addition
- Coupling Interface for SCISEAL-TURBO
  - coupling strategy
  - data transfer procedures

# UNCLE TURBO Applications Group

## ● DEVELOPED FOR PREDOMINANTLY AXIAL FLOW ROTATING MACHINES

- multiple blade row, fans and propellers (ducted and unducted)
- multistage compressors or turbines (no chemistry yet)
- rotating/stationary asymmetric configurations with appendages
  - helicopter rotor (hover configuration)
  - complete airframe – propulsor integration

## ● DEVELOPED FOR UNSTEADY FLOW ANALYSIS

- uneven blade count, unsteady, nonlinear complex flow
- combined internal and external flow
- non – axial inflow conditions
- inviscid or viscous flows

# UNCLE TURBO Release Specs

## ● FLOW MODEL AND SOFTWARE IMPLEMENTATION

- unsteady Euler/Reynolds Averaged Navier Stokes (Cartesian  $\Rightarrow$  Body-fitted)
- implicit time—accurate high-resolution Roe-based finite volume numerics
- “structured multiblock” domain decomposition
  - Baldwin—Lomax turbulence modeling with wall functions — “integrate to wall & compute q<sup>+</sup> and determine if it's need — More of a two layer model Adamczyk put it with Turbo”
  - Non-uniform inlet conditions

## ● SOFTWARE DEVELOPMENT STATUS

- “makefile” installation for SGI, SUN, IBM, and Cray systems
- several example configuration directories
- TIGER grid compatibility
- seamless restart capability for arbitrary NQS queue utilization
- NSS (numerical solution sequencing) software
- queueing system flexibility
- resource stingy

# Advanced Subsonic Technology

## 14.3 Seals/Secondary Air Delivery

### Goal:

Develop and demonstrate advanced seals and design/analysis methods to meet AST engine goals.

### Approach:

Assess feasibility of required sealing technologies through component testing. Demonstrate seal performance under engine-simulated conditions. Transition mature seal technologies to engine service.

### Schedule:

- + Evaluate performance of robust, low leakage, large diameter seal ..... FY96
- + Demonstrate large diameter seal in engine test ..... FY99
- + Measure time averaged/time resolved rim seal cavity conditions ..... FY97/FY98
- + Validate comprehensive secondary/main flow analysis tool ..... FY98
- + Demonstrate performance of CDP seal in gas generator/engine test ..... FY00

### Funding:

WBS	FY96	FY97	FY98	FY99	FY00	FY01	TOTAL
14.3	1337	1932	3105	3250	1100	0	10,724

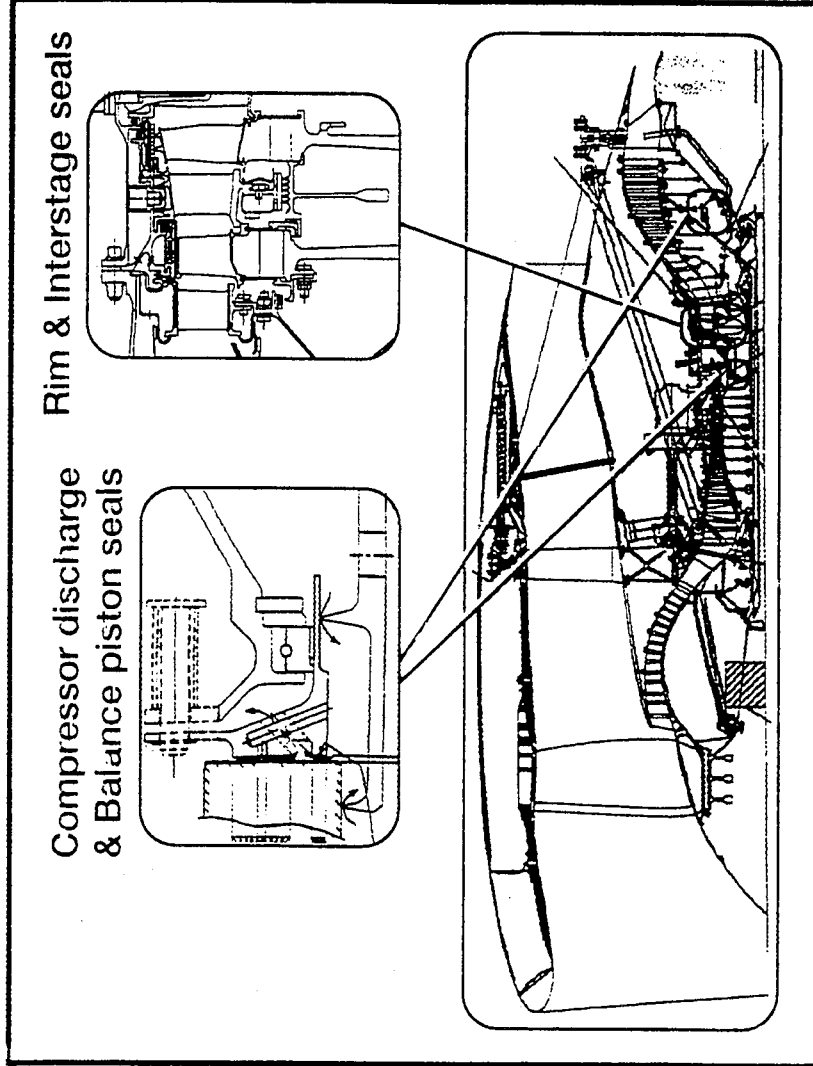


Figure 46. AST Goals

# Engine Seal Locations

Compressor discharge &  
Balance piston seal locations:  
Face & Brush seals

Turbine Rim &  
Interstage seal locations:  
Face & Brush seals

Blade Tip/Clearance  
Control

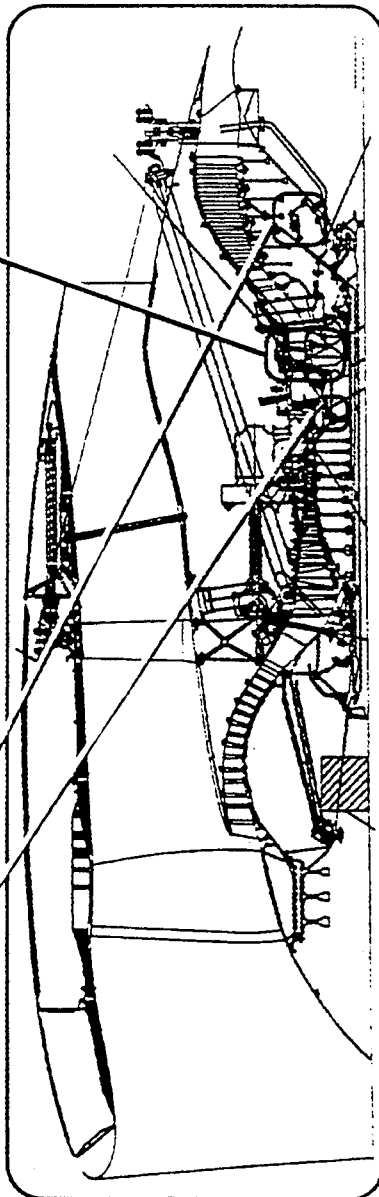
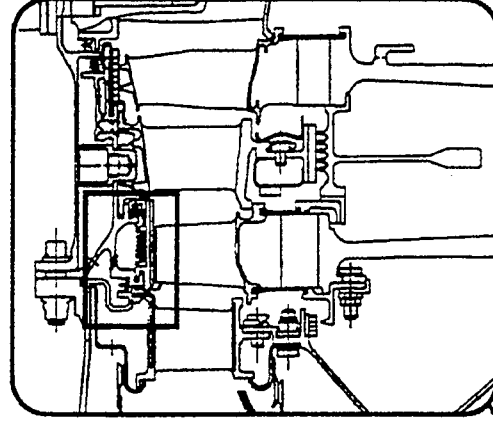
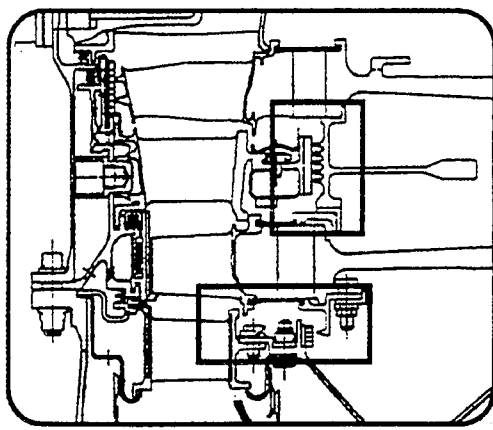
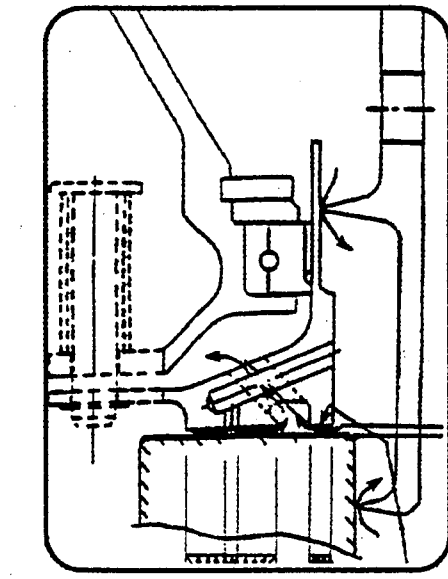


Figure 47. Seals Locations and project description

## UNCLE TURBO Future Releases

- FLOW MODEL
  - relative frame solution capability
  - inclusion of Adamczyk-Chen average passage flow initialization technique
  - turbulence model upgrade
- SOFTWARE DEVELOPMENT
  - input deck preprocessor
  - enhanced resource usage (decrease memory—increase cpu / decrease cpu—increase memory)
  - reduced restrictions regarding zonal cell count
    - I-wall capability
- DOCUMENTATION
  - preliminary users manual

# Transport Aircraft Seal Technology Benefits

## 2005 EIS

Seal Technology	Study Engine	Co.	System Level Benefits
Balance Piston Aspirating Seals (3ea)	GE90/AST Transport	GE	-1.29% SFC
Film Riding Face Seals CDP/Preswirl Locations	AST Regional	Allison	-.76% SFC
Adv. Tech. Brush Seals Turbine Rim Locations (2 ea)	AST Regional	Allison	-1.67% SFC
Film Riding Circumferential Seals	AST Regional	Allison	-1.8% SFC
Turbine Rim Locations (2 ea)	AST Regional	Allison	-1.36% SFC
Turbine Blade Tip Active Clearance Control	T-55	Allied/Lycoming	-.3% SFC
Compressor Blade Tip Passive Clearance Control			

Panel-35 Potential SFC gains seals/secondary flow program

